



THESIS APPROVAL
GRADUATE SCHOOL, KASETSART UNIVERSITY

Master of Engineering (Mechanical Engineering)

DEGREE

Mechanical Engineering

FIELD

Mechanical Engineering

DEPARTMENT

TITLE: Determination of Optimal Cutting Conditions in Parawood Machining
Process on a CNC Wood Router

NAME: Miss Siripen Supadarattanawong

THIS THESIS HAS BEEN ACCEPTED BY

THESIS ADVISOR

(Mr. Supasit Rodkwan, Ph.D.)

COMMITTEE MEMBER

(Assistant Professor Watchara Kruerattikarn, M.S.)

COMMITTEE MEMBER

(Associate Professor Pichit Sukchareonpong, Ph.D.)

DEPARTMENT HEAD

(Associate Professor Thanya Kiatiwat, Ph.D.)

APPROVED BY THE GRADUATE SCHOOL ON 29 DECEMBER 2005

DEAN

(Associate Professor Vinai Artkongharn, M.A.)

THESIS

DETERMINATION OF OPTIMAL CUTTING CONDITONS IN PARAWOOD MACHINING PROCESS ON A CNC WOOD ROUTER

SIRIPEN SUPADARATTANAWONG


**A Thesis Submitted in Partial Fulfillment of
the Requirements for the Degree of
Master of Engineering (Mechanical Engineering)
Graduate School, Kasetsart University
2005**

ISBN 974-9843-60-6

Siripen Supadarattanawong 2005: Determination of Optimal Cutting Conditions in Parawood Machining Process on a CNC Wood Router.
Master of Engineering (Mechanical Engineering), Major Field: Mechanical Engineering, Department of Mechanical Engineering. Thesis Advisor: Mr. Supasit Rodkwan, Ph.D. 138 pages.
ISBN 974-9843-60-6

In this research, series of machining processes of parawood were carried out on a Computer Numerical Control (CNC) wood router to investigate the effect of various machining parameters such as spindle speed, feed speed and depth of cut on the surface quality of parawood machined surface and the wear of the Tungsten Carbide (TC) tool. Using the Design of Experiment (DOE) and statistical methodologies, it is concluded that the optimal cutting conditions for the range of machining parameters studied in this work considering the best surface quality are the spindle speed of 12,000 rpm, the feed speed of 180 ipm and the depth of cut of 0.0625 in. In addition, the conditions with the least cutting tool wear was found at the spindle speed of 15,000 rpm, the feed speed of 360 ipm, and the depth of cut of 0.0625 in. The regression model was also obtained to predict the nose width in each cutting condition. The results provide more understanding on the parawood machining process in order to identify the optimal cutting conditions in which high quality machined surfaces with less surface roughness, less tooling cost, less waste materials, and lower production time are obtained. As a result, the selection of optimal machining parameters can be greatly benefited to the parawood furniture manufacturing industry in terms of productivity improvement.

SIRIPEN SUPADARATTANAWONG
Student's signature


Thesis Advisor's signature

16 / 12 / 05

ACKNOWLEDGMENTS

I would like to express my deep appreciation to all the people for their invaluable support and encouragement during the course of this study. My special thank goes to Dr. Supasit Rodkwan, a chairman of my M.S. Degree advisory committee, for his invaluable support, guidance, endless encouragement; especially, an assistance in improving my technical writing. I am very grateful to Assistance Prof. Watchara Krueattikarn and Associate Prof. Dr. Pichit Sukchareonpong for serving on the committee and for valuable advice.

I also would like to thank Mr. Richard L. Lemaster, Mr. Daniel E. Saloni and Mr. Timothy J. Horn for their support and guidance to conduct the research during a six-month period visiting at Wood Machining & Tooling Research Program (WMTRP), College of Natural Science, North Carolina State University. In addition, valuable advice and technical assistance from N. Laemsak, P. Triyacharoen at Kasetsart University and K. Prommul at King Mongkut University of Technology Thonburi.

I own tremendous gratitude to Mr. Chanate Sangpruk, my brother and my sister for their generous help, encouragement and their endless morale. Mostly, I would like to thank my parents for their love, inspiration, patience and support. They have been the best parents,

Finally, I gratefully acknowledge the financial support from Thailand Research Fund - Master Research Grants: TRF-MAG, contract no. MRG475E028, and the graduate school of Kasetsart University.

Siripen Supadarattanawong
November 2005

TABLE OF CONTENTS

	Page
TABLE OF CONTENTS	i
LIST OF TABLES	v
LIST OF FIGURES	vii
INTRODUCTION	1
The Objective of Proposed Research	2
LITERATURE REVIEW	
Background	
Properties of Wood	3
Physical Properties	3
Mechanical Properties	6
Parawood	8
Physical Properties of Parawood	9
Machining	11
Type of Machining Operation	13
The Cutting Tool	14
Cutting Condition	16
Machining Tool	17
Factors Affecting Tool Life in Machining	18
Tool Materials and Hardening Procedures	19
High Speed Steel	20
Tungsten Carbide	20
Satellites	21
Tool Wear	24
Tool Life	28
Tool Life Criteria	28
Surface Quality	30
Factors Affecting Power and Surface Quality	31
Workpiece Factors	31
Cutterhead Factor	31

TABLE OF CONTENTS (Continued)

	Page
Feed Factor	32
Computer Control of Woodworking Machines in Secondary Manufacture	35
Computer Numerical Controllers	36
Cutting Data Definitions	39
Strategy of Experimentation	40
The Objective of the Experiment	41
Basic Principles	41
Replication	41
Randomization	41
Blocking	42
Guidelines for Designing Experiments	42
Recognition of and Statement of the Problem	42
Choice of Factors, Level, and Range	43
Selection of the Response Variable	43
Choice of Experimental Design	43
Performing the Experiment	44
Statistical Analysis of the Data	44
Conclusions and Recommendation	44
Using Statistical Techniques in Experimentation	45
Hypothesis Testing	46
The use of P-Value in Hypothesis Testing	47
Type of Experimental Design	47
The Randomized Complete Block Design	47
Factorial Design	48
The 2^k Factorial Design	50
The 3^k Factorial Design	50
Fractional Factorial Designs	50

TABLE OF CONTENTS (Continued)

	Page
The Other Techniques in Experimentation	51
Analysis of Variance (ANOVA)	51
The General Factorial Design	53
Model Adequacy Checking	55
The Normal Assumption	56
Plot of Residuals in Time Sequence	56
Plot of Residuals versus Fitted Values	57
Plot of Residuals versus Other Variables	57
Previous Work	58
MATERIALS AND METHODS	60
Materials	60
Preliminary Experimentation	61
Experiment Setup on a CNC Wood Router	61
Experiment Setup for Tool Wear Measurement and Image	
Acquisition of Nose Width of Insert and Surface Roughness	63
Experimental Parameters	64
Methods	65
Locations	67
A period of time for the research	67
RESULTS AND DISCUSSIONS	68
Determination of the Fundamental Machining Parameters	76
Determine the Optimal Solution in Parawood Machining Process	90
CONCLUSIONS	106
LITERATURE CITED	107
APPENDIX	112
Appendix A Measurement of Moisture and Standard	
Measurement of Surface Roughness	113
Appendix B Data from Statistical Analysis	118

TABLE OF CONTENTS (Continued)

	Page
Appendix C Calculation	135
CURRICULUM VITAE	138

LIST OF TABLES

Table		Page
1	Conventional machine tools used for the three common machining operations	18
2	Properties of three classes of cutting tool materials	21
3	Severity of cutting edge wear (loss of sharpness) to tool material and to wood pH and moisture, extractive, and silicon content	23
4	The analysis of variance table for the three-factor fixed model	53
5	Parameter setup for tool wear and surface roughness measurement	64
6	Experiment tree	66
7	Machining conditions in this test	66
8	Code settings for experimental factors	68
9	Results from the machining tests	69
10	Nose width of cutting edge	74
11	Surface roughness of parawood material at 3,000 linear feet	76
12	Analysis of variance of nose width at the first step with 90% confident interval.	76
13	Analysis of variance for surface roughness of parawood material with 90% confident interval.	84
14	Analysis of Variance for transform with 90% confident interval	86
15	Design of parameter for determine the optimal valve	90
16	Analysis of variance for nose width in the second step with 90% confident interval	90
17	Analysis of variance for surface roughness of parawood material at 3,000 linear feet with 90% confident interval	98
18	Analysis of Variance of transform data on step 2 with 90% confident interval	100

LIST OF TABLES (Continued)

Appendix Table	Page
Appendix Table B1. Analysis of variance for nose width in step 1	119
Appendix Table B2 Work sheet for nose width at the first step	120
Appendix Table B3 Regression analysis	122
Appendix Table B4 Analysis of variance	123
Appendix Table B5 Analysis of variance for roughness	123
Appendix Table B6 Work sheet for surface roughness	124
Appendix Table B7 Analysis of variance for transform	125
Appendix Table B8 Analysis of variance for nose width	126
Appendix Table B9 Work sheet of nose width at the second step	127
Appendix Table B10 Regression analysis	130
Appendix Table B11 Analysis of variance	131
Appendix Table B12 Analysis of variance for surface roughness in step 2	131
Appendix Table B13 Work sheet of surface roughness in step 2	132
Appendix Table B14 Analysis of variance for transform	133
Appendix Table C1 Result of nose width of insert using regression model	137

LIST OF FIGURES

Figure		Page
1	a) A cross – section view of the machining process., b) Tool with negative rake angle compare with positive rake angle in (a).	12
2	The three most common types of machining process: a) turning, b) drilling and two forms of milling, c) peripheral milling and d) face milling	14
3	a) A single – point tool showing rake face, flank, and tool point, and b) a helical milling cutter, representative of tools with multiple cutting edges	15
4	Cutting speed, feed, and depth of cut for a turning operation	17
5	Clearance face of a high speed steel knife showing fracture and dulling of the cutting edge	24
6	(Top) Tungsten carbide cutting edges showing chemical corrosive pitting in and adjacent to chipped areas (Bottom left) Same cutting edge at higher magnification. (Bottom right) at still higher magnification, nearly loose grain of tungsten carbide can be seen; the cobalt binder has been eroder	25
7	Typical machining defect on Douglas-fir. a) chip mark and b) Raised grain	31
8	Feed back loop to control worktable position on a computer controlled machine	39
9	General model of a process or system	41
10	A factorial experiments without interaction	49
11	A factorial experiments with interaction	49
12	Schematic of the carbide cutting insert	60
13	Tool holder that used in this research	60

LIST OF FIGURES (Continued)

Figure		Page
14	Nose width of insert at a spindle speed of 18,000 rpm, a feed speed of 180 ipm and a depth of cut of 0.0625 inch	61
15	A Thermwood model 40 Turret router	62
16	Master Wood CNC wood router model Winner 2.45 K	62
17	Keyence optical microscope model VH-6100	63
18	Profilometer, stylus-type by Mitutoyo	64
19	Nose width of an insert used at a spindle speed of 12,000 rpm, a feed speed of 180 ipm and a depth of cut of 0.0625 inch; a) nose width of new insert, b) nose width of insert at 1,000 linear feet, c) nose width of insert at 2,000 linear feet and d) nose width of insert at 3,000 linear feet	69
20	Nose width of an insert used at a spindle speed of 12,000 rpm, a feed speed of 180 ipm and a depth of cut of 0.1250 inch; a) nose width of new insert, b) nose width of insert at 1,000 linear feet, c) nose width of insert at 2,000 linear feet and d) nose width of insert at 3,000 linear feet	70
21	Nose width of an insert used at a spindle speed of 12,000 rpm, a feed speed of 360 ipm and a depth of cut of 0.0625 inch; a) nose width of new insert, b) nose width of insert at 1,000 linear feet, c) nose width of insert at 2,000 linear feet and d) nose width of insert at 3,000 linear feet	70
22	Nose width of an insert used at a spindle speed of 12,000 rpm, a feed speed of 360 ipm and a depth of cut of 0.1250 inch; a) nose width of new insert, b) nose width of insert at 1,000 linear feet, c) nose width of insert at 2,000 linear feet and d) nose width of insert at 3,000 linear feet	70

LIST OF FIGURES (Continued)

Figure		Page
23	Nose width of an insert used at a spindle speed of 18,000 rpm, a feed speed of 180 ipm and a depth of cut of 0.0625 inch; a) nose width of new insert, b) nose width of insert at 1,000 linear feet, c) nose width of insert at 2,000 linear feet and d) nose width of insert at 3,000 linear feet	71
24	Nose width of an insert used at a spindle speed of 18,000 rpm, a feed speed of 180 ipm and a depth of cut of 0.1250 inch; a) nose width of new insert, b) nose width of insert at 1,000 linear feet, c) nose width of insert at 2,000 linear feet and d) nose width of insert at 2,500 linear feet	71
25	Nose width of an insert used at a spindle speed of 18,000 rpm, a feed speed of 360 ipm and a depth of cut of 0.0625 inch; a) nose width of new insert, b) nose width of insert at 1,000 linear feet, c) nose width of insert at 2,000 linear feet and d) nose width of insert at 3,000 linear feet	71
26	Nose width of an insert used at a spindle speed of 18,000 rpm, a feed speed of 360 ipm and a depth of cut of 0.1250 inch; a) nose width of new insert, b) nose width of insert at 1,000 linear feet, c) nose width of insert at 2,000 linear feet and d) nose width of insert at 3,000 linear feet	72
27	Nose width of an insert used at a spindle speed of 15,000 rpm, a feed speed of 180 ipm and a depth of cut of 0.0625 inch; a) nose width of new insert, b) nose width of insert at 1,000 linear feet, c) nose width of insert at 2,000 linear feet and d) nose width of insert at 3,000 linear feet	72
28	Nose width of an insert used at a spindle speed of 15,000 rpm, a feed speed of 180 ipm and a depth of cut of 0.1250 inch; a) nose width of new insert, b) nose width of insert at	

LIST OF FIGURES (Continued)

Figure		Page
	1,000 linear feet, c) nose width of insert at 2,000 linear feet and d) nose width of insert at 3,000 linear feet	72
29	Nose width of an insert used at a spindle speed of 15,000 rpm, a feed speed of 360 ipm and a depth of cut of 0.0625 inch; a) nose width of new insert, b) nose width of insert at 1,000 linear feet, c) nose width of insert at 2,000 linear feet and d) nose width of insert at 3,000 linear feet	73
30	Nose width of an insert used at a spindle speed of 15,000 rpm, a feed speed of 360 ipm and a depth of cut of 0.1250 inch; a) nose width of new insert, b) nose width of insert at 1,000 linear feet, c) nose width of insert at 2,000 linear feet and d) nose width of insert at 3,000 linear feet	73
31	The relationship between nose width of all inserts that used to machine parawood and cutting distance	73
32	Residual plots for nose width at the first step	78
33	Plot of residuals versus spindle speed (rpm)	78
34	Plot of residual versus feed speed (ipm)	79
35	Plot of residual versus depth of cut (in)	79
36	Plot of residual versus cutting distance (feet)	79
37	Main effects plot (data means) for nose width	80
38	The interaction plot between spindle speed and feed speed	81
39	The interaction plot between spindle speed and depth of cut	81
40	The interaction plot between feed speed and depth of cut	82
41	The interaction plot between depth of cut and cutting distance	82
42	The interaction plot between spindle speed, feed speed and depth of cut	82
43	The interaction plot between spindle speed, feed speed and cutting distance	83

LIST OF FIGURES (Continued)

Figure		Page
44	The spindle speed - depth of cut - cutting distance interaction	83
45	The spindle speed -feed speed-depth of cut and cutting distance interaction	83
46	Residual plots for surface roughness at 3,000 linear	85
47	Box-Cox plot of surface roughness at step 1	85
48	Normal probability plot of the residual of transform data	86
49	Residuals plot versus spindle speed	87
50	Residuals plot versus feed speed	87
51	Residuals plot versus depth of	88
52	Main effect plot for roughness at the first step	88
53	Interaction plot between spindle speed and feed speed	89
54	Interaction plot between spindle speed, feed speed and depth of cut	89
55	Residual plots of nose width in stage 2	91
56	Residuals versus spindle speed at stage 2	92
57	Residuals versus feed speed at stage 2	93
58	Residuals versus depth of cut at stage 2	93
59	Residuals versus cutting distance at stage 2	93
60	Plot of main effect of nose width in stage 2	94
61	The interaction plot between spindle speed and feed speed	95
62	The interaction plot between spindle speed and depth of cut	95
63	The interaction plot between spindle speed and cutting distance	96
64	The interaction plot between depth of cut and cutting	96
65	The interaction plot between spindle speed, feed speed and depth of cut	96
66	The interaction plot between spindle speed, feed speed and cutting distance	97
67	The interaction plot between spindle speed, depth of cut and cutting distance	97

LIST OF FIGURES (Continued)

Figure		Page
68	The interaction plot between spindle speed, feed speed, depth of cut and cutting distance	97
69	Residual plots for surface roughness at 3,000 linear feet	99
70	Box-Cox plot of surface roughness at stage 2	99
71	Normal probability plot of the residual of transform data	100
72	Residuals plot versus spindle speed	101
73	Residuals plot versus feed speed	101
74	Residuals plot versus feed speed	102
75	Main effect plot for roughness at stage 2	102
76	Interaction plot between spindle speed and feed speed	103
77	Interaction plot between spindle speed, feed speed and depth of cut	103

Appendix Figure

Appendix Figure A1	Calculation of roughness average (Ra)	117
Appendix Figure B1	Normal probability plot of residuals for surface roughness	124
Appendix Figure B2	Box-Cox plot for surface roughness	125
Appendix Figure B3	Normal probability plot of residuals for transform data	125
Appendix Figure B4	Normal probability plot of residuals for surface roughness	132
Appendix Figure B5	Box-Cox plot for surface roughness	133
Appendix Figure B6	Normal probability plot of residuals for transform data	134

LIST OF ABBREVIATION

adj	=	Adjust
CNC	=	Computer numerical control
DoC	=	Depth of cut
DoF	=	Degree of freedom
ipm	=	Inch per minute
LT	=	linear feet, cutting distance
MS	=	Mean square
MS _E	=	Mean square due to error
NW	=	Nose width
PW	=	Parawood
RESI	=	Residual
rpm	=	Revolution per minute
SS	=	Sum of square
TC	=	Tungsten carbide
μinch	=	Microinch

DETERMINATION OF OPTIMAL CUTTING CONDITIONS IN PARAWOOD MACHINING PROCESS ON A CNC WOOD ROUTER

INTRODUCTION

In the past few years, wood machining has often been treated as the last factor on improving productivity as an integrated part in furniture manufacturing; nevertheless, with growing concern on the future supply of wood resources, it becomes significant for researchers to gain a better understanding of wood machining process nowadays. Currently, parawood becomes more popular as an important raw material in Thailand furniture manufacturing industry due to unique properties of parawood such as excellent white wood texture and color similar to high quality hardwoods. Parawood demand is increasing since the Thai Government issued a royal enactment to close forestry concession around the country.

The furniture industry has become a major industry with an increase in parawood value. To make parawood having the highest value, it is necessary to reduce production time by developing the process for more efficiency. A variability of process must be improved such as the maintenance and the quality control. This improvement can reduce errors in the process, make the lifetime of equipment longer and decrease the cost of maintenance. State of cutting tool during machining of wood was mainly diagnosed by the skilled workers; however, for high production efficiency and cost reduction due to the significant increase in labor cost and raw materials in recent years, it is necessary to introduce process monitoring and control in wood machining. These techniques are not intended to replace the workers in the production lines, instead, they can help those workers to verify the condition of process more accurately and faster. As a result, downtime can be greatly reduced.

Consequently, in order to improve the productivity of using parawood in furniture manufacturing industry, more understanding of parawood machining process and its optimal cutting conditions are needed to obtain high quality wood products and to reduce production time with less tooling cost and less waste materials.

The Objective of Proposed Research

Because of a regulation on commercial logging in national forest areas, Thai furniture industry has successfully developed parawood from rubber plantation to substitute typical timber. Parawood, which is considered a hardwood, is derived from rubber trees, production of parawood has increased significantly in past decade. Regarding wooden furniture, parawood furniture currently accounts for about sixty percent of total production.

Many different schemes have been proposed and developed for the monitoring of machining conditions. Critical process variables of interest in machining include tool wear, surface finish, vibration, chip breakage, residual stress, etc. Among these machining process variables, tool wear and workpiece surface finish are very important parameters affecting the productivity of a machining process and they are related to many other machining parameters. (Elanayar et al., 1990)

The objective of this research is to investigate the effect of various machining parameters such as spindle speed, feed speed, depth of cut on product quality and tool wear through parawood machining process on a Computer Numerical Control (CNC) wood router. Additionally, optimal cutting conditions on parawood machining are determined using a statistical procedure.

In summary, the major tasks to accomplish this research are listed as:

- 1) Identification of various machining parameters which are important in parawood machining process through an investigated of tool wear and surface quality of finished product.
- 2) Determination of optimal conditions in parawood machining using statistical procedure.

LITERATURE REVIEW

Background

1. Properties of Wood (Forest Products Laboratory General Technical, 1999)

1.1 Physical Properties

Specific gravity: the ratio is found by dividing the weight of a substance by the weight of an equal volume of pure water at its greater density (being the specific gravity of pure water equal to 1.0). Any substance with a specific gravity more than 1.0 will sink in water, if less than 1.0 it will float. Next to the actual tests of wood strength, the specific gravity of wood is the best indication of its strength properties. The true specific gravity of wood is based on its oven-dry weight and volume; however, the specific gravity may also be based upon the volume of wood in the green air-dry condition.

Moisture content: moisture content of wood is defined as the weight of water in wood expressed as a fraction, usually a percentage, of the weight of oven dry wood. Weight, shrinkage, strength, and other properties of wood depend upon the moisture content of wood. Variability of moisture content exists even within individual boards cut from the same tree.

Green wood and fiber saturation point: green wood is often defined as freshly sawn wood in which the cell walls are completely saturated with water; however, green wood usually contains additional water in the lumens. The moisture content at which both the cell lumens and cell walls are completely saturated with water is the maximum possible moisture content. Conceptually, the moisture content at which only the cell walls are completely saturated (all bound water) but no water exists in cell lumen is called the fiber saturation point. The fiber saturation point of wood averages about 30% moisture content, but in individual species and individual pieces of wood it can vary by several percentage points from that value. The fiber

saturation point also is often considered as that moisture content below which the physical and mechanical properties of wood begin to change as a function of moisture content. During drying, the outer parts of a board can be less than fiber saturation while the inner part is still greater than fiber saturation.

Equilibrium moisture content: the moisture content of wood below the fiber saturation point is a function of both relative humidity and temperature of the surrounding air. Equilibrium moisture content (EMC) is defined as that moisture content at which the wood is neither gaining nor losing moisture; an equilibrium condition has been reached. The objective of wood drying is to bring the wood close to the moisture content a finished product will have in service.

Weight: weight of wood is technically expressed as the pounds of wood substance and water present in a cubic foot. The weight of resins and gums are not considered.

Density: density is the mass (quantity of matter) of a body per unit volume. Density of wood is the mass of wood substance in a given volume. In its dry state, the density of wood is numerically equal to its specific gravity. The density, or specific gravity of the actual wood substance itself is about 1.54. This value is practically the same for all species of wood. Because wood is porous, it contains air in the cells which reduces the weight of a given volume and permits it to float on water. The dry weight of different species varies because of these hollow cells.

Grain and texture: the general term grain is normally used to cover many different characteristics of wood, strictly speaking it should only denote the direction or arrangement of the wood fibers in relation to the longitudinal axis of the tree or of the converted plank or board. The term texture is descriptive of the relative size and arrangements of the constituent cells whereas the term figure denotes the ornamental markings brought about by structural characteristics.

Hardness: hardness is measured of the capability of a wood to resist indentation. It represents the capability of a wood to resist abrasion, scratching or denting. Hardness is primarily dependent on the density or amount of wood substance present in a given volume. Toughness, size and arrangement of fibers are also factors. The wearing qualities of any given wood may also be altered by the manner in which it is cut. Hardness values are expressed as the pounds of the wood. The following table presents average hardness values of radial and tangential side grain surfaces.

Shrinking: shrinking is an inherent property of wood and is beyond ordinary mechanical control. Any piece of wood is constantly seeking a moisture balance with the atmosphere. Since the atmospheric humidity is constantly changing, the moisture content of the wood is constantly changing and correspondingly the dimensions of the wood. Furthermore, the use of artificial heating has greatly increased the shrinkage values and, unfortunately, the greatest degree of shrinkage takes place between the critical moisture contents of air dried wood (20 percent) and fully conditioned wood (4 to 6 percent). It is important to realize that wood is not a homogeneous solid and the movement is not equal in all directions. The probable extent and direction of the shrinkage is best understood by visualizing the tree as a compact cylinder composed of innumerable smaller cylinders or annual rings fitted tightly within each other. As the tree dries out, the shrinkage will take place in every direction except in the length. The circumference of the outer cylinder will grow shorter and the cylinders within will grow smaller and more tightly packed. This circumferential shrinkage along the length of the annual rings is always greater than the shrinkage between the rings.

Working qualities: the ease of working wood with hand tools generally varies directly with the specific gravity of the wood. The lower the specific gravity, the easier it is to cut the wood with a sharp tool.

A wood species that is easy to cut does not necessarily develop a smooth surface when it is machined. Consequently, tests have been made with parawood to evaluate them for machining properties. Three major factors other than density can

affect generation of smooth surfaces during wood machining: interlocked and variable grain, hard mineral deposits, and reaction wood, particularly tension wood in hardwoods.

1.2 Mechanical Properties

Strength: ability of the material to carry applied loads or forces, in general sense, resistance of body to applied stress.

Stress: force applied per unit area.

Modulus of rupture: reflects the maximum load carrying capacity of a member in bending and is proportional to maximum moment borne by the specimen. Modulus of rupture is an accepted criterion of strength, although it is not a true stress because the formula by which it is computed is valid only to the elastic limit.

Work to maximum load in bending: ability to absorb shock with some permanent deformation and more or less injury to a specimen. Work to maximum load is a measure of the combined strength and toughness of wood under bending stress.

Compressive strength: compressive strength is a measure of the force parallel to the grain that a specimen will support. It is an evaluation of the strength of posts or short blocks that might be used support load.

Compressive strength parallel to grain: maximum stress sustained by a compression parallel to grain specimen having a ratio of length to least dimension of less than 11.

Compressive stress perpendicular to grain: reported as stress at proportional limit. There is no clearly defined ultimate stress for this property.

Shear strength parallel to grain: ability to resist internal slipping of one part upon another along the grain. Values presented are average strength in radial and tangential shear planes.

Impact bending: in the impact bending test, a hammer of given weight is dropped upon a beam from successively increased heights until rupture occurs or the beam deflects 152 mm (6 in) or more. The height of the maximum drop, or the drop that causes failure, is a comparative value that represents the ability of wood to absorb shocks that cause stresses beyond the proportional limit.

Tensile strength perpendicular to grain: resistance of wood to force acting across the grain that tends to split a member. Values presented are the average of radial and tangential observation.

Hardness: generally defined as resistance to indentation using a modified Janka hardness test, measured by the load required to embed an 11.28 mm. (0.444 in) ball to one-half its diameter. Values presented are the average of radial and tangential penetrations.

Tensile strength parallel to grain: maximum tensile stress sustained in direction parallel to grain. Relatively few data are available on the tensile strength of various species of clear wood parallel to grain. In the absence of sufficient tension test data, modulus of rupture values are sometimes substituted for tensile strength of small, clear, straight grained pieces of wood. The modulus of rupture is considered to be low or conservative estimate of tensile strength of clear specimens (this is not true for lumber)

Factors affecting strength:

1. Specific gravity generally the higher the specific gravity, the “stronger” the wood.

2. Moisture content as % M.C. increase up to fiber saturation point (fsp), strength decreases, remember that at moisture contents above fsp the additional water goes into the lumen and so the strength properties of wood at fsp and higher Moisture contents are similar.

3. Direction stress applied this is a characteristic of wood related to the anatomy of the wood, most of cells in wood have a longitudinal orientation, the micro fibrils in the thickest cell wall layer, the S2, normally have an orientation near parallel to the long axis of the longitudinal cells.

4. Duration the longer the load is applied, the more likely the wood will change shape.

5. Temperature at very high temperatures the cell wall chemicals degrade. High temperature drying of wood needed to be carefully monitored.

2. Parawood

Vegetable gum of the parawood is the name for the timber of 'Hevea Brasiliensis'. It comes from the parawood tree, which not only produces latex from which natural gum derives, but it is also a valuable source of timber, which can be utilized in many different ways. The parawood tree reaches its prime in 25 years, after which it is no longer economical to produce latex. The trees are felled and the logs taken to the factory where they are peeled in the saw mill. Most logs are in excess often meters long, but they are cut down to 1.8 meter lengths for handling purposes. Parawood is a light hardwood. It is 'whitish yellow' in color when freshly cut, which mellows to a cream, color in time. It is usually kiln dried in order to achieve quicker drying with minimum degrade. The high temperatures and humidity used in this method effectively prevent fungal and insect infestation as well as reduce warping. Also, before the timber reaches the manufacturing stage, preservatives are forced into the timber with hydraulic pressure, providing permanent protection against the likes of woodworm and other parasites. Parawood, with its inherent properties such as light

density, aesthetic appearance and easy workability, is a versatile timber suitable for a number of uses - none more so than for manufacturing furniture. In its natural state, parawood looks much like pine, but it is considerably harder and due to its abundance in the Far East, it is a good deal cheaper. Parawood is well sustainable resource to produce various kinds of products such as Flooring, Doors, Frame, Dining Table, Chair and so on. Japan and European Countries have been familiar with and appreciate Parawood quality for more decades. Parawood is an exiting new concept and comes as a sensational relief the wood consuming industries. Finally, parawood from the Far East is used for most furniture made in the part or the world. The wood is as hard as maple or ash and takes a very nice even stain. It is yellow in color, with a grain similar to mahogany (Design in Wood, 2003).

2.1 Physical Properties of Parawood

Green density	800 Kg/m ³
Average air dry density	560 – 640 Kg/m ³ at 16% m.c.
Density at 12% m.c.	600 – 620 Kg/m ³
Relative density	0.63 – 0.66 (moderately heavy timber)
Volume shrinkage	Negligible and comparable to Dark Red Meranti Tangential 1.4%, Radial 1%
Compression strength	
Parallel to grain	32
Perpendicular to grain	4.69 N/m ²
Bending strength	
Modulus of rupture	66 N/mm ² at 12% m.c.
Sheer parallel to grain	11 N/mm ²
Modus of elasticity	9240 N/mm ²
Chemical composition	Similar to hard wood, but has a higher content of extractive compounds, starch and solucarbohydrates.
Weight	Comparable to Oak and Teak with a density of 0.55 to 0.65 gm/cm ³

Hardness

On tangential face	485 kgs
On radial face	590 kgs
On end face	975 kgs

Compression parallel to grain

Average compressive strength	620 kg/sqcm
Type of failure	Crushing

Static bending test

Average flexural strength	734 kg/sqcm
Type of failure	Simple tension

Shear parallel to grain

Average shear strength along radial face	88.6 kg/sqcm
Average shear strength along tangential face	115kg/sqcm

Nail Withdrawal Strength

Average load on radial face	145 kg
Average load on tangential face	204 kg
Average load on cross face	140 kg

Screw withdrawal strength

Average load on radial face	310 kg
Average load on tangential face	400 kg
Average load on cross face	200 kg

Tensile perpendicular to grain

Average tensile strength along radial face	44 kg/sqcm
Average tensile strength along tangential face	55 kg/sqcm

Tensile parallel to grain

Average tensile strength	1267 kg/sqcm
--------------------------	--------------

Comparison with teakwood

	Teakwood	Treated
Parawood		
Specific gravity	0.604	0.557
Weight (kg/m ²)	676	624
Compression perpendicular to the grain (kg/cm ²)	101	101
Permissible stress along grain (kg/cm ²)	153	126
Janka (Side) Rating Hardness	1000	933

Working properties

Durability	Resistant to many fungal, bacterial and mold attacks can also be made resistant to other specific susceptibilities.	
Gluing	Good and compatible with almost all industrial grade adhesives--its glue bond strength is high.	
Machining	Easy to saw, machine, plane, turn and bore. The resultant surfaces are fairly smooth.	
Nail holding	Average of radial tangential value	91 kg.
	Average of end values	53 kg.
Screw holding	Average of radial tangential value	267 kg.
	Average of end values	164 kg.

3. Machining (Anonymous, 1999)

Machining is a manufacturing process in which a cutting tool is used to remove excess material from a workpart so that the remaining material is the desired part shape. The predominant cutting action involves shear deformation of the work material to form a chip; as the chip is removed, a new surface is exposed. Machining is most frequently applied to shape metals. The process is illustrated in the diagram of Figure 1.

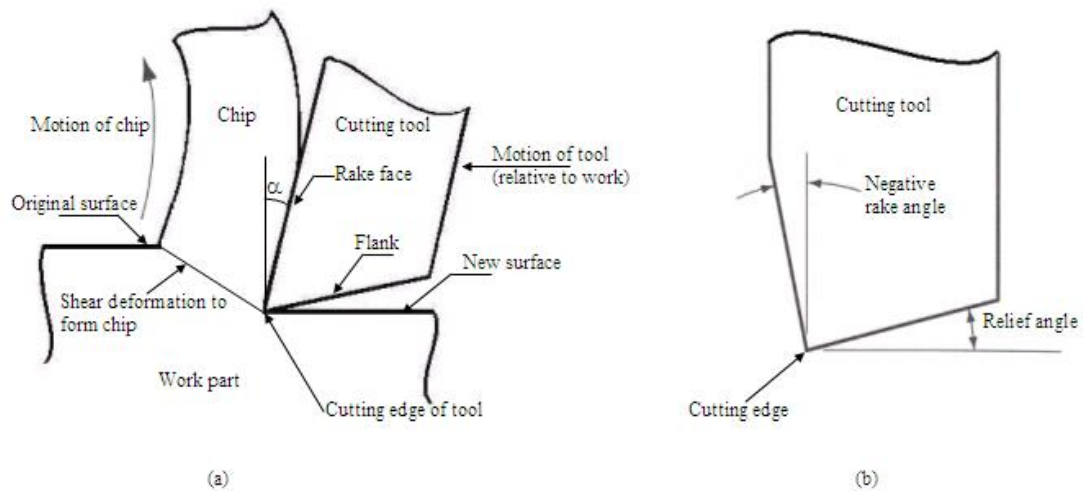


Figure 1 a) A cross – section view of the machining process., b) Tool with negative rake angle compare with positive rake angle in (a).

Machining is one of the most important manufacturing processes. The industrial revolution and the growth of the manufacturing-based economies of the world can be traced largely to the development of the various machining operation. Machining is important commercially and technologically includes the following: machining can be applied to a wide variety of work materials. Virtually all solid metals can be machined. Plastics and plastic composites can also be cut by machining. Ceramics pose difficulties because of their high hardness and brittleness; however most ceramic can be successfully cut by the abrasive machining processes.

Machining can be used to generate any regular geometry, such as flat planes, round holes, and cylinders. By combining several machining operations in sequence, shapes of almost unlimited complexity and variety can be produced. Machining can produce dimensions to very close tolerances of less than 0.001 in. (0.025 mm). It is more accurate than most other processes. Machining is capable of creating very smooth surface finishes of better than 16 μ in. (0.4 μ m). Some abrasive processes can achieve even better finishes.

Because of these characteristic, machining is generally performed after other manufacturing process such as casting or bulk deformation. The other processes

create the general shape of the part, and machining provides the final geometry, dimensions, and finish.

Machining is a family of processes. The common feature is the use of cutting tool to form a chip that is removed from the workpart. To perform the operation, relative motion is required between the tool and work. This relative motion is achieved in most machining operations by means of a primary motion, called the speed, and a secondary motion, called the feed. The shape of the tool and its penetration into the work surface, combined with these motions produce the desired shape of the resulting work surface.

3.1 Type of Machining Operation

There are many kinds of machining operations, each of which is capable of generating a certain part geometry and surface texture. Nowadays, it is appropriate to identify and define three most common types: turning, drilling, and milling, illustrated in Figure 2.

In turning, a cutting tool with a single cutting edge is used to remove material from a rotating workpiece to form a cylindrical shape, as in Figure 2 (a). The speed motion in turning is provided by the rotating workpart, and the feed motion is achieved by the cutting tool moving slowly in a direction parallel to the axis of rotation of the workpiece. Drilling is used to create a round hole. It is usually accomplished with a rotating tool that has two cutting edges. The tool is fed in direction parallel to its axis of rotation into the workpart to form the round hole, as in Figure 2 (b). In milling, a rotating tool with multiple cutting edges is moved slowly relative to the material to generate a plane or straight surface. The direction of the feed motion is perpendicular to the tool's axis of rotation. The speed motion is provided by the rotating milling cutter. There are various forms of milling, the two most basic being peripheral milling and face milling, as in Figure 2 (c) and (d).

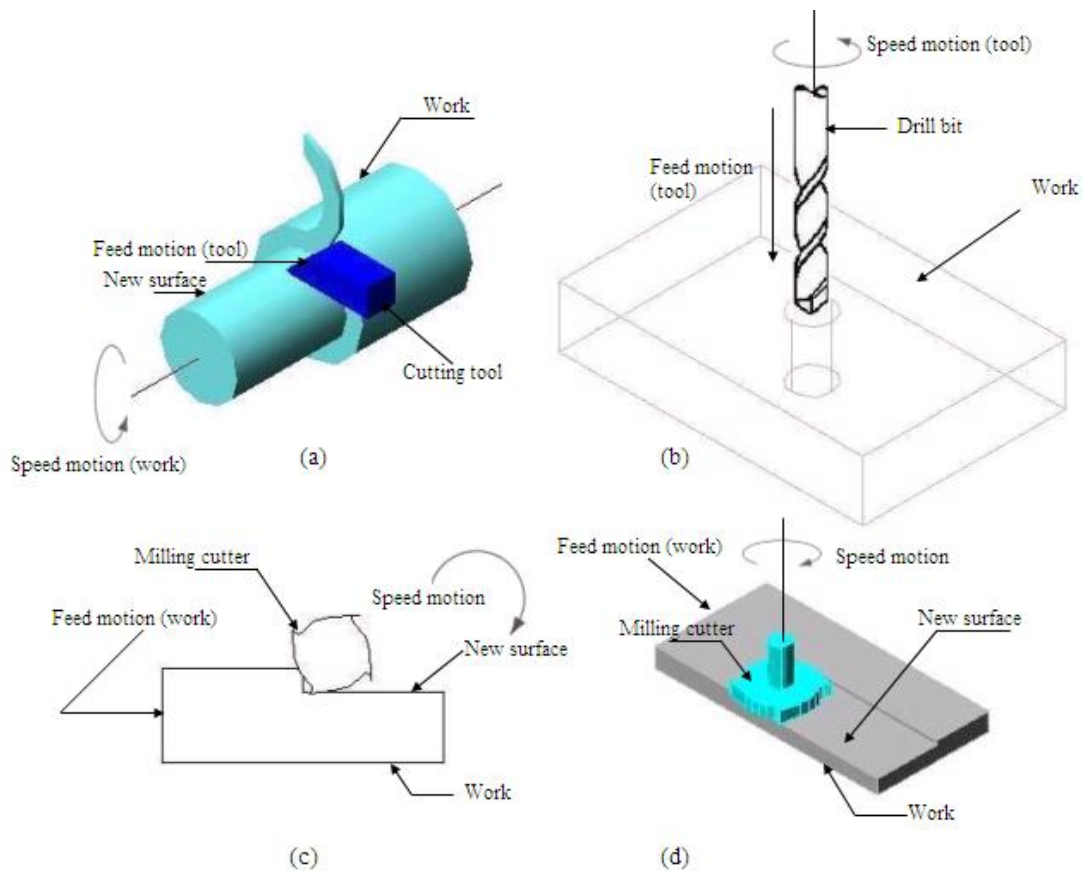


Figure 2 The three most common types of machining process: a) turning, b) drilling and two forms of milling, c) peripheral milling and d) face milling.

In addition to turning, drilling and milling, other conventional machining operations included shaping, planing, broaching, and sawing. Another group of processes often included within the category of machining is those that utilize abrasive to cut material. These processes included grinding and similar operations that are commonly used to achieve a superior surface finish on a workpart.

3.2 The Cutting Tool

A cutting tool has one or more sharp cutting edges. The cutting edge serves to separate a chip from the parent work material, as in Figure 1 Connected to the cutting edge are two surfaces of the tool; the rake face and the flank. The rake face, which directs the flow of the newly formed chip, is oriented at a certain angle call the

“rake angle, α ”. The angle is measured relative to a plane perpendicular to the work surface. The rake angle can be positive as in Figure 1 (a) or negative as in part (b). The flank of the tool provides a clearance between the tool and the newly generated work surface, thus protecting the surface from abrasive, which would degrade the finish. This flank surface is oriented at an angle called “relief angle”. Because of the harsh environment in which the tool operates, its design is very important. It must be of the proper tool geometry to effectively cut the material, and it must be made of a material that is harder than the work material.

Most cutting tool in practice has more complex geometries than those in Figure 1. There are two basic types, examples of which are illustrated in Figure 3: (a) single point tools and (b) multiple-cutting-edge tools. A single point tool has one cutting edge and is used for operation such as turning. A typical geometry for a single point tool is illustrated in Figure 3 (a). Multiply-cutting-edge tools have more than one cutting edge and usually achieve their motion relative to the workpart by rotating. Drilling and milling use rotating multiply-cutting-edge tools. Significant variety exists in these tools and their geometries. Figure 3 (b) shows a helical milling cutter used in peripheral milling. Although the shape is quite different from a single-point tool, many element of tool geometry is similar.

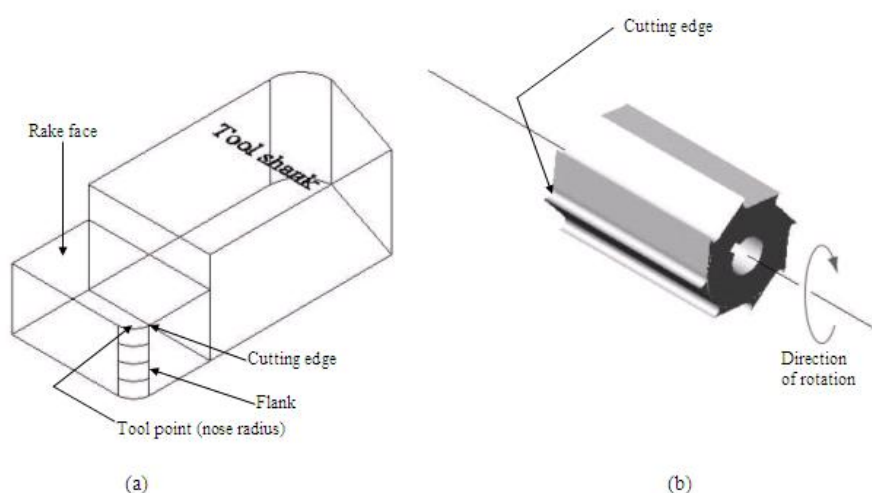


Figure 3 a) A single – point tool showing rake face, flank, and tool point, and b) a helical milling cutter, representative of tools with multiple cutting edges.

3.3 Cutting Condition

Relative motion is required between tool and work to perform a machining operation. The primary motion is accomplished at a certain cutting speed, v . In addition, the tool must be moved laterally across the work. This is a much slower motion, called the feed, f . The remaining dimension of the cut is the penetration of cutting tool below the original work surface, called the depth of cut, d . Collectively, speed, feed, and depth of cut are called the cutting conditions. They form the three dimensions of the machining process, and for certain operation (for example, most single-point tool operations) their product can be used to obtain the material removal rate for the process:

$$MRR = vfd \quad (1)$$

where

MRR	=	material removal rate, in. ³ /min (mm. ³ /s)
v	=	cutting speed, ft/min (m/s) or in. /min (mm/s)
f	=	feed, in. (mm)
d	=	depth of cut, in. (mm)

The cutting conditions for a turning operation are depicted in Figure 4. Typical units used for cutting speed are ft/min (m/s). Feed in turning is usually expressed in in/rev (mm/rev), and depth of cut is expressed in in (mm). In other machining operations, these units may be different. Machining operation usually divide into two categories, distinguished by purpose and cutting condition: roughing cuts and finishing cuts. Roughing cuts are used to remove large amounts of material from the starting workpart as rapidly as possible in order to produce a shape close to the desired from, but leaving some material on the piece for a subsequent finishing operation. Finishing cuts are used to complete the part and achieve the final dimensions, tolerances, and the surface finish. In production machining job, one or more roughing cuts are usually performed on the work, follow by one or two finishing cuts. Roughing operations are performed at high feeds and depths. Finishing

operations are carried at low feeds and depth. Cutting speeds are lower in roughing than in finishing.

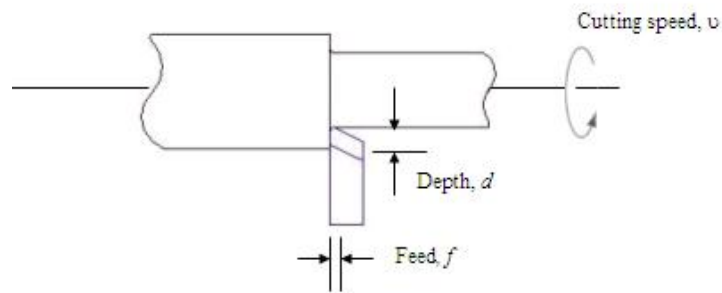


Figure 4 Cutting speed, feed, and depth of cut for a turning operation.

3.4 Machining Tool

A machining tool is used to hold the workpart, position the tool relative to the work, and provide power for the machining process at the speed, feed, and depth that have been set. By controlling the tool, work, and cutting conditions, machine tools permit parts to be made with great accuracy and repeatability to tolerance of 0.001 in (0.025 mm) and better. The term machine tool applies to any power-driven machine that perform a machining operation, including grinding. The machine tools traditionally used to perform the three common machine operation are identified in Table 1. The speed and feed motions accomplished on these machine tools are also indicated.

Conventional machine tools are usually used by human operator, although modern machine tools are often designed to accomplish their processes with a high degree of automation. These automated machines generally operate under a form of control called numerical control.

Table 1 Conventional machine tools used for the three common machining operations

Operation	Machine tool	Definitions of speed, feed, depth
Turning	Lathe	Work rotates for speed motion. Tool is fed parallel to work axis. Depth of cut is tool penetration beneath original work surface.
Drilling	Drill press	Work is held stationary. Tool rotates and feeds in direction determines hole diameter. Depth of cut is depth of hole.
Milling	Milling machine	Tool rotates for speed motion. Work is fed in direction perpendicular to tool axis. Depth of cut is tool penetration beneath original surface.

The geometry of most practical machining operation is somewhat complex. A simplified model of machining is available, which neglects many of the geometric complexities, yet describes the mechanics of the process fairly accurately. It is called the orthogonal cutting model. Although an actual machining process is three-dimensional, the orthogonal model has only two dimensions that play an active role in the analysis.

3.5 Factors Affecting Tool Life in Machining (Rodkwan, 2000)

Two major factors play the important roles in tool life when:

1. Tool material: the most common tool materials in machining parawood are carbide, diamond tooling, and ceramic tooling. Ceramic and diamond tooling usually last many times longer than carbide cutting tool do; however, they are typically much more expensive than carbide tools.

2. Tool wear: density, type and amount of resin binder, wood species, wood size, and abrasiveness will vary among parawood. Resin binders tend to build

up on the cutting tool and, when coupled with silica found naturally in the wood, have an abrasive action on the cutting tool. This can result in dull cuts, excessive tool wear, and shortened tool life. Heat buildup on the cutting tool is one of the most significant causes for tool wear, tool breakage, and poor quality cuts. Tool balancing is also the key factor that determines whether a cutting tool functions properly since improper balance tools can cause excessive tool wear, increased tool and maintenance cost, excessive noise generation.

3.6 Tool Materials and Hardening Procedures

The American Society of Tool and Manufacturing Engineering defines tool steel as “either carbon or alloy steels capable of being hardened and tempered.” These steels are utilized for machining materials at ordinary and elevated temperatures. All steel is composed of a combination of iron and carbon with varying amounts of other elements. Carbon added to iron at levels as low as 0.01 percent forms an interstitial solid solution. That is, the carbon atoms move into spaces between the iron atoms and remain there when the solution solidifies from the liquid form. These carbon atoms act to lock up the matrix and transform normally soft, malleable iron into the harder, stronger material known as steel (Kohn, n. d.).

Other materials present as alloys play an important part in developing desired properties. Certain metallic elements can replace iron atoms in the matrix and enhance performance. Other combinations can reform the carbon into very hard structural configurations, the structures known as carbides. The most useful elements used in tool steel are chromium, tungsten, molybdenum, vanadium, and cobalt. Combinations of these elements must be hardenable. To harden steel, a heat treatment is necessary.

All steels are hardened by causing an unnatural formation of the basic elements to occur. Surface hardening can be accomplished by causing carbon or nitrogen atoms to migrate into the matrix. The terms carbonizing or nitriding describe such processes. The hardening process requires heating above a critical temperature

and the controlling the cooling process to lock certain crystalline structures into the resulting metallic system.

Hardness, which promotes long wear, and toughness, which promotes resistance to fracture, are contradictory properties in most tool materials; i.e., hard steels are usually not tough. The tool designer must compromise to insure that the cutting edge can withstand cutting impacts as well as resist dulling.

3.6.1 High Speed Steel: high-speed steel is a tool steel originally designed to machine other metals at high rates of removal. The term is now also part of the nomenclature in wood machining. The most important properties of a high-speed steel are its resistance to crack propagation and hardness sufficient for the cutting task.

3.6.2 Tungsten Carbide: carbides are compressed assemblies of hard crystals held together by a binder which gives flexibility and toughness to the composite. Most carbide is produced by reducing a tungstick oxide or ammonium paratungstate in hydrogen to tungsten powder; the tungsten powder is carburized by heating with pure carbon and then ball milling with cobalt to produce the final compound to be pressed into the shape of a cutting tool. This process of hard metal pressing requires careful cutting-tip design to insure an accurate, non-stressed part. Sintering (agglomerating by heating) is employed to control hardness and carbon content of the material. A controlled atmosphere of hydrogen or carbon monoxide is used, as well as vacuum sintering, to regulate the diffusion process which produces the tungsten carbide configuration desired. Both systems have their proponents and the choice of process is limited mainly by cost. Vacuum sintering can produce superior material, but is more subject to process variables and requires sophisticated equipment of high cost and complexity. Tungsten carbides are more dense than high-speed steel, harder, and have much higher modulus of elasticity. The properties of three classes of cutting tool materials are shown in Table 2.

Table 2 Properties of three classes of cutting tool materials.

Material	Hardness R _c	Modulus of elasticity (Psi)	Density (G/cm ³)	Thermal conductivity (cal/°C/m/s)	Coefficient of thermal expansion up to 650°C x 10 ⁶ /°C
High-speed steel, Medium- carbon, heat treated....	66 (max)	32,500,000	8.6	0.61	12.6
High-carbon (1.10 percent C), heat treated....	62 (max)	29,500,000	7.8	0.41	14.7
Tungsten carbides...	67 - 68	61,000,000 - 94,300,000	11.1 – 15.2	0.068 – 0.029	4.5 – 7.2
Stellites....	63 -67	30,000,000	8.4 – 8.8	low	14.5 – 16.9

Source: Kohn (n. d.)

3.6.3 Satellites: satellites encompass a family of cobalt-chromium alloys noted for hardness, stability and wear resistance, even at high temperature. Satellite is used most commonly as a coating or tipping material; it is deposited on a clean cutting edge in a process similar to conventional welding. The edge is then ground to desired tool configuration, a slow and labor intensive process. Tipped tools may, however, be resharpened a few times before the coating needs replacement. Recently developed machinery can deposit satellite in a performed shape on a cutting surface, reducing preparation costs and grinding losses. A typical satellite comprised of 50 percent cobalt and 30 percent chromium (with carbon, nickel, molybdenum, iron and other alloying ingredients making up the remainder) will have a modulus of elasticity comparable to steel and other properties as notes in the Table 3.

The three modes of tool failure can be used to identify some of the important properties required in a tool material

(1) Toughness: to avoid fracture failure, the tool material must possess high toughness. Toughness is the capacity of a material to absorb energy without failing. It is usually characterized by a combination of strength and ductility in the material.

(2) Hot hardness: hot hardness is the ability of a material must process high temperatures. This is required because of the high-temperature environment in which the tool operates.

(3) Wear resistance: hardness is the single most important property needed to resist abrasive wear. All cutting tool materials must be hard. However, wear resistance in metal cutting depends on more than just tool hardness, because of the other tool wear mechanisms. Other characteristics affecting wear resistance include surface finish on the tool (a smoother surface means a lower coefficient of friction), chemistry of tool and work materials, and whether or not a cutting fluid is used.

Table 3 Severity of cutting edge wear (loss of sharpness) to tool material and to wood pH and moisture, extractive, and silicon content

Material	Hardness	Dry wood (<15 percent moisture content)	Green wood (above fiber saturation)	Effect of high extractives content, e.g., oak or cedar	Effect of high silicon content	Effect of low pH
-----Wear factor -----						
High-speed steel (reference material)	42-48	1.0	1.0	severe loss	severe loss	moderate loss
Carbide tip (tungsten-C)	65-84	0.05-0.20	0.10-0.30	severe loss	moderate loss	mild loss
Stellite tips	60-62	.15- .20	.20- .25	moderate loss	moderate loss	mild loss
Hard chromium plating	66-70	.10- .50	.20- .75	moderate loss	moderate loss	mild loss
High frequency induction hardened tip	60-70	.30- .50	.60+	severe loss	severe loss	moderate loss

¹Guideline data tabulated are from a variety of sources in the literature, and from personal communications. Each combination of wood and tool material requires tests to determine severity of cutting edge wear.

Source: Kohn (n. d.)

3.7 Tool Wear

Wear between two sliding surfaces can occur by plastic deformation, diffusion, viscous flow, and fracture. Figure 5 is show clearance face of a high speed steel knife showing fracture and dulling of the cutting edge.



Figure 5 Clearance face of a high speed steel knife showing fracture and dulling of the cutting edge.

Source: Kohn (n. d.)

Viscous flow, and perhaps other wear mechanisms, is accelerated by chemical/electrical reactions at the interface which soften tool material, e.g., the cobalt in carbide cutter is shown in Figure 6.

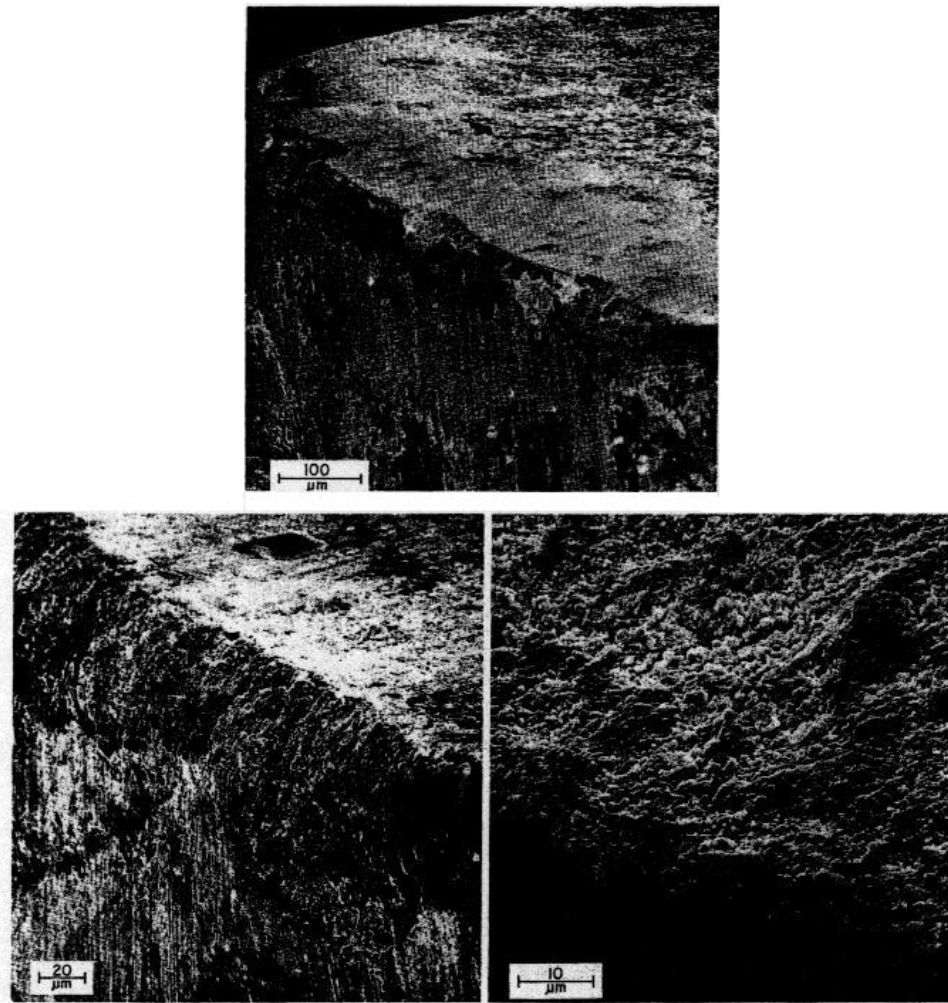


Figure 6 (Top) Tungsten carbide cutting edges showing chemical corrosive pitting in and adjacent to chipped areas. (Bottom left) Same cutting edge at higher magnification. (Bottom right) at still higher magnification, nearly loose grain of tungsten carbide can be seen; the cobalt binder has been eroded.

Source: Kohn (n. d.)

All commercial cutting tools are crystalline materials and have planes of strength and weakness. Because it is impossible to orient the cutting face so that only strong planes are exposed to the applied forces, it is necessary to examine how weaker planes behave. The micro structures of high-speed steel and carbide tools expose planes of atoms which can slide more readily than others. These planes can be shifted by high stresses at impact during cutting, and atoms are dislodged to be carried away

with the chips formed by the workpiece. Even diamond has these weak planes which are exploited by the diamond cutter to cause easy fracture. After these planes are fractured by the workpiece, the more rigid planes remaining must continue the work of material removal.

To minimize dulling, then, the tool designer attempts to place the hardest yet most energy absorbent and chemically inert cutting surface possible at the wood tool interface. It is a difficult task with no easy solutions. Researchers across the world have attempted to model the systems involved in tool wear and have developed some interesting and potentially useful concepts.

The most common approach is to separate tool wear into mechanical and electro-mechanical categories. These are looked at separately and interactive schemes are modeled. Another approach is to measure heat-friction wear and that due to silica and other abrasive inclusions. These parameters can then be weighted to develop a relative wear scale for species of varying specific gravity (surface wear from heat) and crystal inclusions (wear from abrasion).

Galvanic corrosion and cathodic-anodic ion transfer can develop and be accelerated by certain combinations of species, moisture content, and extractives. Some work has indicated that keeping workpiece-tool voltages balanced or over-balanced can decrease wear rates significantly. Whether, such systems have commercial value for mass production remains to be shown. Possibly ceramic cutting edges could better resist such wear.

It has been shown that surface hardening or treatment can improve wear significantly. Coating techniques involving chromium, satellite, and other hard surfaces show some value, but increased temperature from heavy use can soon negate the benefit. Once coating on the treated zone is materially reduced in depth, overall wear rate may not be greatly reduced. The success of chromium suggests that smoothness can be as important as hardness. Some hard-cased tools do not perform as well as chromium plated tools in some applications.

The data in Table 3 suggest how wear on cutting edges varies with tool material and cutting situation. Wear is least on tungsten carbide edges cutting dry wood with low extractives and silicon content, and high pH. The specific mechanisms that cause tool wear can be summarized as follows:

Abrasion: this is a mechanical wearing action due to hard particle in the work material gouging and removing small portions of the tool. This abrasive action occurs in both flank wear and crater wear; it is a dominant cause of flank wear.

Adhesion: when two metals are forced in to contact under high pressure and temperature, adhesion or welding occurs between them. These conditions are presented between chip and the rake face of the tool. As the chip flows across the tool, small particle of the tool are broken away from the surface, resulting in attrition of the surface.

Diffusion: diffusion is a process in which and exchange of atom takes place across a close contact boundary between two materials. In the case of tool wear, diffusion occurs at the tool-chip boundary, causing the tool surface to become depleted of the atoms responsible for its hardness. As this process continues, the tool surface becomes more susceptible to abrasion and adhesion. Diffusion is believed to be a principal mechanism of crater wear.

Plastic deformation: another mechanism that contributes to tool wear is plastic deformation of the cutting edge. The cutting forces acting on the cutting edge at high temperature cause the edge to deform plastically, making it more vulnerable to abrasion of the tool surface. Plastic deformation contributes mainly to flank wear.

Most of these tool wear mechanisms are accelerated at higher cutting speeds and temperature.

3.8 Tool Life

There are three possible modes by which a cutting tool can fail in machining, (Kohn, n. d.):

1) Fracture failure: this mode of failure occurs when the cutting force at the tool point becomes excessive, causing it to fail suddenly by brittle fracture.

2) Temperature failure: this failure occurs when the cutting temperature is too high for the tool material, causing the material at the tool point to soften, which leads to plastic deformation and loss of the shape edge.

3) Gradual wear: gradual wearing of the cutting edge causes loss of tool shape, reduction in cutting efficiency, accelerated wear, and final tool failure in manner similar to temperature failure

Fracture and temperature failure result in premature loss of the cutting tool. These two modes of failure are therefore undesirable. Of the three possible tool failures, gradual wear is preferred because it leads to the longest possible use of the tool, with the associated economic advantage of that longer use. Product quality must also be considered when attempting to control the mode of tool failure. When the tool point fails suddenly during a cut, it often causes damage to the work surface the damage requires either rework of the surface or possible scrapping of the part. The damage can be avoided by selecting cutting condition that the favor gradual wearing of the tool, rather than fracture or temperature failure, and by changing the tool before the final catastrophic loss of the cutting edge occurs.

3.8.1 Tool Life Criteria

Tool wear is normally undesirable and should be minimized, as a loss of material from the tool or both the tool and the work piece results in a change in the desired geometry of the system. A tool life criterion is defined as pre-determined

threshold values of a tool wear measure or the occurrence of a phenomenon. When the tool life, based on a limiting wear land of flank wear, is plotted using log-log coordinates, it has been found that the relationship between tool life, T and cutting speed, V , is given by the Equation 2.

$$VT^n = C, \quad (2)$$

where n and C are constants for a given work and tool material and machining conditions other than cutting speed, such as feed, depth of cut and tool geometry, etc. T is usually measured in minutes and V in m/s. This relationship is known as Taylor's equation. Following are nine alternative tool life criteria that are more convenient to use in a production machining operation, some of which are admittedly subjective:

- 1) Complete failure of the cutting edge (fracture failure, temperature failure, or wearing unit complete breakdown of the tool has occurred
- 2) Visual inspection of flank wear (or crater wear) by the machine operator (without a toolmaker's microscope). This criterion is limited by the operator's judgment and ability to observe tool wear with the naked eye.
- 3) Fingernail test across the cutting edge by the operator.
- 4) Changes in the sound emitting from the operation, as judged by the operator.
- 5) Chip becomes ribbony, stringy, and difficult to dispose of.
- 6) Degradation of the surface finish on the work.
- 7) Increased power consumption in the operation, as measure by a wattmeter connected to the machine tool.

8) Workpiece count. The operator is instructed to change the tool after a certain specified number of parts have been machined.

Cumulative cutting time, which is similar to the previous workpiece count, except the length of time the tool has been cutting is monitored. This is possible on machining tool controlled by computer is programmed to keep data on the total cutting time for each tool.

3.9 Surface Quality

Surface irregularities can be listed in three categories, (Kohn, 1964):

1. Surface quality as a function of geometry. The feed speed per knife, the wave height, and the instantaneous radius of knife-path curvature can all be regulated as desired by altering the cutting-circle diameter, cuttinghead (rpm), feed speed, depth of cut, and the number of jointed knives in the cutterhead.

2. Surface quality as a function of chip type.

3. Surface quality as an obscure function of several factors. The defect of “chip mark” is illustrated in Figure 7 (a). It appears to be caused by shavings, or more frequently by minute fiber bundles that split over, or otherwise adhere to, the extreme knife tip. These chips, particles, or fiber bundles are carried around and indented into the finished surface of the lumber. The defect appears to be associated with the character of the wood itself, and no standard procedure is effective in eliminating it. Under some circumstances wiping each knife edge with a solvent will accomplish temporary relief from this defect. Inadequate suction in the blow pipe system aggravates the problem.

The defect “raised grain” is illustrated in Figure 7 (b). It is a roughened condition in which hard summerwood is raised above the softer springwood, but not torn loose from it. It can be induced by using low rake angles, by allowing knives to

become dull or by jointing knives too heavily. The defect may show up subsequent to machining as a swelling phenomenon associated with moisture change and thus have no direct connection with the machining process.

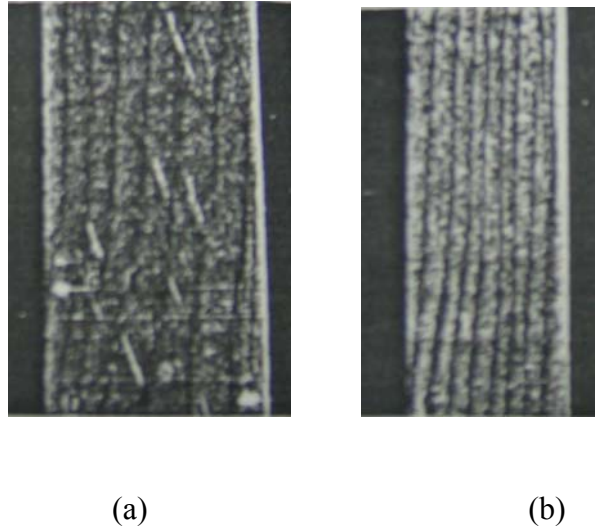


Figure 7 Typical machining defect on Douglas-fir. a) chip mark and b) Raised grain.
Source: Kohn (1964)

3.10 Factors Affecting Power and Surface Quality

Principle factors are listed in the following tabulation;

3.10.1 Workpiece Factors

- a) Species
- b) Moisture content
- c) Specific gravity
- e) Flat grain compared to edge grain

3.10.2 Cutterhead Factors

- a) Cutting velocity

- b) Cutting – circle diameter
- c) Number of jointed knives cutting
- d) Rake angle
- e) Clearance angle
- f) Sharpness of cutting edge
- g) Width of joint
- h) Knife extension beyond face of gib
- i) Shape of gib face
- l) Angle between rotational axis of cutterhead and direction of

feed

3.10.3 Feed Factors

- a) Feed speed
- b) Depth of cut
- c) Direction of cutterhead rotation with relation to direction of

feed

The effects of these factors are discussed on the follow pages:

Cutting velocity: the relative importance of cutting velocity as an isolated factor affecting cutting forces is not firmly established at this time. With small chip thicknesses and low densities, the effect may be on the order of a 5 percent increase in tool force over a range up to 30,000 fpm cutting velocity. With thick chip and high densities, an increase of over 20 percent in tool forces might be encountered as cutting velocities range from creeping speed to 30,000 fpm. As a further comment, some woods tend to have fuzzy grain when machined. The fuzziness is caused by projecting fibers that have not been completely severed at the cutting plane. With high cutting velocity, chip inertia gives the effect of greater rigidity to the wood structure and assists in accomplishing clean severance of the projecting fibers.

Cutting circle diameter: the large cutterhead produces the best surface, all other being equal, because of the geometry of the situation. The large cutterhead develops a lesser wave height and a greater instantaneous radius of curvature than does the small cutterhead. Whether the higher cutting velocity of the larger head contributes to a superior surface is debatable.

Number of jointed knives cutting: feed per knife, F_t , is a fairly good guide to cutterhead power consumption and surface quality. In the special case where feed speed is adjusted to hold F_t constant, then a direct proportionality exists between number of jointed knives cutting and net horsepower demand. In this situation doubling the number knives will double the net horsepower demand.

The feed per knife or chip load is defined as the amount of material to be removed per cutting knife per cutting revolution. The definition is given as follow:

$$F_t = F / Nn \quad (3)$$

where

F_t	=	feed per knife or chip load (in./rev./knife, usually denoted by in.)
F	=	feed speed (in/min)
N	=	number of knives cutting
n	=	cutterhead or spindle speed (rev./min)

The average undeformed chip thickness is another important machining parameter to be explored. It can be written as follow:

$$t_a = (F / Nn) / (d / D)^{1/2} \quad (4)$$

or
$$t_a = F_t / (d / D)^{1/2} \quad (5)$$

or
$$t_a = F_t d / L \quad (6)$$

Rake angle: in peripheral milling, the nominal rake angle is defined as the angle between the face of the knife and a plane containing the cutting edge and passing through the rotational axis of the cutting cutterhead this angle is constant in Figure 1. The effect of rake angle is the instantaneous angle that made between the face of the knife and a plane containing the cutting edge and perpendicular to the direction (relative to workpiece) of tool travel. This angle varies continuously along the tool path.

Clearance angle: this nominal clearance angle is constant in Figure 1. The effect of clearance angle is the instantaneous angle that made between the back of the knife and the instantaneous direction (relative to workpiece) of tool travel. This angle varies continuously along the tool path.

Feed speed: in the special case where F_t is held constant while feed speed is increased (i.e., if the number of knives in the cutterhead is doubles each time the feed speed is doubled), the horsepower requirement per knife is approximately constant with in the feed speed range from 100 to 1000 fpm. At the higher feed speeds the horsepower requirement per knife should rise slightly due to the increased kinetic energy of the undeformed chip. In the more general case in which all of factors remain constant, an increase in feed speed increase the instantaneous radius of curvature of the knife path, increase of the height of the individual knife marks, and increases the distance between knife marks. The last two results mentioned because surface quality to suffer as feed speed increases. With relatively heavy cuts, i.e., 1/16 to 1/8 inch, only with heavy cuts on the other of 1/8 inch deep does the slope of the curve become such that the horsepower requirement doubles with the doubling of feed speed. As more knives are add to the head, this degree of slope comes about in the higher speed range. With smaller depths of cut a doubling of feed rate does not result in a doubling of horsepower requirement.

Depth of cut: in orthogonal cutting, depth of cut is synonymous with thickness of the undeformed chip. A somewhat linear relationship between net

cutterhead horsepower demand and depth of cut of 1/16 inch and greater can be observed. , In general, heavy cut are more efficient than light cuts.

3.11 Computer Control of Woodworking Machines in Secondary Manufacture

In the late 1800's innovative automatic machines were developed rapidly, and by the turn of the century, woodworking machines could turn out thousands of identical parts with little human interaction. While productivity improved, such automatic machines were limited in that they could only perform a series of sequential operations. That is, the "program" was created by a series of cams and ratchets that actuated tools needed to manufacture the part. Little change could be made in the variety of sequences and the cost of creating new "hard ware" programs was high.

It was clear that more versatile machines were needed. Much more desirable would be a machine that could be guided by a set of written instructions, then on command carry out operations described in the instructions –e.g., position the workpiece, route grooves, or drill holes in specified locations with no human intervention. Refined concepts of feedback and the modern digital computer have made such machines possible. In 1966, a numerically controlled routing and shaping machine was introduced into the wood industry. The machine could mill, drill and bore at any angle on the workpiece using a punched-paper-tape program read by an electronic controller. The program positioned the tool and dictated its depth and rate of cut. To alter the shape of the part or create an entirely different one, it was necessary only to amend the old punched tape or create a new one.

These early machines were expensive due to the cost of the computer controller, and the industry was slow to respond. By 1982 the cost of micro processor based controllers no larger than desktop calculators has decreased dramatically, magnetic media and solid state bubble memory were replacing punched paper tape, and microprocessor controllers added relatively little to the cost of numerically controlled machines.

Aside from reduced machine cost, other factors favor increased introduction of computer numerically controlled equipment for secondary wood conversion. Costs associated with labor are such that returns on investments for programmable machinery are attractive. But perhaps more important is the potential for improved productivity. In many applications, computer numerical control of machines can materially increase production, reduce rejects and waste, minimize material handling, and improve dimensional accuracy

3.11.1 Computer Numerical Controllers

At heart of the computerized numerical control (CNC) is a low cost, small microprocessor that is the central arithmetic and logic unit of the system. Such microprocessors are miniaturized to fit on a single silicon chip and frequently hold thousands of transistors, resistors, and related circuit elements. By adding additional chips to provide timing, program memory interfaces for input/output signals, random-access memory, and other ancillary functions, it is possible to assemble a numerical controller on boards no larger than 8 by 10 inch pieces of paper.

It is the function of the microprocessor to accept data in the form of binary digit (0's and 1's), to store the data, and to perform arithmetic and logic operations in accordance with a previously programmed set of instructions. After processing, the microprocessor must then deliver the results to a user output mechanism. Typically, a microprocessor contains the following components, a decode and code control unit to interpret instructions from programs, an arithmetic and logic unit, registers for manipulating data, an accumulation register, address buffers to provide access to sequential instructions, and input-output buffers to read instructions or data into the microprocessor or to send them out.

A computer numerical controller consists of an operator control panel, part program data reader, and peripheral device connector panel. Typically the components are also available for individual mounting according to the machine tool builder's requirements.

The controller's power supply usually operates at 60 Hz, 120 volts AC, and is normally provided with over and under voltage protection as well as over temperature detection display circuitry and automatic shutdown if excessive internal temperatures are reached. Some power supplies feature battery backup to maintain part program data storage during power failures as well as diagnostic indicators and external voltage test points.

The operators' control panel usually consists of a CRT video display, various push buttons, indicators, and selector switches used to initiate, monitor, and govern control operations. Typical operations include control on/off, manual axis jog, machine home, and part program load/execute functions. A serial communication link is usually provided between the operator control panel and the controller circuit boards so that the control panel may be on or near the machine tool with the controller and power supply placed in a more desirable location.

A typewriter-like alphanumeric keyboard enables the operator to manually enter part program data and tool offsets as well as edit programs and initiate various control operations. Some control panels contain space for additional hardware used in specialized applications; they may also provide for emergency termination of machine operation and interlocks to prevent unauthorized modification of stored part programs.

The electronic circuitry needed to implement machine operations are some times contained on individual printed circuit modules assigned to specific slots within the controller chassis. In other controllers, the functions of individual digital logic boards are combined and incorporated on a single board using very large scale integrated (VLSI) circuitry. Each module or operational circuit performs specific control functions such as data processing or input/output/servo control.

The main processor module containing the system microprocessor executes the control program and provides supervisory control over

system operations. It additionally performs CNC functions, such as part program data decoding and distribution, arithmetic and logic, and interpolation. A programmable interface provides the necessary circuitry to interface the CNC with machines and allows the user to define and store in program from his own sequential machine tool logic. A microprocessor on the module executes the programmable interface program, and coordinates functions with the main processor module.

One or several-part memory circuits provide random access storage for part program data. Such data are read from punched paper tape, or from magnetic media such as tape and disks. In some controllers, part program data are permanently stored in recently developed magnetic bubble memories eliminating the need for interfacing punched tape or magnetic readers. Lastly the input/output/servo circuitry facilitates the electronic interface between the CNC and the external machine tool. The input/output modules actuate such devices as relays, limit, and proximity switches; they vary in number depending on user needs. One or more servo modules provide the electronic interface with position feedback devices and servo drives.

The concept of feedback is characteristic common to most computer controlled machines. Feedback involves the interaction of machine servomechanisms and the controller. As an example, Figure 8 shows a schematic diagram of a feedback loop that determines the position of movable work table. The part program data storage device first instructs the controller what position is desired. The drive motor and lead screw then move the table until the position transducer reports to the controller through a comparison unit that the correct position has been reached. Various types of feedback transducers are used such as encoders, tachometers, Selsyn motors, variable resistors or in highly accurate machines, optical interferometers. Depending on the sophistication of the feedback system, computer controlled machines are routinely accurate to within a 0.001 inch or less.

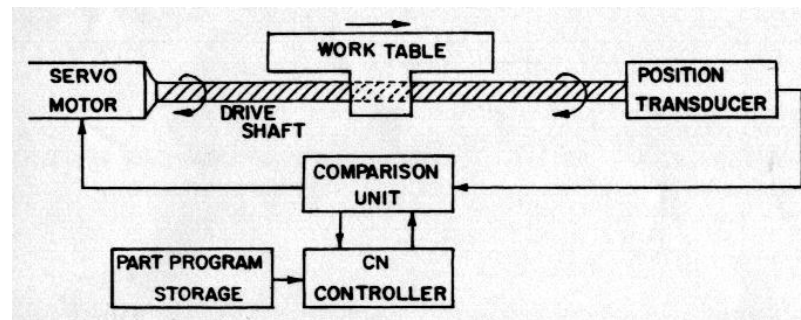


Figure 8 Feedback loop to control worktable position on a computer controlled machine.

Source: Kohn (1964)

3.12 Cutting Data Definitions

Cutting speed, feed and depth of cut are the basic cutting data used in turning. In addition, a set of specifications pertaining to tools and tool geometry must be provided for each operation. Theoretically, basic cutting data can easily be changed during the process, whereas additional cutting data must be kept constant.

Technical limitations can be reached during a cutting operation through lack of power or torque, excessive force, bad surface finish or feed speed range constraints. Cutting data that produce acceptable results and meet the specified technical limitation are called technical cutting data (TCD). Most industrial cutting data are obtained from recommendations in standard or company files, recommended cutting data (RCD). Such cutting data are usually rather conservative or “safe” and uneconomical. Cutting data that only take the economic situation into account and disregard technical limitations are called global economic optimum cutting data (GEOCD) and are usually unreasonably high. If both the economic optimum as well as the technical limitations of the specific machining situation are considered the optimum cutting data (OCD) are selected. OCD are usually higher than RCD. The aim of the on-line AC system is to realize control of the basic cutting data in such a way that the cutting operation will work with OCD, regardless of changes in the process during machining. This does not exclude, but rather emphasizes, the

importance of integration with an off-line optimization system that can provide the AC system with reliable initial OCD.

Advanced process monitoring to prevent breakdowns

- Tool flank wear
- Chipping
- Tool breakage
- Collisions
- Vibration
- Motor currents

4. Strategy of Experimentation

Experiments are performed by investigators in virtually all fields of inquiry, usually to discover something about a particular process or system (Montgomery, 2001). Literally, an experiment is a test. More formally, it can define an experiment as a test or series of tests in which purposeful changes are made to the input variables of a process or system so that it may observe and identify the reasons for changes that may be observed in the input response. In engineering, experimentation plays an important role in new product design, manufacturing process development, and process improvement. The objective in many cases may be to develop a robust process, that is, a process affected minimally by external sources of variability.

In general, experiments are used to study the performance of processes and systems. The process or system can be represented by the model shown in Figure 9. It can usually visualize the process as a combination of machines, methods, people, and other resources that transforms some input into an output that has one or more observable responses. Some of the process variables x_1, x_2, \dots, x_p are controllable, whereas other variables z_1, z_2, \dots, z_q are uncontrollable.

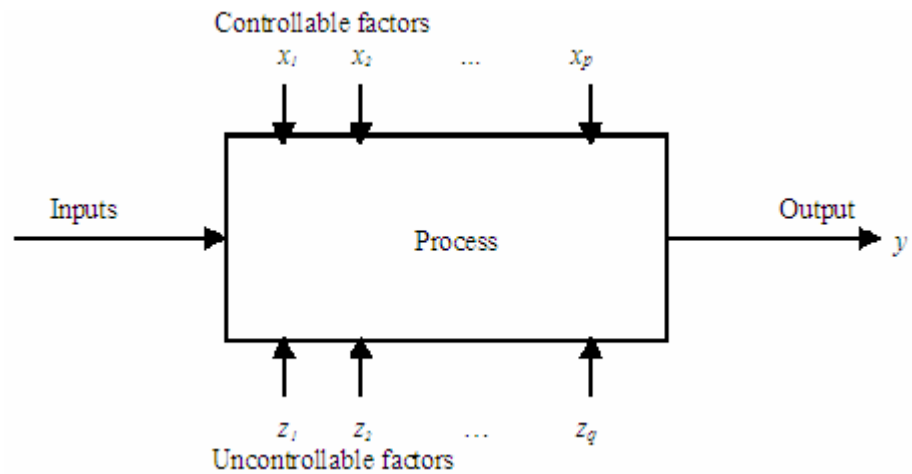


Figure 9 General model of a process or system.

4.1 The Objectives of the Experiment

The objectives of the experiment may include the following:

1. Determine which variables are most influential on the response y .
2. Find where to set the influential x 's so that y is almost always near the desired nominal value.
3. Determine where to set the influential x 's so that variability in y is small.
4. Discover where to set the influential x 's so that the effects of the uncontrollable variables z_1, z_2, \dots, z_q are minimized.

4.2 Basic Principles

Statistical methods are applied for analyzing the data which are collected during three basic principles of experimental design; replication, randomization, and blocking.

4.2.1 Replication: replication is a repetition of the basic experiment. Replication would consist of treating a specimen. It has two important properties. First, it allows the experimenter to obtain an estimate of the experimental error. This

estimate of error becomes a basic unit of measurement for determining whether observed differences in the data are really statistically different. Second, if the sample mean is used to estimate the effect of a factor in the experiment, replication permits the experimenter to obtain a more precise estimate of this effect.

4.2.2 Randomization: randomization is the cornerstone underlying the use of statistical methods in experimental design. By randomization it means that both the allocation of the experimental material and the order in which the individual runs or trials of the experiment are to be performed are randomly determined. Statistical methods require that the observation be independently distributed random variables. Randomization usually makes this assumption valid.

4.2.3 Blocking: blocking is a design technique used to improve the precision with which comparisons among the factors of interest are made. Often blocking is used to reduce or eliminate the variability transmitted from nuisance factors; that is, factors that may influence the experimental response but in which it is not directly interested.

4.3 Guidelines for Designing Experiments

To use the statistical approach in designing and analyzing an experiment, it is necessary for everyone involved in the experiment to have a clear idea in advance of exactly what is to be studied.

4.3.1 Recognition of and Statement of the Problem

It is usually helpful to prepare a list of specific problems or questions that are to be addressed by the experiment. A clear statement of the problem often contributes substantially to better understanding of the phenomenon being studied and the final solution of the problem.

4.3.2 Choice of Factors, Level, and Range

When considering the factors that may influence the performance of a process or system, the experimenter usually discovers that these factors can be classified as either potential design factors or nuisance factors. The potential design factors are those factors that experimenter may wish to vary in the experiment. Nuisance factors may have large effects that must be accounted for. Nuisance factors are often classified as controllable, uncontrollable, or noise factors. A controllable nuisance factor is one whose levels may be set by the experimenter. The blocking principal is often useful in dealing with controllable nuisance factors. If a nuisance factor is uncontrollable in the experiment, but it can be measure, an analysis procedure called the analysis of covariance can often be used to compensate for it effect. When a factor that varies naturally and uncontrollably in the process can be controlled for purposes of an experiment, it often calls a noise factor. In such situations, the objective is usually to find the settings of the controllable design factors that minimize the variability transmitted from the noise factors.

4.3.3 Selection of the Response Variable

The experimenter should be certain that this variable really provides useful information about the process under study. Most often, the average or standard deviation (or both) of the measured characteristic will be the response variable. Multiple responses are not unusual. Gauge capability (or measurement error) is also an important factor. If gauge capability is inadequate, only relatively large factor effects will be detected by the experiment or perhaps additional replication will be required.

4.3.4 Choice of Experimental Design

Choice of design involves the consideration of sample size (number of replicates), the selection of a suitable run order for the experimental trials,

and the determination of whether or not blocking or other randomization restrictions are involved.

4.3.5 Performing the Experiment

It is vital to monitor the process carefully to ensure that everything is being done according to plan. Errors in experimental procedure at this state will usually destroy experimental validity. Up-front planning is crucial to success. It is easy to underestimate the logistical and planning aspects of running a designed experiment in a complex manufacturing or research and development environment.

4.3.6 Statistical Analysis of the Data

Statistical methods should be used to analyze the data so that results and conclusions are objective rather than judgmental in nature. There are many excellent software packages designed to assist in data analysis direct interface to the statistical analysis. Because many of the questions that the experimenter wants to answer can be cast into a hypothesis-testing framework, hypothesis testing and confidence interval estimation procedures are very useful in analyzing data from a designed experiment. It is also usually very helpful to present the results of many experiments in terms of an empirical model, that is, an equation derived from the data that expresses the relationship between the response and the important design factors. Residual analysis and model adequacy checking are also important analysis techniques.

4.3.7 Conclusions and Recommendation

Once the data have been analyzed, the experimenter must draw practical conclusion about the results and recommend a course of action. Graphical methods are often useful in this stage, particularly in presenting the results to others.

Follow-up runs and confirmation testing should also be performed to validate the conclusions from the experiment.

4.4 Using Statistical Techniques in Experimentation

The proper use of statistical techniques in experimentation requires that the experimenter keep the following points in mind:

1. Use the nonstatistical knowledge of the problem. Experimenters are usually highly knowledgeable in their fields. This type of nonstatistical knowledge is invaluable in choosing factors, determining factor levels, deciding how many replicates to run, interpreting the results of the analysis, and so forth. Using statistics is no substitute for thinking about the problem.

2. Keep the design and analysis as simple as possible. Don't be overzealous in the use of complex, sophisticated statistical techniques. Relatively simple design and analysis methods are almost always best.

3. Recognize the difference between practical and statistical significance. Just because two experimental conditions produce mean responses that are statistically different, there is no assurance that this difference is large enough to have any practical value.

4. Recall that in most situations it is unwise to design too comprehensive an experiment at the start of a study. Successful design requires knowledge of the important factors, the ranges over which these factors are varied, the appropriate number of levels for each factor, and the proper methods and the units of measurement for each factor and response.

4.5 Hypothesis Testing

A statistical hypothesis is a statement either about the parameters of a probability distribution or the parameters of a model. The hypothesis reflects some conjecture about the problem situation. This may be stated formally as

$$H_0: \mu_1 = \mu_2 \quad (7)$$

$$H_i: \mu_1 \neq \mu_2 \quad (8)$$

where μ_i is the mean of the response at the i th factor level. The statement $H_0: \mu_1 = \mu_2$ is called the null hypothesis and $H_i: \mu_1 \neq \mu_2$ is called the alternative hypothesis. The alternative hypothesis specified here is called a two-side alternative hypothesis because it would be true if $\mu_1 < \mu_2$ or if $\mu_1 > \mu_2$

To test a hypothesis, they devise a procedure for taking a random sample, computing an appropriate test statistic, and then rejecting or failing to reject the null hypothesis H_0 . Part of this procedure is specifying the set of values for the test statistic that leads to rejection of H_0 . This set of values is called the critical region or rejection region for the test.

Two kinds of errors may be committed when testing hypotheses. If the null hypothesis is rejected when it is true, a type I error has occurred. If the null hypothesis is not rejected when it is false, a type II error has been made. The probabilities of these two errors are given special symbols:

$$\alpha = P(\text{type I error}) = P(\text{reject } H_0 \mid H_0 \text{ is true}) \quad (9)$$

$$\beta = P(\text{type II error}) = P(\text{fail to reject } H_0 \mid H_0 \text{ is false}) \quad (10)$$

Sometimes it is more convenient to work with the power of the test, where

$$\text{Power} = 1 - \beta = P(\text{reject } H_0 \mid H_0 \text{ is false}) \quad (11)$$

The general procedure in hypothesis testing is to specify a value of the probability of type I error α , often called the significance level of the test, and then design the test procedure so that the probability of type II error β has suitably small value.

4.6 The use of P-Values in Hypothesis Testing

One way to report the results of a hypothesis test is to state that the null hypothesis was or was not rejected at a specified α - level or level of significance. To avoid these difficulties, the P-Value approach has been adopted widely in practice. The P-value is the probability that the test statistic will take on the value that is at least as extreme as the observed value of the statistic when the null hypothesis H_0 is true. Thus, a P-value conveys much information about the weight of evidence against H_0 , and so a decision maker can draw a conclusion at any specified level of significance. More formally, they define the P-value as the smallest level of significance that would lead to rejection of the null hypothesis H_0 .

It is customary to call the test statistic (and the data) significant when the null hypothesis H_0 is rejected; therefore, we may think of the P-value as the smallest level α at which the data are significant. Once the P-value is known, the decision maker can determine how significant the data are without the data analyst formally imposing a preselected level of significance.

4.7 Type of Experimental Design

4.7.1 The Randomized Complete Block Design

In any experiment, variability arising from a nuisance factor can affect the results. Generally, they define a nuisance factor as a design factor that probably has an effect on the response, but they are not interested in that effect. Sometime the nuisance factor is unknown and uncontrolled; that is, they don't know that the factor exists and it may even be changing levels while we are conducting the

experiment. Randomization is the design technique used to guard against such a “lurking” nuisance factor. In other cases, the nuisance factor is known but uncontrollable. If they can at least observe the value that the nuisance factor takes on at each run of the experiment, they can compensate for it in the statistical analysis by using the analysis of covariance. When the nuisance source of variability is known and controllable, a design technique called blocking can be used to systematically eliminate its effect on the statistical comparisons among treatments. Blocking is an extremely important design technique, used extensively in industrial experimentation.

4.7.2 Factorial Design

Many experiments involve the study of the effects of two or more factors. In general, factorial designs are most efficient for this type of experiment. By the factorial design, it means that in each complete trial or replication of the experiment all possible combinations of the levels of the factors are investigated. For example, if there are a levels of factor A and b levels of factor B , each replicate contains all ab treatment combinations. When factors are arranged in a factorial design, they are often said to be crossed.

The effect of a factor is defined to be the change in response produced by a change in the level of the factor. This is frequently called a main effect because it refers to the primary factors of interest in the experiment. In some experiments, it may find that the difference in response between the levels of one factor is not the same at all levels of the other factors. When this occurs, there is an interaction between the factors. These ideas may be illustrated graphically. Figure 10 plots the response data against factor A for both levels of factor B . Note that the B^- and B^+ lines are approximately parallel, indicating a lack of interaction between factors A and B . Similarly, Figure 11 plots the response data that the B^- and B^+ lines are not parallel. This indicates an interaction between factors A and B . Graphs such as these are frequently very useful in interpreting significant interactions and in reporting results to nonstatistically trained personnel. However, they should not be utilized as

the sole technique of data analysis because their interpretation is subjective and their appearance is often misleading.

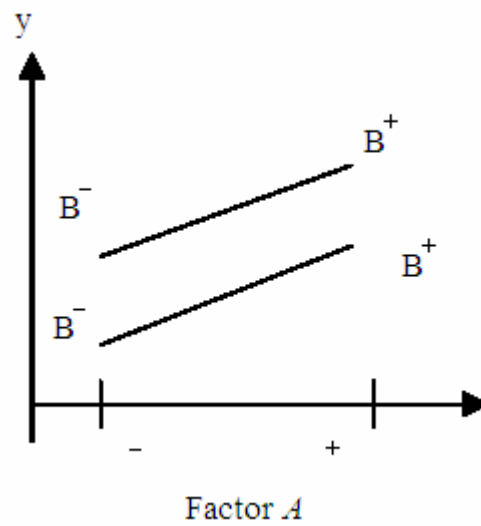


Figure 10 A factorial experiment without interaction.

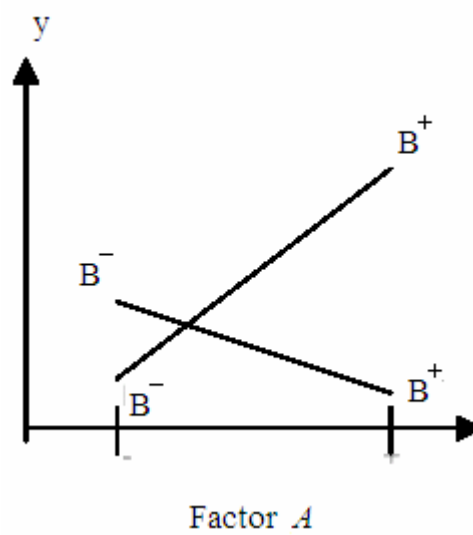


Figure 11 A factorial experiment with interaction.

4.7.3 The 2^k Factorial Design

The 2^k factorial design is a design with k factors, each at only two levels. These levels may be qualitative, such as two values of temperature, pressure or time; or may be qualitative, such as two machines, two operators, the “high” and “low” level of a factor, or perhaps the presence and absence of a factor. In the 2^k design the low and high level are denoted by “-” and “+” respectively. Thus, - represents the low level, whereas + represents the high level.

The 2^k design is particularly useful in the early stages of experimental work, when there are likely to be many factors to be investigated. It provides the smallest number of runs with which k factors can be studied in a complete factorial design. Consequently, these designs are widely used in factor screening experiments.

4.7.4 The 3^k Factorial Design

The 3^k factorial design is a factorial arrangement with k factors each at three levels. Factors and interactions will be denoted by capital letters. It will refer to the three levels of the factors as low, intermediate, and high. There are several different notations used to represent these factor levels; one possibility is to represent the factor levels by the digits 0 (low), 1 (intermediate), 2 (high). In the 3^k system of designs, when the factors are quantitative, it is often denoted the low, intermediate, and high levels by -1, 0, and +1, respectively. The 3^k design is certainly a possible choice by an experimenter who is concerned about curvature in the response function.

4.7.5 Fractional Factorial Designs

A major use of fractional factorials is in screening experiments. These are experiments in which many factors are considered and the objective is to identify those factors (if any) that have large effects. Screening experiments are usually performed in the early stages of a project when it is likely that many of the

factors initially considered have little or no effect on the response. The factors that are identified as important are then investigated more thoroughly in subsequent experiments.

4.7.6 The Other Techniques in Experimentation

4.7.6.1 Latin Square Design

4.7.6.2 Nested Design

4.7.6.3 Split – Plot Design

4.7.6.4 Response Surface Design

4.8 Analysis of Variance (ANOVA)

Suppose they have a treatments or different levels of a single factor that they wish to compare. The observed response from each of the a treatments is random variable. Models for the data, they will find it useful to describe the observations from an experiment with a model. One way to write this model is

$$y_{ij} = \mu + \tau_i + \varepsilon_{ij}, i = 1, 2, \dots, a \text{ and } j = 1, 2, \dots, n \quad (12)$$

where y_{ij} is the ij th observation, μ_i is a parameter common to all treatments called the overall mean, τ_i is a parameter unique to the i th treatment called the i th treatment effect, and ε_{ij} is a random error component that incorporates all other sources of variability in the experiment including measurement, variability arising from uncontrolled factors, differences between the experimental units such as test treatment, etc. to which the treatments are applied, and the general background noise in process (such as variability over time, effects of environmental variables, and so forth).

The statistic model describes two different situations with respect to the treatment effects. First, the a treatments could have been specifically chosen by the experimenter. In this situation, they wish to test hypotheses about the treatment means and the conclusions will apply only to the factor levels considered in the analysis. The

conclusion cannot be extended to similar treatments that it was not explicitly considered. It may also wish to estimate the model parameters. This is called the “fixed effect model”. Alternatively, the a treatments could be a random sample from a larger population of treatments. This is called the “random effects model or components of variance model”. Analysis of variance is derived from a partitioning of total variability into its component parts. The different between the observed treatment averages and the grand average is measure of the differences between treatment means, whereas the difference of observations within a treatment from the treatment average can be due only to random error. Thus it may write Equation as

$$SS_T = SS_{Treatment} + SS_E \quad (13)$$

where SS_T = total some of squares
 $SS_{Treatment}$ = sum of squares due to treatment (i.e., between treatment)
 SS_E = sum of square due to error (i.e., within treatment)

To measure variability in the data, the best estimate variable is mean square value (MS). It may also show that

$$MS = SS/DoF \quad (14)$$

where SS = sum of squares
 DoF = degree of freedom

Test statistic for the hypothesis that use to compare variable is

$$F = MS_{Tr} / MS_E \quad (15)$$

where MS_{Tr} is mean square due to treatment and MS_E is mean square due to error.

Compare test statistic for the hypothesis (F) with distributed chi-square random variables (F-test, $F_{(\alpha, v_1, v_2)}$)

$$\begin{aligned} \text{If } F &\geq F_{(\alpha, \nu_1, \nu_2)} && \text{reject } H_0 \\ \text{If } F &< F_{(\alpha, \nu_1, \nu_2)} && \text{accept } H_0 \end{aligned}$$

where α = level of significant
 ν_1 = the treatment number of degree of freedom
 ν_2 = the error number of degree of freedom

4.9 The General Factorial Design

The result for the two factor factorial design may be extended to the general case where there are a levels of factor A , b levels of factor B , c levels of factor C , and so on, arranged in a factorial experiment. In general, there will be $abc\dots n$ total observations if there are n replicates of the complete experiment. Once again, note that we must have at least two replicate to determine a sum of squares due to error if all possible interactions are include in the model. Consider the three-factor analysis of variance model:

$$y_{ijkl} = \mu + \tau_i + \beta_j + \gamma_k + (\tau\beta)_{ij} + (\tau\gamma)_{ik} + (\beta\gamma)_{jk} + (\tau\beta\gamma)_{ijk} + \varepsilon_{ijkl} \quad (16)$$

Assuming that A , B and C are fixed, the analysis of variance table is shown in Table 4. The F test on main effects and interactions follow directly from the expected mean squares.

Table 4 The analysis of variance table for the three-factor fixed model

Source of variation	Sum of Square	Degree of Freedom	Mean Square	F_0
A	SS_A	$a-1$	$SS_A/(a-1)$	MS_A/MS_E
B	SS_B	$b-1$	$SS_B/(b-1)$	MS_B/MS_E
C	SS_C	$c-1$	$SS_C/(c-1)$	MS_C/MS_E
AB	SS_{AB}	$(a-1)(b-1)$	$SS_{AB}/(a-1)(b-1)$	MS_{AB}/MS_E
AC	SS_{AC}	$(a-1)(c-1)$	$SS_{AC}/(a-1)(c-1)$	MS_{AC}/MS_E
BC	SS_{BC}	$(b-1)(c-1)$	$SS_{BC}/(b-1)(c-1)$	MS_{BC}/MS_E
ABC	SS_{ABC}	$(a-1)(b-1)(c-1)$	$SS_{ABC}/(a-1)(b-1)(c-1)$	MS_{ABC}/MS_E
Error	SS_E	$abc(n-1)$	$SS_E/abc(n-1)$	
Total	SS_T	$abcn-1$		

$$SS_T = \sum_{i=1}^a \sum_{j=1}^b \sum_{k=1}^c \sum_{l=1}^n y_{ijkl}^2 - \frac{y_{...}^2}{abcn} \quad (17)$$

$$SS_A = \frac{1}{bcn} \sum_{i=1}^a y_{i...}^2 - \frac{y_{...}^2}{abcn} \quad (18)$$

$$SS_B = \frac{1}{acn} \sum_{j=1}^b y_{.j..}^2 - \frac{y_{...}^2}{abcn} \quad (19)$$

$$SS_C = \frac{1}{abc} \sum_{k=1}^c y_{...k.}^2 - \frac{y_{...}^2}{abcn} \quad (20)$$

$$SS_{AB} = \frac{1}{cn} \sum_{i=1}^a \sum_{j=1}^b y_{ij..}^2 - \frac{y_{...}^2}{abcn} - SS_A - SS_B \quad (21)$$

$$SS_{AC} = \frac{1}{bn} \sum_{i=1}^a \sum_{k=1}^c y_{i.k.}^2 - \frac{y_{...}^2}{abcn} - SS_A - SS_C \quad (22)$$

$$SS_{BC} = \frac{1}{an} \sum_{j=1}^b \sum_{k=1}^c y_{.jk.}^2 - \frac{y_{...}^2}{abcn} - SS_B - SS_C \quad (23)$$

$$SS_{ABC} = \sum_{i=1}^a \sum_{j=1}^b \sum_{k=1}^c y_{ijkl}^2 - \frac{y_{...}^2}{abcn} - SS_A - SS_B - SS_C - SS_{AB} - SS_{AC} - SS_{BC} \quad (24)$$

$$SS_E = SS_T - SS_{ABC} \quad (25)$$

If all factors in the experiment are fixed, it may easily formulate and test hypotheses about the main effects and interactions. For a fixed effect model, test

statistics for each main effect and interactive may be constructed by dividing the corresponding mean square for the effect or interactive by the mean square error. All of these F tests will be upper-tail, one-tail tests. The number of degrees of freedom for any main effect is the number of levels of the factor minus one, and the number of degrees of freedom for and interaction is the product of the number of degrees of freedom associated with in individual components of the interaction.

4.10 Model Adequacy Checking

The decomposition of the variability in the observations through an analysis of variance identity is a purely algebraic relationship. However, the use of partitioning to test formally for no difference in treatment means requires that certain assumptions be satisfied. Examination of the residuals should be an automatic part of any analysis of variance. If the model is adequate, the residuals should be structureless; that is, they should contain no obvious patterns. Through a study of residuals, many types of model inadequacies and violations of the underlying assumptions can be discovered. The observations are adequately described by the model

$$y_{ij} = \mu + \tau_i + \varepsilon_{ij} \quad (26)$$

and that the errors are normally and independently distributed with mean zero and constant but unknown variance σ^2 . If these assumptions are valid, the analysis of variance procedure is an exact test of the hypothesis of no difference in treatment mean.

In practice, however, these assumptions will usually not hold exactly. Consequently, it is usually unwise to rely on the analysis of variance until the validity of these assumptions has been checked. Violations of the basic assumptions and model adequacy can be easily investigated by the examination of residuals. it define the residual for observation j in treatment i as

$$e_{ij} = y_{ij} - \hat{y}_{ij} \quad (27)$$

where \hat{y}_{ij} is an estimate of the corresponding observation y_{ij} obtained as follows:

$$\begin{aligned} \hat{y}_{ij} &= \hat{\mu} + \hat{\tau}_i \\ &= \bar{y}_{..} + (\bar{y}_{i.} - \bar{y}_{..}) \\ &= \bar{y}_{i.} \end{aligned} \quad (28)$$

Equation 28 gives the intuitively appealing result that the estimate of any observation in the i th treatment is just the corresponding treatment average.

4.10.1 The Normal Assumption

A check of the normality assumption could be made by plotting a histogram of the residuals. An extremely useful procedure is to construct a normal probability plot of the residuals. They used a normal probability plot of the raw data to check the assumption of normality when using t-test. In the analysis of variance, it is usually more effective (and straightforward) to do this with the residuals. If the underlying error distribution is normal, this plot will resemble a straight line.

4.10.2 Plot of Residuals in Time Sequence

Plotting the residuals in the time order of data collection is helpful in detecting correlation between the residuals. A tendency to have runs of positive and negative residuals indicates positive correlation. This would imply that the independence assumption on the errors has been violated. This is a potentially serious problem and one that is difficult to correct, so it is important to prevent the problem if possible when the data are collected. Proper randomization of the experiment is an important step to obtaining independence.

4.10.3 Plot of Residuals versus Fitted Values

If the model is corrected and if the assumptions are satisfied, the residuals should be structureless; in particular, they should be unrelated to any other variable including the predicted response. A simple check is to plot the residuals versus the fitted values \hat{y}_{ij} . This plot should not reveal any obvious pattern.

4.10.4 Plot of Residuals versus Other Variables

If data have been collected on any other variables that might possibly affect the response, the residuals should be plotted against these variable.

Previous Work

Wood machining is generally performed under very high cutting speed with very sharp cutting edges. It is a predominant abrasive process and therefore, the erosion of the cutting tool material is the main wear mechanism. Low wedge angles are necessary for machining massive wood and generally give a better surface quality; however, the lower angle generates the higher the wear (Endler, et. al., 1999). The amount of wear generally decreases with an increase of hardness, a decrease in grain size and a decrease of binder content of the cutting tool material. Several wear mechanisms may contribute to overall wear of the cutting tool. Among these wear mechanisms are gross fracture or chipping, abrasion, erosion, microfracture, chemical and electrochemical corrosion and oxidation. Corrosion can be easily removed from the cutting edge by abrasion depending on the cutting condition, e. g., moisture content, composition, etc. (Sheikh-Ahmad and Bailey, 1999). Some wear could occur through tool edge chipping when wood products with low moisture content are machined. Tool life and tool performance in a given operation improve considerably when the cemented tungsten carbides are used to replace either high carbon steel or high speed steels (Bailey, et. al, 1983).

There are many different methods to cut materials; routing process is often used to compare different material's wear on the cutting tool. There are distinct characteristics in tool wear and surface roughness among different wood fiber plastic products. Differences also exist when these materials are compared to solid wood. A better understanding of the necessary process parameters to cut these materials would lead to the improved results with respect to tool wear and surface roughness (Buehlmann, et. al, 2001). Researchers have attempted to gain more understanding in wood machining process. The relationship between the cutting process parameters such as feed rate, cutting speed and wood machining productivity was developed (Diei and Dornfeld, 1987). The effects of tool wear, cutting direction, spindle speed on edge chipping of melamine coated particle board using a CNC wood router was studied. The relationship of workpiece quality, tool wear and machining conditions was also verified with the empirical monitoring indices. (Rodkwan, 2000).

The investigation of mechanics of machining for other materials, besides metals and wood, such as elastomers were also performed (Rodkwan and Strenkowski, 2003), (Strenkowski, et. al., 2003), (Strenkowski, et. al, 2002). In their research, the effects of various machining parameters on chip morphology, surface roughness and the associated machining force were examined using the orthogonal cutting test of elastomers. The feed speed and rake angle were found to have significant effect on the type of chips generated during orthogonal cutting (Rodkwan, 2002).

Currently, parawood makes up seventy percents of raw materials used in Thai wooden furniture industry (AsiaPulse News, 2003). Nevertheless, a little research has been performed in understanding various furniture manufacturing processes such as machining, sanding using parawood. The use of Computer Numerical Control (CNC) wood router to machine parawood Laminated Veneer Lumber (LVL) and solid parawood using cemented tungsten carbide tool was carried out (Ratnasingam and Perkins, 1998). In this work, it was found that the tool wear rate and power consumption are increased as cutting continues. Parawood LVL was also discovered to be four times as abrasive as solid parawood. The fundamental understanding of parawood sanding process was revealed (Ratnasingam, et. al., 2002). It was found that sanding of parawood using silicon carbide abrasive belts was performed better than using aluminum oxide abrasive belt. The optimal cutting conditions of parawood machining using a Polycrystal Diamond (PCD) cutting tool were investigated (Prommul, et. al., 2002). In this work, spindle speed, feed speed and cutting direction are the major controlled parameters to study their effects on surface roughness and wood splinter. It was discovered that the condition which has the best surface finish and no wood splinter was occurred at the spindle speed of 15,000 rpm and feed speed of 8 m/min. The best surface quality of parawood were found when the spindle speed of 16,000 rpm and feed speed of 12 m/min were used with Tungsten Carbide (TC) cutting tool (Arlai, et. al., 2003).

MATERIALS AND METHODS

1. Materials

Parawood obtained from Chatpisan Co., Ltd. was selected as the workpiece material. Parawood and the workpiece geometry is 39.4 inch in length, 4 inch in width and 1 inch in board thickness. The mean specific gravity is 0.557. The insert geometry is 30 mm. in length, 12 mm. in width and 1.5 mm. in blade thickness. Tungsten carbide grade T10MG with 10% cobalt binder (0.5 μm) insert type was mainly used throughout experiment as cutting blades since it is one of blade types widely used in the wood routing industry. The tungsten carbide and the tool holder are shown in Figure 12 and Figure 13, respectively. An experimental series of tests were conducted to verify the machining condition in process monitoring to determine the effects of the process parameters on routing process. The description of experimental surface measurement, tool wear measurement, and images acquisition of nose width of parawood are given.

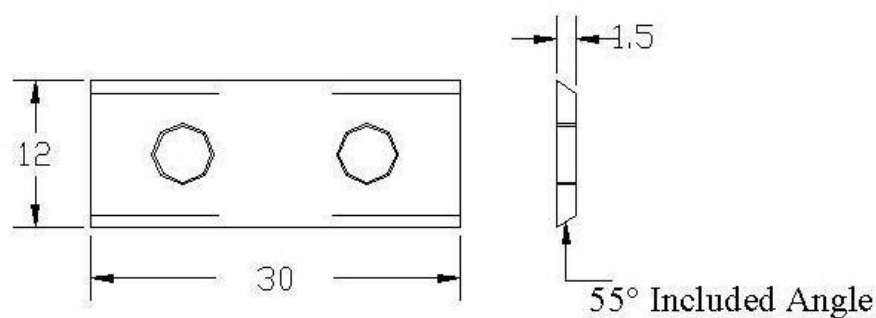


Figure 12 Schematic of the carbide cutting insert (all dimensions in mm).



Figure 13 Tool holder that used in this research.

1.1 Preliminary Experimentation

In order to obtain some preliminary results, the preliminary runs from series of test one were performed. Parawood machining was conducted using a spindle speed of 18,000 revolution per minute (rpm), a feed speed of 180 inch per minute (ipm) and depth of cut of 0.0625 inch. In this way, it was possible to adjust the feed length, width of cut for the final setting so the approximation of time used in machining process can be obtained. It is noted that the cutting rate is one hour per 500 feet length. In addition, the experiment was carried out to investigate the tool wear off-line. Tool wear for the worn insert was measured at 100 length feet until 1,000 length feet and then at 1,200, 1,800, 2,000, 2,500 length feet. Figure 14 shows the nose width of an insert at a spindle speed of 18,000 rpm, a feed speed of 180 ipm and a depth of cut of 0.0625 inch.

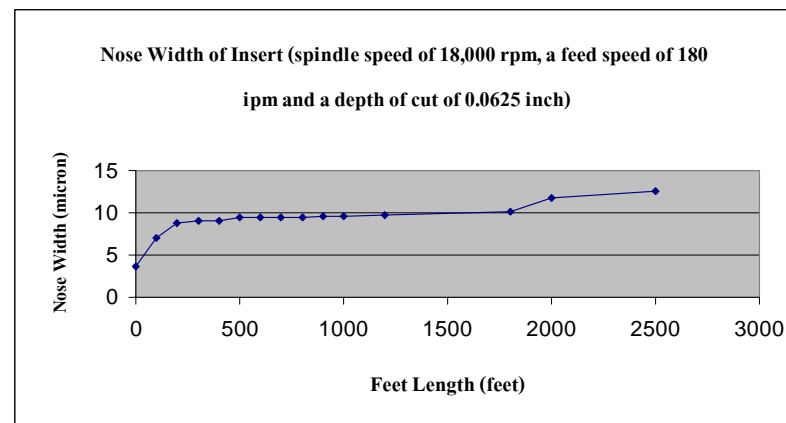


Figure 14 Nose width of insert at a spindle speed of 18,000 rpm, a feed speed of 180 ipm and a depth of cut of 0.0625 inch.

1.2 Experiment Setup on a CNC Wood Router

A Thermwood model 40 turret router and Master Wood model Winner 2.45 K were used in this research as testing machines. The Thermwood model 40 has capacity of 10 horsepower, spindle speed ranged up to 24,000 revolutions per minute (rpm), a feed speed ranged up to 3,400 inch per minute (ipm) and the machining travel

is 60 x 60 x 6 in. The Master Wood model Winner 2.45 K has spindle speed ranged up to 24,000 rpm, a feed speed ranged up to 945 ipm and the machining travel is 118 x 59 in. Workpiece was mounted rigidly on CNC machine table using specifically-designed vacuum system. Prior to cutting with the test's insert, a cut with a minimum depth of cut of 1/16 inch was done to check the corner and to remove potential contaminants of the sample. The Thermwood model 40 CNC wood router and the Master Wood model Winner 2.45 K are shown in Figure 15 and Figure 16, respectively.



Figure 15 A Thermwood model 40 Turret router.



Figure 16 Master Wood CNC wood router model Winner 2.45 K.

1.3 Experiment Setup for Tool Wear Measurement and Image Acquisition of Nose Width of Insert and Surface Roughness

Tool wear for both unused and worn insert was measured off-line using the Keyence optical microscope model VH-6100 with lighting and digital picture capturing. The nose width of insert can be obtained by setting the angular rotation of insert holding to 293 degree. The microscope model VH-6100 is depicted in Figure 17. Surface roughness was also measured off-line using profilometer, stylus-type by Mitutoyo as shown in Figure 18. The instrument is widely used and generally accepted as a fulfilled method of surface roughness measurement providing numerical value in agreement with current standards (ASME B46.1-1995). In addition, the need to calibrate apparatus using calibration block provided by the manufacturer was fulfilled. The block used for calibration had 116 micro inch ($R_a=116$) arithmetical average roughness. Calibration should be done whenever the detector is replaced or reset and it should be done when the filter setting is changed. If R_a value is correct, the measurement will also display the values for the other parameters. The Root Mean Square Roughness (R_q) in horizontal plane was used to quantify the surface roughness.



Figure 17 Keyence optical microscope model VH-6100.



Figure 18 Profilometer, stylus-type by Mitutoyo.

1.4 Experimental Parameters

Three independent parameters were used in respect to the final surface quality of the workpiece and tool wear in the process. Parameters used in the research are shown in Table 5.

Table 5 Parameter setup for tool wear and surface roughness measurement

1.Spindle Speed (rpm)	12,000, 15,000, 18,000
2.Feed Rate (ipm)	180, 360
3.Depth of Cut, DOC (inch/pass)	0.0625, 0.125
7.Number of Passes	To be determined based on wood size and DOC
8.Width of Cut (inch)	0.75
9. Tool Geometry (Included Angle)	55 degrees
10.Length of Cut (inch)	34
11.Number of Tests	3

The spindle speed, feed rate and depth of cut were varied with various parameters such as a direction (conventional cutting), an insert type T10MG, a width of cut 0.75 inch, a tool geometry (an included angle of 55 degree).

2. Methods

The overall design of the experiment includes preparation of wood sample, calibration of measuring equipment, statistical design of results analysis. A Thermwood model 40 Turret router and Master Wood model Winner 2.45 K were used in the research as testing machines. The steps for determination the tool wear and surface quality investigation are described as follows:

1. Identify the workpiece and measure the nose width of all inserts.
2. Clamp the wood sample for the test on the CNC wood router table and set up spindle speed, feed speed and depth of cut following the experimental design as shown in Table 6, then place the blade into the blade-holder for the first cut and next run for one pass to clean up the edge of workpiece, and then stop the router.
3. Replace the blade and place test's insert into the blade-holder.
4. Run the test for 1,000 linear feet and measure the nose width of each insert and take the pictures using microscope. Next, calculate arithmetic for the nose width.
5. Repeat step (2) to step (4) again for the insert in 1,000 increments linear feet, stopping at 2,000, 3,000 linear feet to measure nose width, take photograph and measure surface roughness of workpiece after 3,000 linear feet of machining.
6. After three replications, calculate the average of surface roughness of workpiece and nose width of test blades.

Table 6 Experiment design

Spindle Speed (rpm)	Feed speed (ipm)	Depth of cut (inch)	Name's code	Cutting Distance (feet)		
12,000	180	0.0625	PW1	1000	2000	3000
				1000	2000	3000
	360	0.1250	PW2	1000	2000	3000
				1000	2000	3000
		0.0625	PW3	1000	2000	3000
				1000	2000	3000
18,000	180	0.0625	PW5	1000	2000	3000
				1000	2000	3000
	360	0.1250	PW6	1000	2000	3000
				1000	2000	3000
		0.0625	PW7	1000	2000	3000
				1000	2000	3000
15,000	180	0.0625	PW9	1000	2000	3000
				1000	2000	3000
	360	0.1250	PW10	1000	2000	3000
				1000	2000	3000
		0.0625	PW11	1000	2000	3000
				1000	2000	3000
				1000	2000	3000
				1000	2000	3000

Consequently, the relationship among cutting distance, surface roughness, and nose width with various machining conditions was found by using a statistical program (Minitab14[®]). The machining conditions are listed in Table 7

Table 7 Machining conditions in this test

Machining conditions	Level
Tool type	T10MG
Spindle speed (rpm)	12,000, 15,000, 18,000
Feed speed (ipm)	180, 360
Depth of cut (inch)	0.0625, 0.125

3. Locations

1. Wood Machining & Tooling Research Program (WMTRP), College of Natural Science, North Carolina State University, Raleigh, NC, USA.
2. Research and Development Institute of Industrial Production Technology (RDipt), Faculty of Engineering, Kasetsart University, Bangkok, Thailand.
3. Department of Tool and Materials, King Mongkut's University of Technology, Thonburi, Bangkok, Thailand.
4. Department of Materials Engineering, Faculty of Engineering, Kasetsart University, Bangkok, Thailand.

4. A period of time for the research

The research project started in October, 2003 and completed in September, 2005.

RESULTS AND DISCUSSIONS

In this section, the data generated from 36 experimental sets are presented. The specific code for each parameter is shown in Table 8. Also, the machining conditions of parawood are denoted from PW1 to PW12 for ease of representation.

Table 8 Code settings for experimental factors.

Spindle Speed (rpm.)	Code	Feed Speed (ipm.)	Code	Depth of Cut (in.)	Code
12,000	-1	180	+	0.0625	+
15,000	0	360	-	0.1250	-
18,000	1				

The results from all cutting conditions described in Table 6 are shown in Table 9. In this study, blade wear was obtained by measuring Nose Width (NW) along various locations on the cutting edge. Figures 19-30 display the cutting edge with various cutting distances on the blade; 1,000, 2,000 and 3,000 feet. Figure 31 shows the relationship between tool wear and cutting distance of the insert for different cutting conditions. Nose width was measured using an image analysis software, Image J[®]. For this technique, it is assumed that the blade is homogeneous and the applied force is constant along the cutting edge.

Table 9 Results from the machining tests.

PW*	Variables			Nose Width (μin)				Roughness** (μin)	Machining Time*** (hr:min)
	Spindle Speed (rpm)	Feed Speed (ipm)	Depth of Cut (in)	Cutting Distance (feet)					
				0	1,000	2,000	3,000		
1	12,000	180	0.0625	114.75	230.49	301.13	359.86	111.25	4:47
2	12,000	180	0.1250	132.54	215.58	278.75	306.83	142.29	4:56
3	12,000	360	0.0625	128.58	222.59	336.64	399.22	175.78	2:55
4	12,000	360	0.1250	142.57	242.34	280.75	344.97	142.30	2:56
5	18,000	180	0.0625	116.34	269.06	365.78	441.70	132.04	4:30
6	18,000	180	0.1250	140.83	225.41	271.97	341.14	207.70	4:24
7	18,000	360	0.0625	119.40	256.83	300.95	359.61	119.00	2:40
8	18,000	360	0.1250	145.22	224.80	258.40	296.98	171.76	2:40
9	15,000	180	0.0625	125.53	201.35	237.06	276.30	149.54	4:27
10	15,000	180	0.1250	137.32	201.68	278.78	322.63	125.34	4:28
11	15,000	360	0.0625	93.62	168.89	237.69	296.65	132.56	2:43
12	15,000	360	0.1250	121.59	183.48	243.56	315.20	189.04	2:44

* Code number

** Surface roughness of parawood material at cutting distance of 3,000 feet

*** Machining time after running the machine for a cutting distance of 3,000 feet

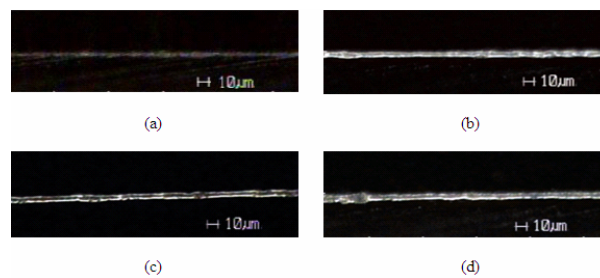


Figure 19 Nose width of an insert used at a spindle speed of 12,000 rpm, a feed speed of 180 ipm and a depth of cut of 0.0625 inch; a) nose width of new insert, b) nose width of insert at 1,000 linear feet, c) nose width of insert at 2,000 linear feet and d) nose width of insert at 3,000 linear feet.

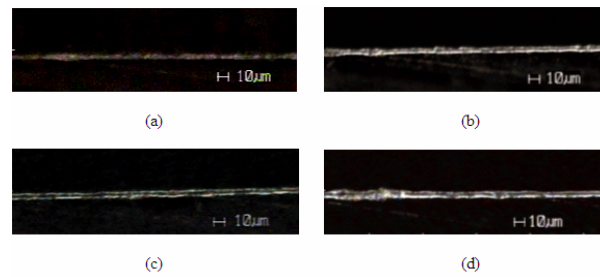


Figure 20 Nose width of an insert used at a spindle speed of 12,000 rpm, a feed speed of 180 ipm and a depth of cut of 0.1250 inch; a) nose width of new insert, b) nose width of insert at 1,000 linear feet, c) nose width of insert at 2,000 linear feet and d) nose width of insert at 3,000 linear feet.

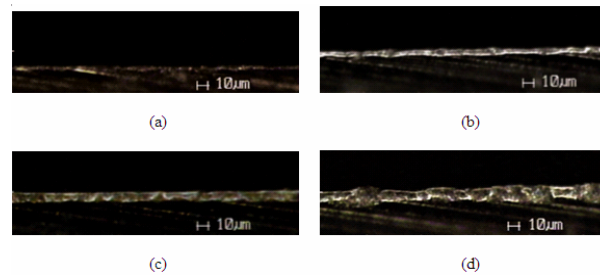


Figure 21 Nose width of an insert used at a spindle speed of 12,000 rpm, a feed speed of 360 ipm and a depth of cut of 0.0625 inch; a) nose width of new insert, b) nose width of insert at 1,000 linear feet, c) nose width of insert at 2,000 linear feet and d) nose width of insert at 3,000 linear feet.

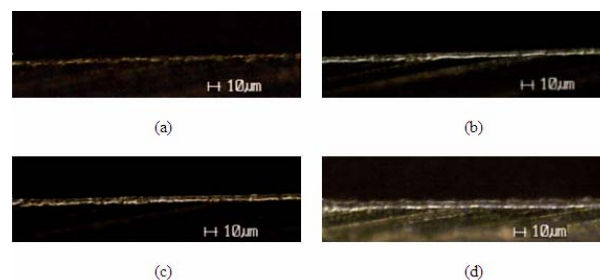


Figure 22 Nose width of an insert used at a spindle speed of 12,000 rpm, a feed speed of 360 ipm and a depth of cut of 0.1250 inch; a) nose width of new insert, b) nose width of insert at 1,000 linear feet, c) nose width of insert at 2,000 linear feet and d) nose width of insert at 3,000 linear feet.

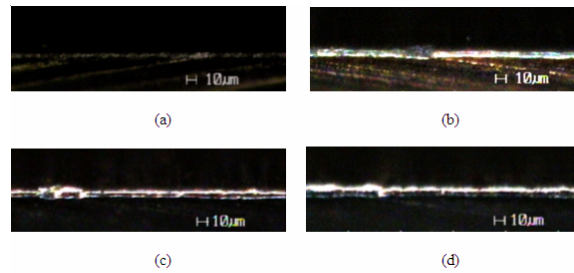


Figure 23 Nose width of an insert used at a spindle speed of 18,000 rpm, a feed speed of 180 ipm and a depth of cut of 0.0625 inch; a) nose width of new insert, b) nose width of insert at 1,000 linear feet, c) nose width of insert at 2,000 linear feet and d) nose width of insert at 3,000 linear feet.

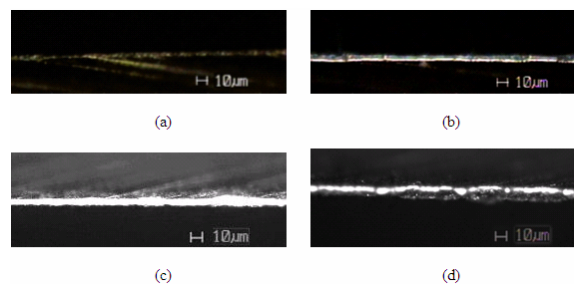


Figure 24 Nose width of an insert used at a spindle speed of 18,000 rpm, a feed speed of 180 ipm and a depth of cut of 0.1250 inch; a) nose width of new insert, b) nose width of insert at 1,000 linear feet, c) nose width of insert at 2,000 linear feet and d) nose width of insert at 2,500 linear feet.

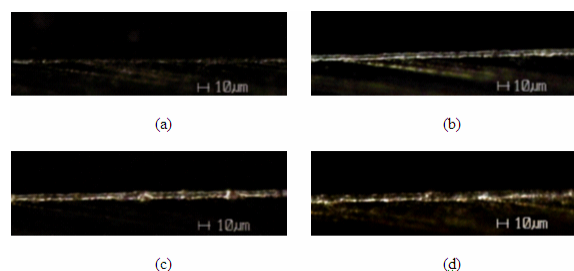


Figure 25 Nose width of an insert used at a spindle speed of 18,000 rpm, a feed speed of 360 ipm and a depth of cut of 0.0625 inch; a) nose width of new insert, b) nose width of insert at 1,000 linear feet, c) nose width of insert at 2,000 linear feet and d) nose width of insert at 3,000 linear feet.

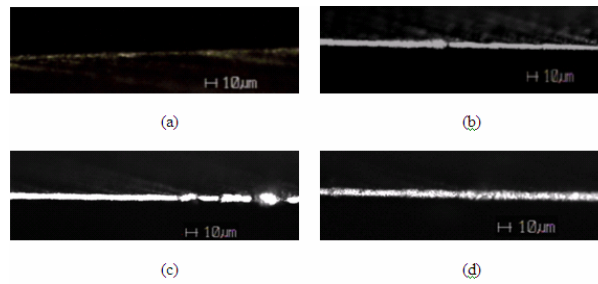


Figure 26 Nose width of an insert used at a spindle speed of 18,000 rpm, a feed speed of 360 ipm and a depth of cut of 0.1250 inch; a) nose width of new insert, b) nose width of insert at 1,000 linear feet, c) nose width of insert at 2,000 linear feet and d) nose width of insert at 3,000 linear feet.

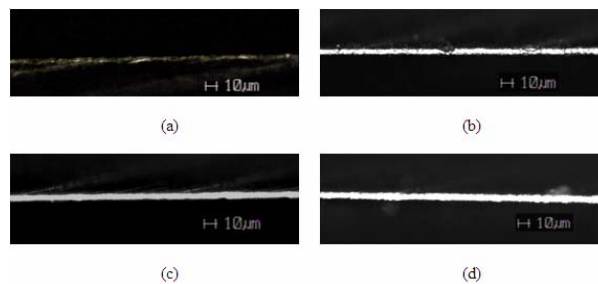


Figure 27 Nose width of an insert used at a spindle speed of 15,000 rpm, a feed speed of 180 ipm and a depth of cut of 0.0625 inch; a) nose width of new insert, b) nose width of insert at 1,000 linear feet, c) nose width of insert at 2,000 linear feet and d) nose width of insert at 3,000 linear feet.

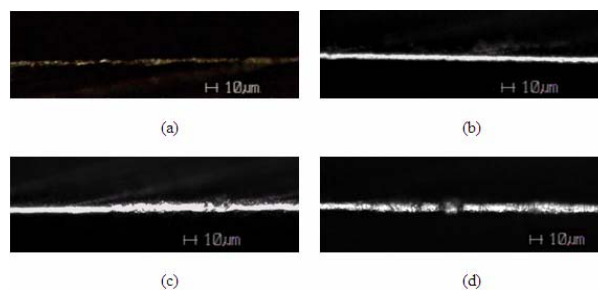


Figure 28 Nose width of an insert used at a spindle speed of 15,000 rpm, a feed speed of 180 ipm and a depth of cut of 0.1250 inch; a) nose width of new insert, b) nose width of insert at 1,000 linear feet, c) nose width of insert at 2,000 linear feet and d) nose width of insert at 3,000 linear feet.

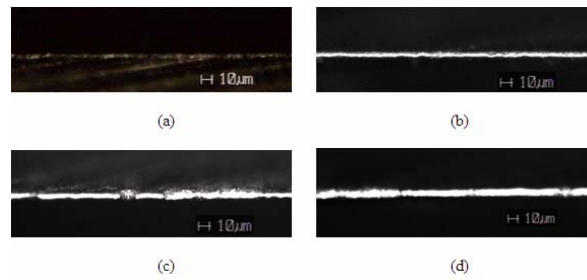


Figure 29 Nose width of an insert used at a spindle speed of 15,000 rpm, a feed speed of 360 ipm and a depth of cut of 0.0625 inch; a) nose width of new insert, b) nose width of insert at 1,000 linear feet, c) nose width of insert at 2,000 linear feet and d) nose width of insert at 3,000 linear feet.

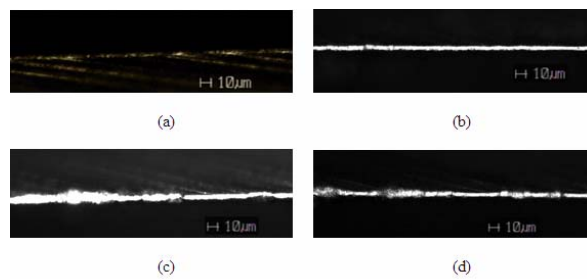


Figure 30 Nose width of an insert used at a spindle speed of 15,000 rpm, a feed speed of 360 ipm and a depth of cut of 0.1250 inch; a) nose width of new insert, b) nose width of insert at 1,000 linear feet, c) nose width of insert at 2,000 linear feet and d) nose width of insert at 3,000 linear feet.

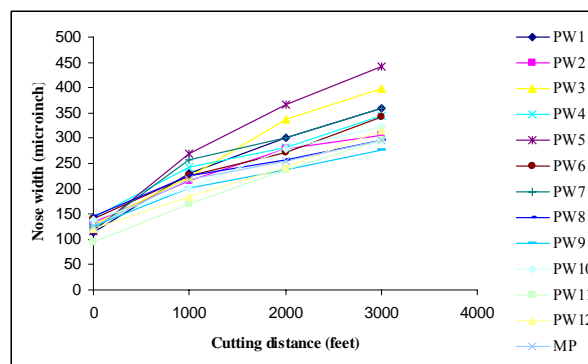


Figure 31 The relationship between nose width of all inserts that used to machine parawood and cutting distance.

The factorial design 2^3 was used to determine the fundamental machining parameters. In general, factorial design 2^3 has three factors; A, B and C, each at two levels is of interest. This design is particularly useful in the early stages of experimental procedure, where several parameters are investigated. In addition, the general factorial design was used to obtain the optimal solution in parawood machining process. Subsequently, all data in Table 9 was analyzed with statistical software, Minitab®, to obtain the optimal condition of parawood machining process. The input parameters are spindle speeds at 12,000, 15,000 and 18,000 rpm, feed speeds at 180, 360 ipm and depths of cut at 0.0625 and 0.1250 in and the output parameters are surface quality and nose width. The testing hypothesis about the equality of treatment effects was shown in Equation 29.

$$H_0: \tau_1 = \tau_2 = \dots = \tau_a$$

$$H_1: \text{at least one } \tau_i \neq \tau_j \text{ for all } i, j \text{ that } i \neq j \quad (29)$$

In this research, it is assumed that 1) the factors are fixed 2) the design is completely randomized and 3) the usual normality assumption is satisfied. The data from the experiment with an analysis with Minitab release 14® are shown in Table 10 and Table 11 for nose width and surface roughness, respectively.

Table 10 Nose width of cutting edge.

No.	Variables				Nose Width (μin)		
	Spindle Speed (rpm)	Feed Speed (ipm)	Depth of Cut (in)	Cutting Distance (feet)	Block 1	Block 2	Block 3
1	12,000	180	0.0625	0	113.02	115.62	115.62
2	12,000	180	0.0625	1,000	229.17	230.49	231.81
3	12,000	180	0.0625	2,000	293.67	313.41	296.30
4	12,000	180	0.0625	3,000	354.21	366.06	359.32
5	12,000	180	0.1250	0	137.74	126.03	133.84
6	12,000	180	0.1250	1,000	214.70	213.38	218.65
7	12,000	180	0.1250	2,000	279.19	275.24	281.82
8	12,000	180	0.1250	3,000	305.51	300.25	314.73
9	12,000	360	0.0625	0	125.91	128.61	131.23
10	12,000	360	0.0625	1,000	217.33	222.59	222.59
11	12,000	360	0.0625	2,000	276.56	375.20	358.16

Table 10 Continued.

No.	Variables				Nose Width (μ in)		
	Spindle Speed (rpm)	Feed Speed (ipm)	Depth of Cut (in)	Cutting Distance (feet)	Block 1	Block 2	Block 3
12	12,000	360	0.0625	3,000	390.99	398.81	407.87
13	12,000	360	0.1250	0	146.95	144.31	136.46
14	12,000	360	0.1250	1,000	226.54	256.82	242.34
15	12,000	360	0.1250	2,000	269.98	287.09	285.95
16	12,000	360	0.1250	3,000	334.39	376.59	323.94
17	15,000	180	0.0625	0	133.80	120.72	122.06
18	15,000	180	0.0625	1,000	201.96	203.83	198.26
19	15,000	180	0.0625	2,000	241.63	238.01	231.53
20	15,000	180	0.0625	3,000	277.84	278.75	272.31
21	15,000	180	0.1250	0	135.14	135.14	141.69
22	15,000	180	0.1250	1,000	208.40	201.08	201.68
23	15,000	180	0.1250	2,000	280.54	283.36	272.43
24	15,000	180	0.1250	3,000	313.97	339.01	314.92
25	15,000	360	0.0625	0	89.38	102.09	89.38
26	15,000	360	0.0625	1,000	159.27	164.91	182.48
27	15,000	360	0.0625	2,000	238.01	237.09	237.97
28	15,000	360	0.0625	3,000	300.89	301.96	287.10
29	15,000	360	0.1250	0	139.06	112.86	112.84
30	15,000	360	0.1250	1,000	170.56	177.00	202.87
31	15,000	360	0.1250	2,000	236.10	241.79	252.80
32	15,000	360	0.1250	3,000	308.48	328.71	308.40
33	18,000	180	0.0625	0	128.57	110.23	110.23
34	18,000	180	0.0625	1,000	261.20	273.00	272.98
35	18,000	180	0.0625	2,000	370.15	358.26	368.94
36	18,000	180	0.0625	3,000	448.26	428.42	448.42
37	18,000	180	0.1250	0	148.27	131.21	143.01
38	18,000	180	0.1250	1,000	202.34	237.00	231.43
39	18,000	180	0.1250	2,000	252.90	286.10	276.92
40	18,000	180	0.1250	3,000	377.01	325.97	320.45
41	18,000	360	0.0625	0	123.33	120.72	114.16
42	18,000	360	0.0625	1,000	269.14	251.99	249.35
43	18,000	360	0.0625	2,000	308.38	288.71	305.77
44	18,000	360	0.0625	3,000	360.89	359.64	358.30
45	18,000	360	0.1250	0	164.01	137.78	133.86
46	18,000	360	0.1250	1,000	214.04	226.88	233.48
47	18,000	360	0.1250	2,000	249.14	244.49	281.57
48	18,000	360	0.1250	3,000	287.97	302.88	300.09

Table 11 Surface roughness of parawood material at 3,000 linear feet.

PW	Variables			Roughness (μin)		
	Spindle Speed (rpm)	Feed speed (ipm)	Depth of cut (in)	Block 1	Block 2	Block 3
1	12,000	180	0.0625	108.11	121.98	103.67
2	12,000	180	0.1250	126.33	141.33	156.22
3	12,000	360	0.0625	205.89	171.00	150.44
4	12,000	360	0.1250	128.56	149.11	149.22
5	18,000	180	0.0625	137.56	123.15	135.41
6	18,000	180	0.1250	164.57	356.77	101.76
7	18,000	360	0.0625	127.22	117.78	112.11
8	18,000	360	0.1250	131.07	132.62	171.76
9	15,000	180	0.0625	146.36	151.49	150.78
10	15,000	180	0.1250	131.62	122.22	122.19
11	15,000	360	0.0625	137.61	135.67	124.40
12	15,000	360	0.1250	117.26	172.54	217.32

Determination of the Fundamental Machining Parameters

The ranges of machining parameters studied in this step are spindle speeds of 12,000, and 18,000 rpm.; feed speeds of 180 and 360 ipm.; and depths of cut of 0.0625 and 0.1250 in. In this work, null hypotheses are rejected when 90% confident interval is found. An analysis of variance table of nose width is shown in Table 12.

Table 12 Analysis of variance of nose width at the first step with 90% confident interval.

Source	DF	SS	MS	F	P
Blocks	2	326	163	0.67	0.516
Spindle speed (rpm)	1	718	718	2.94	0.092
Feed speed (ipm)	1	297	297	1.22	0.274
Depth of cut (in)	1	21735	21735	88.94	0.000
Cutting distance (ft)	3	681688	227229	929.82	0.000
Spindle speed*Feed speed	1	13079	13079	53.52	0.000
Spindle speed*Depth of cut	1	3220	3220	13.18	0.001
Spindle speed*Cutting distance	3	1096	365	1.49	0.225
Feed speed*Depth of cut	1	833	833	3.41	0.070
Feed speed*Cutting distance	3	1478	493	2.02	0.121
Depth of cut* Cutting distance	3	27091	9030	36.95	0.000
Spindle speed* Feed speed*Depth of cut	1	943	943	3.86	0.054

Table 12 Continued.

Source	DF	SS	MS	F	P
Spindle speed*Feed speed*Cutting distance	3	8092	2697	11.04	0.000
Spindle speed*Depth of cut*Cutting distance	3	1815	605	2.48	0.070
Feed speed*Depth of cut* Cutting distance	3	687	229	0.94	0.428
Spindle speed*Feed speed*Depth of cut * Cutting distance	3	2484	828	3.39	0.023
Error	62	15152	244		
Total	95	780735			

$$S = 15.6327 \quad R\text{-Sq} = 98.06\% \quad R\text{-Sq (adj)} = 97.03\%$$

The result of analysis of variance considering P-Value shows that spindle speed, depth of cut, cutting distance, interaction between spindle speed and feed speed, interaction between spindle speed and depth of cut, interaction between feed speed and depth of cut, interaction between depth of cut and cutting distance, interaction between spindle speed, feed speed and depth of cut, interaction between spindle speed, feed speed and cutting distance, interaction between spindle speed, depth of cut and cutting distance and interaction between spindle speed, feed speed, depth of cut and cutting distance have P-Value less than 0.10. As a result, the main effect and the interaction above significantly affect the nose width at the first step.

The residual plots for nose width at the first step are shown in Figure 32. Normal probability plot of residual resembles as a straight line. It shows that the underlying error distribution is normal. The model of plot of residuals and the fitted values is correct because it does not correlate well as expected, the assumptions are satisfied and the residuals are structureless.

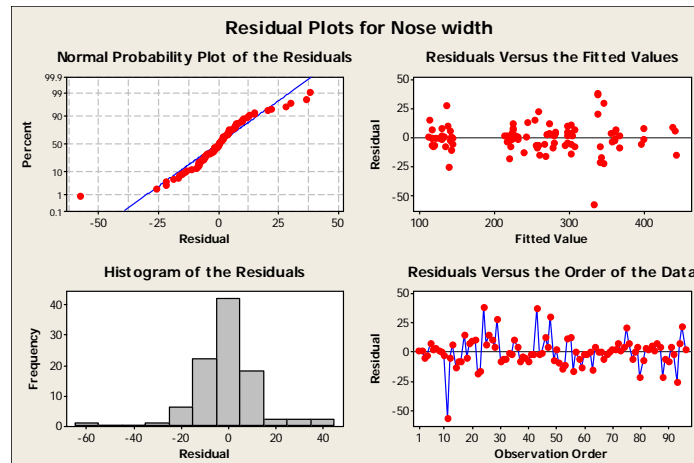


Figure 32 Residual plots for nose width at the first step.

The residual versus spindle speed is shown in Figure 33. The plot reveals that there are much less scatter in the residual at spindle speed of 18,000 rpm than at the spindle speed of 12,000 ipm. Figure 34 plots the residual versus feed speed. The graph shows that there are much less scatter in the residual at feed speed of 180 ipm than at the feed speed of 360 ipm. and Figure 35 displays the residual versus depth of cut. The plot indicates that there are much less scatter in the residual at depth of cut of 0.1250 in. than at the depth of cut of 0.0625 in. In addition, residual versus cutting distance is shown in Figure 36.

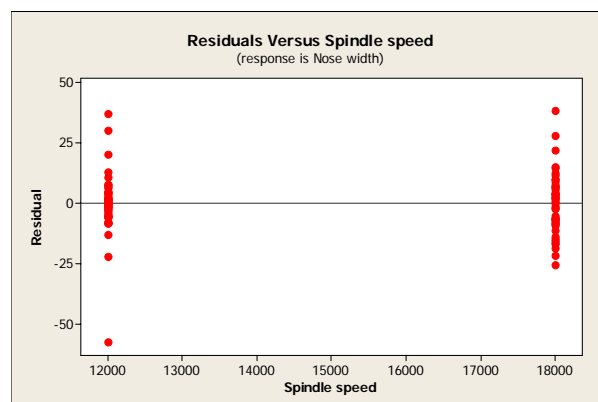


Figure 33 Plot of residuals versus spindle speed (rpm).

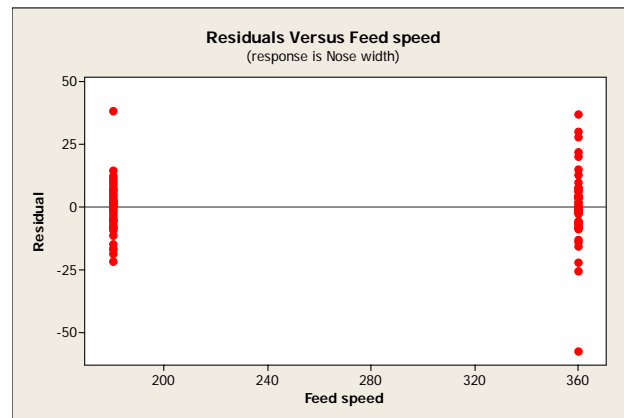


Figure 34 Plot of residual versus feed speed (ipm).

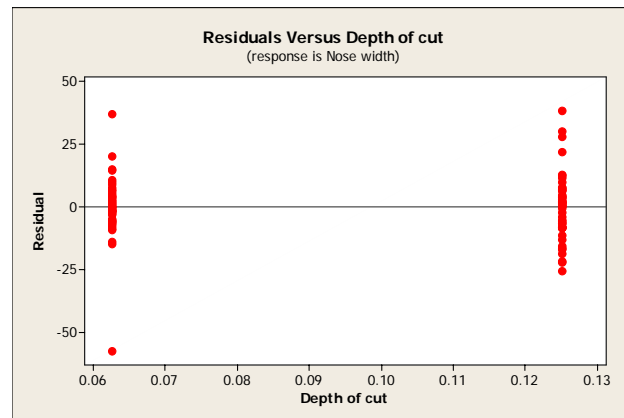


Figure 35 Plot of residual versus depth of cut (in).

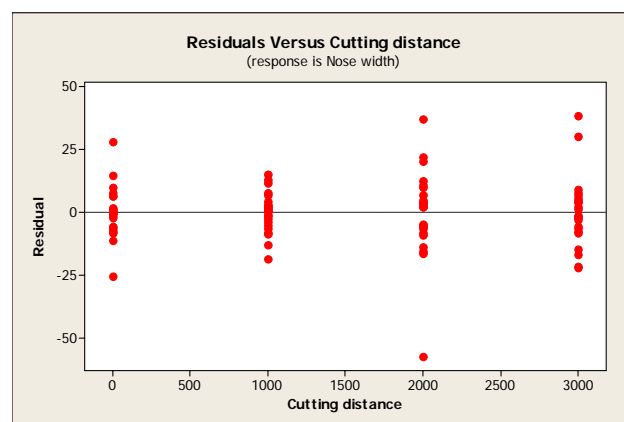


Figure 36 Plot of residual versus cutting distance (feet).

The main effect of spindle speed, depth of cut and cutting distance are plotted in Figure 37. The spindle speed effect reveals a few inequality of nose width, with the treatment combination of 18,000 rpm. possibly having larger nose width than 12,000 rpm., depth of cut effect indicates of nose width, with the treatment combination at depth of cut of 0.0625 in. possibly having larger nose width than a depth of cut of 0.125 in., and if the main effect is considered, two factors at spindle speed of 12,000 rpm, and depth of cut of 0.1250 in. are needed to include to minimize the nose width from the blade test. However, any important interactions are necessary to be examined because the main effects do not have much meaning when the interaction significantly affects.

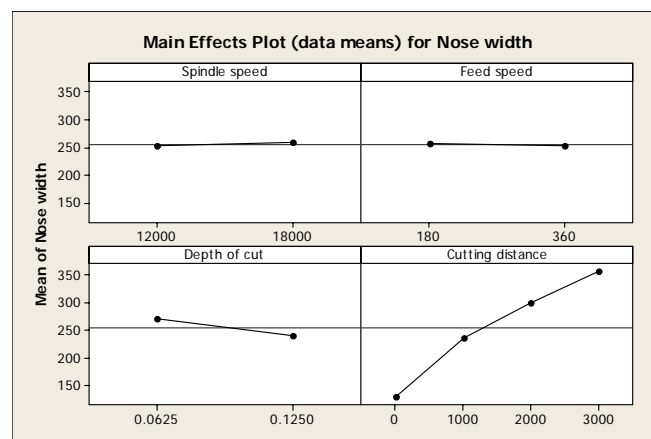


Figure 37 Main effects plot (data means) for nose width.

The spindle speed – feed speed interaction, the spindle speed – depth of cut interaction, the feed speed – depth of cut interaction, the depth of cut – cutting distance interaction, the spindle speed - feed speed – depth of cut interaction, the spindle speed - feed speed – cutting distance interaction, the spindle speed – depth of cut – cutting distance interaction, and the spindle speed – feed speed – depth of cut – cutting distance are plotted in Figures 38 - 45. The spindle speed - feed speed interaction shows that the spindle speed effect is small when feed speed is at the 360 ipm. and it is large when the feed speed is at the 180 ipm., as a result, it is possible to have smaller nose width at the spindle speed of 12,000 rpm and the feed speed of 180 ipm. The spindle speed – depth of cut interaction presents that the smaller nose width

would appear when a spindle speed at 18,000 rpm. and a depth of cut at 0.125 in. The depth of cut - linear feet interaction indicates that depth of cut has smaller effect at 0.125 in. As a result, the smaller nose width is obtained when a spindle speed is 12,000 rpm, a feed speed is 180 ipm. and a depth of cut is 0.125 in.

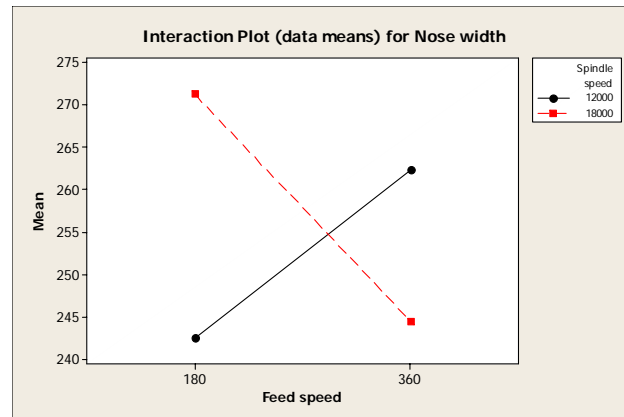


Figure 38 The interaction plot between spindle speed and feed speed.

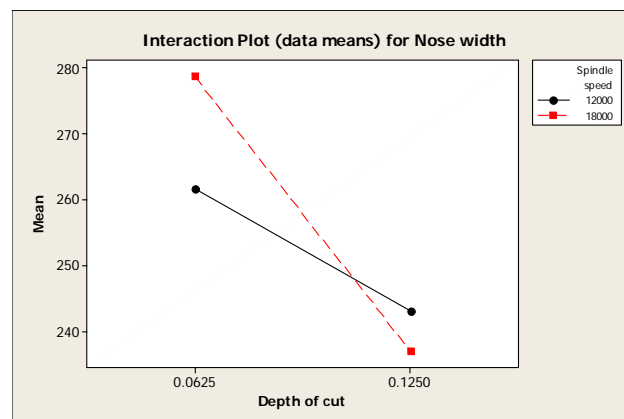


Figure 39 The interaction plot between spindle speed and depth of cut.

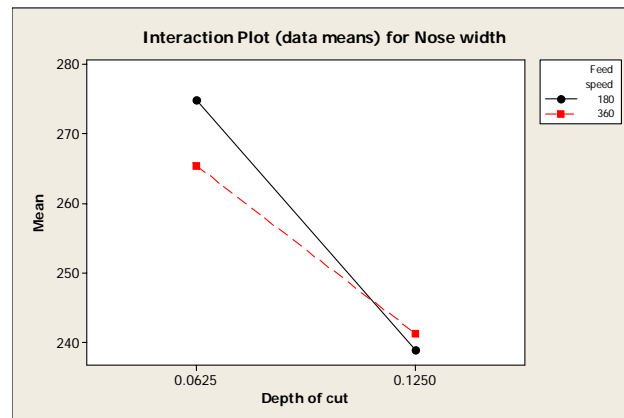


Figure 40 The interaction plot between feed speed and depth of cut.

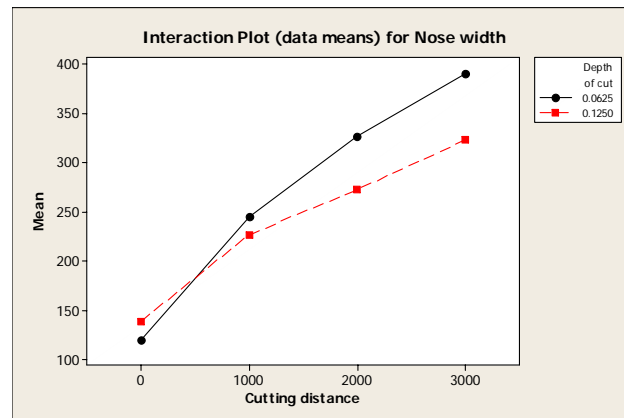


Figure 41 The interaction plot between depth of cut and cutting distance.

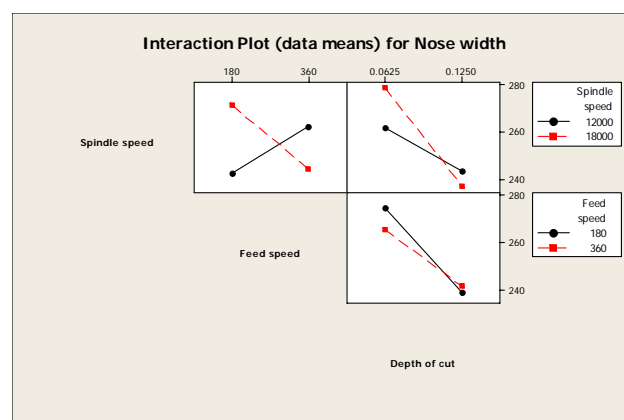


Figure 42 The interaction plot between spindle speed, feed speed and depth of cut.

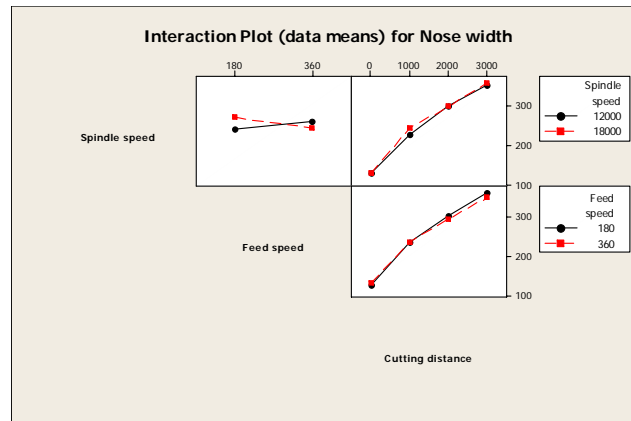


Figure 43 The interaction plot between spindle speed, feed speed and cutting distance.

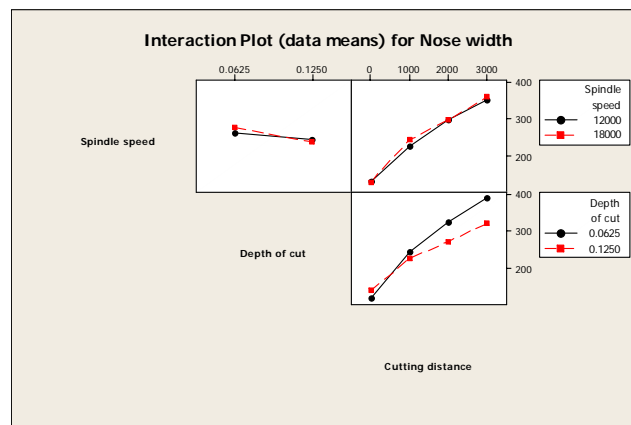


Figure 44 The spindle speed - depth of cut - cutting distance interaction.

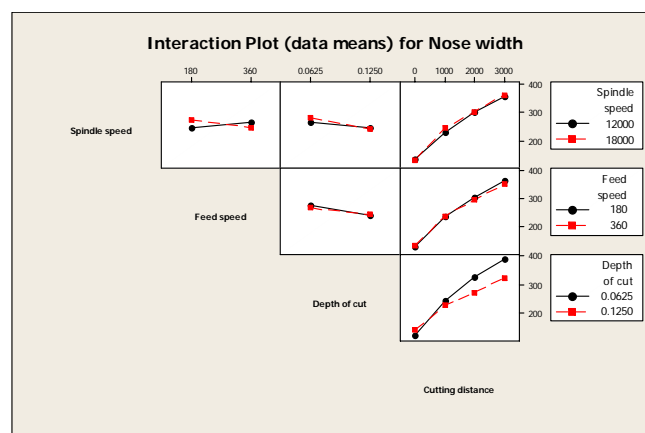


Figure 45 The spindle speed -feed speed-depth of cut and cutting distance interaction.

As a result, the regression model is obtained for process optimization of parawood machining at the first stage as shown in Equation 30;

$$\begin{aligned} \text{Nose Width } (\mu\text{inch}) = & -283 + 0.0278 \text{ rpm} + 1.05 \text{ ipm} + 2550 \text{ DoC} \\ & + 0.132 \text{ LF} - 0.000073 \text{ rpm} \times \text{ipm} - 0.173 \text{ rpm} \times \text{DoC} - \\ & 4.52 \text{ ipm} \times \text{DoC} - 0.589 \text{ DoC} \times \text{LF} + 0.000367 \text{ rpm} \times \\ & \text{ipm} \times \text{DoC} + 0.000007 \text{ rpm} \times \text{DoC} \times \text{LF} \end{aligned} \quad (30)$$

where rpm = spindle speed (revolution per minute)
 ipm = feed speed (inch per minute)
 DoC = depth of cut (inch)
 LF = cutting distance (feet)

For the case of surface roughness of parawood at a cutting distance of 3000 feet, an analysis of variance for surface roughness table is shown in Table 13.

Table 13 Analysis of variance for surface roughness of parawood material with 90% confident interval.

Source	DF	SS	MS	F	P
Blocks	2	3781	1891	0.75	0.491
Spindle speed (rpm)	1	416	416	0.16	0.691
Feed speed (ipm)	1	38	38	0.01	0.904
Depth of cut (in)	1	3626	3626	1.44	0.250
Spindle speed*Feed speed	1	7464	7464	2.96	0.107
Spindle speed*Depth of cut	1	4151	4151	1.65	0.220
Feed speed*Depth of cut	1	4794	4794	1.90	0.190
Spindle speed*Feed speed*Depth of cut	1	73	73	0.03	0.867
Error	14	35309	2522		
Total	23	59652			

S = 50.2200 R-Sq = 40.81% R-Sq (adj) = 2.76%

The result of analysis of variance considering P-Value shows that all of the main effect and interaction have P-Value more than 0.10. As a result, the main effect

and the interaction do not significantly affect the surface roughness of parawood material at a cutting distance of 3000 feet.

The normal probability plot of residual is shown in Figure 46. This plot could resemble a straight line. It shows that the underlying error distribution is normal. The model of plot of residuals versus the fitted values is incorreced because it is correlated well, the assumptions are unsatisfied and the residuals are structure.

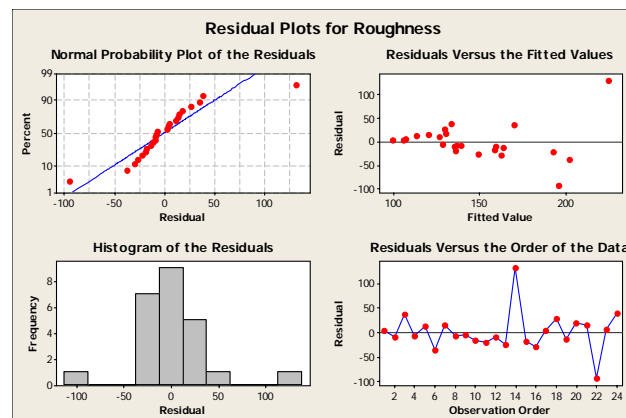


Figure 46 Residual plots for surface roughness at 3,000 linear feet.

To continue an analysis of surface roughness, Box-Cox technique used to transform the data. The Box-Cox plot of surface roughness, an analysis of variance table of transform data and the normal probability plot of the residual of transform data are presented in Figure 47, Table 14 and Figure 48, respectively.

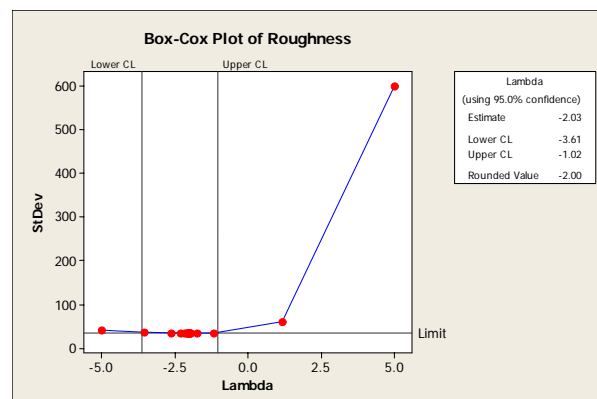


Figure 47 Box-Cox plot of surface roughness at step 1.

Table 14 Analysis of Variance for transform with 90% confident interval.

Source	DF	SS	MS	F	P
Blocks	2	0.0000000	0.0000000	0.66	0.533
Spindle speed (rpm)	1	0.0000000	0.0000000	0.07	0.793
Feed speed (ipm)	1	0.0000000	0.0000000	1.11	0.310
Depth of cut (in)	1	0.0000000	0.0000000	2.20	0.160
Spindle speed*Feed speed	1	0.0000000	0.0000000	4.26	0.058
Spindle speed*Depth of cut	1	0.0000000	0.0000000	0.31	0.585
Feed speed*Depth of cut	1	0.0000000	0.0000000	1.31	0.272
Spindle speed*Feed speed*Depth of cut	1	0.0000000	0.0000000	3.36	0.088
Error	14	0.0000000	0.0000000		
Total	23	0.0000000			

S = 0.0000192717 R-Sq = 49.90% R-Sq (adj) = 17.69%

The result of analysis of variance considering P-Value shows that the interaction between spindle speed and feed speed and the interaction between spindle speed, feed speed and depth of cut have P-Value less than 0.10. As a result, spindle speed – feed speed interaction and the spindle speed – feed speed – depth of cut significantly affect the surface roughness of parawood material significantly affect the surface roughness of parawood material at a cutting distance of 3000 feet.

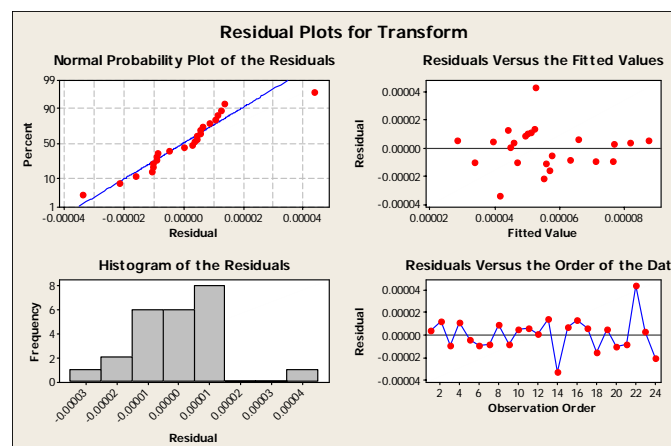


Figure 48 Normal probability plot of the residual of transform data.

In Figure 48, normal probability plot of residual resembles as a straight line. It shows that the underlying error distribution is normal. The model of plot of residuals and the fitted values is correct because it does not correlate well as expected, the assumptions are satisfied and the residuals are structureless. The residual versus spindle speed is shown in Figure 49. The plot reveals that there are much less scatter in the residual at spindle speed of 12,000 rpm than at the spindle speed of 18,000 ipm. Figure 50 displays the residual versus feed speed. The graph indicates that there are much less scatter in the residual at feed speed of 360 ipm than at the feed speed of 180 in. and Figure 51 plots the residual versus depth of cut. The plot depicts that there are much less scatter in the residual at a depth of cut of 0.0625 in than at a depth of cut of 0.1250 in.

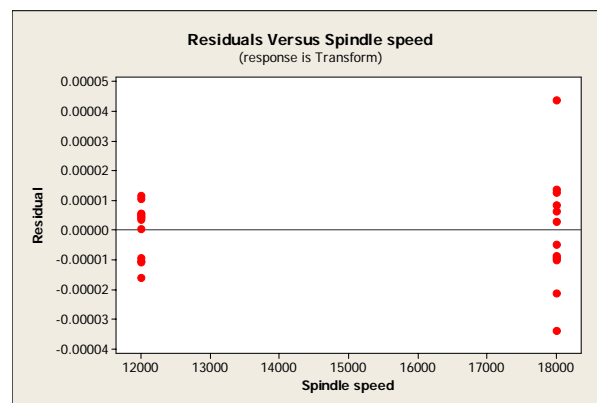


Figure 49 Residuals plot versus spindle speed.

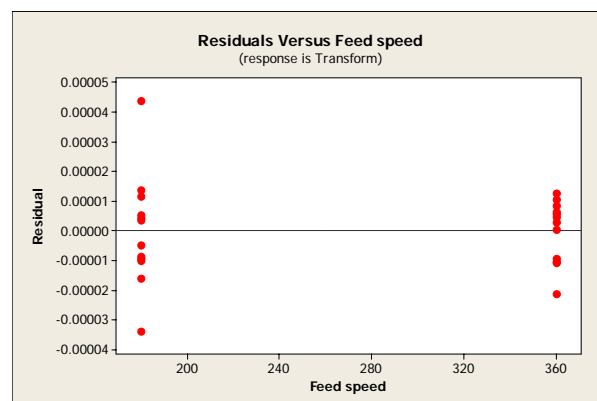


Figure 50 Residuals plot versus feed speed.

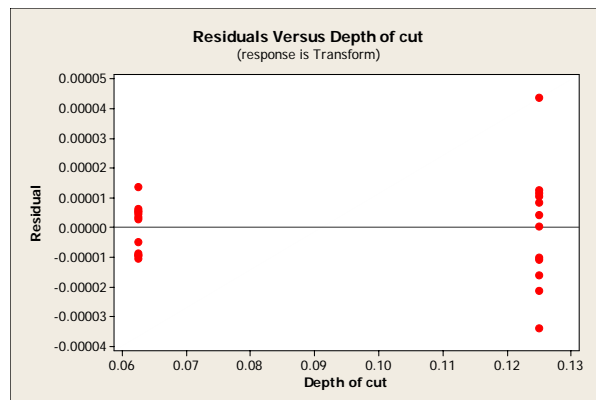


Figure 51 Residuals plot versus depth of cut.

The main effect of spindle speed, feed speed and depth of cut are plotted in Figure 52. The spindle speed effect and feed speed effect indicates mind inequality of surface roughness , with the treatment combination at spindle speed of 12,000 rpm and feed speed of 360 ipm possibly having smaller roughness than a spindle speed of 18,000 rpm and at feed speed of 180 ipm., depth of cut effect reveals larger surface roughness, with the treatment combination of 0.125 in. and if the main effect is considered, three factors at spindle speed of 12,000 rpm, feed speed at 360 ipm and depth of cut of 0.0625 in. are needed to include to minimize the surface roughness from the workpiece. However, any important interactions are necessary to be examined because the main effects do not have much meaning when the interaction significant affects.

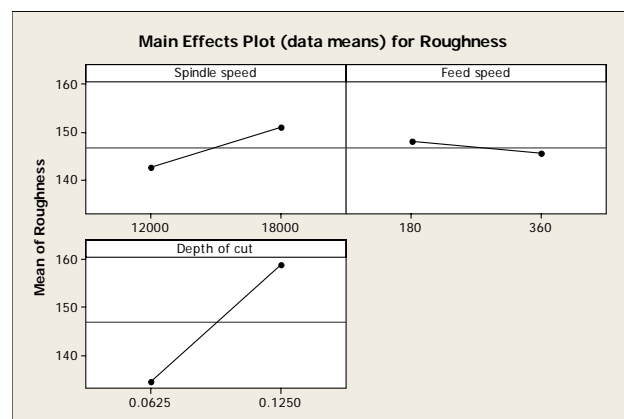


Figure 52 Main effect plot for roughness at the first step.

The spindle speed – feed speed interaction and the spindle speed - feed speed - depth of cut interaction are shown in Figures 53 and 54. From the spindle speed - feed speed interaction, it is possible to have smaller surface roughness at the spindle speed of 12,000 rpm and the feed speed of 180 ipm. The spindle - feed speed - depth of cut interaction indicates that spindle speed has smaller surface roughness at spindle speed of 12,000 rpm, depth of cut of 0.0625 in. As a result, the best surface quality would appear to be obtained when a spindle speed is 12,000 rpm, a feed speed is 180 ipm and a depth of cut is 0.0625 in.

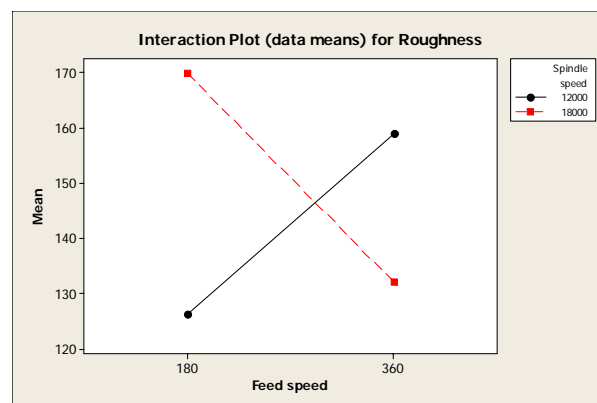


Figure 53 Interaction plot between spindle speed and feed speed.

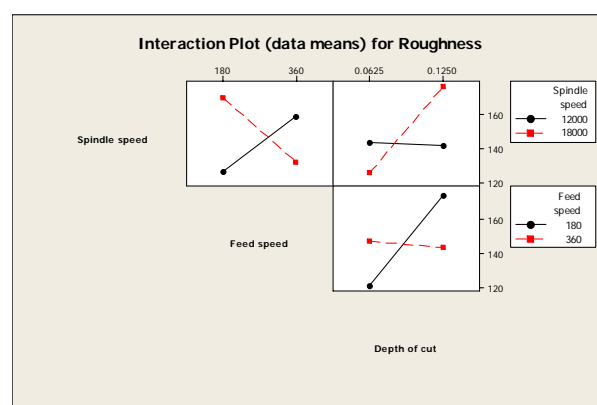


Figure 54 Interaction plot between spindle speed, feed speed and depth of cut.

The result at the fundamental machining process was shown that the conditions with the least cutting tool wear were found at a spindle speed of 12,000

rpm, a feed speed of 180 ipm and a depth of cut 0.1250 in. In addition, the cutting conditions for the range of machining parameters studied in this stage considering the surface quality include a spindle speed of 12,000 rpm, a feed speed of 180 ipm and a depth of cut 0.0625 in.

Determine the Optimal Solution in Parawood Machining Process

In the second stage, the parameters used to analyze are shown in Table 15.

Table 15 Design of parameter for determine the optimal value

Machining conditions	Level
Tool type	T10MG
Spindle speed (rpm)	12,000, 15,000, 18,000
Feed rate (ipm)	180, 360
Depth of cut (inch)	0.0625, 0.125

The work sheet from this experiment is shown in Appendix Table B7. It is used to analyze for determine optimal parameter of parawood machining process using Minitab release 14[®]. In this step, null hypotheses are rejected when 90% confident interval is found. Analysis of variance table of nose width in the second step was presented in Table 16 and the normal probability plot is also presented in Figure 55.

Table 16 Analysis of variance for nose width in the second step with 90% confident interval.

Source	DF	SS	MS	F	P
Blocks	2	286	143	0.75	0.476
Spindle speed (rpm)	2	52060	26030	136.19	0.000
Feed speed (ipm)	1	1942	1942	10.16	0.002
Depth of cut (in)	1	6175	6175	32.31	0.000
Cutting distance (ft)	3	895716	298572	1562.1	0.000
Spindle speed*Feed speed	2	14133	7067	36.97	0.000
Spindle speed*Depth of cut	2	24019	12009	62.83	0.000
Spindle speed*Cutting distance	6	11066	1844	9.65	0.000
Feed speed*Depth of cut	1	233	233	1.22	0.272
Feed speed*Cutting distance	3	379	126	0.66	0.578

Table 16 Continued.

Source	DF	SS	MS	F	P
Depth of cut* Cutting distance	3	15539	5180	27.10	0.000
Spindle speed* Feed speed*Depth of cut	2	1750	875	4.58	0.013
Spindle speed*Feed speed*Cutting distance	6	11143	1857	9.72	0.000
Spindle speed*Depth of cut*Cutting distance	6	14337	2390	12.50	0.000
Feed speed*Depth of cut* Cutting distance	3	854	285	1.49	0.223
Spindle speed*Feed speed*Depth of cut * Cutting distance	6	4003	667	3.49	0.004
Error	94	17967	191		
Total	143	1071601			

S = 13.8253 R-Sq = 98.32% R-Sq (adj) = 97.45%

The result of analysis of variance considering P-Value shows that spindle speed, feed speed, depth of cut, cutting distance, the spindle speed - feed speed interaction, the spindle speed - depth of cut interaction, the spindle speed – cutting distance interaction, the depth of cut – cutting distance interaction, the spindle speed - feed speed – depth of cut interaction, the spindle speed - feed speed – cutting distance interaction, the spindle speed - depth of cut – cutting distance interaction and the spindle speed – feed speed – depth of cut – cutting distance interaction have P-Value less than 0.10. As a result, the main effect and interaction above significantly affect the nose width at the second stage.

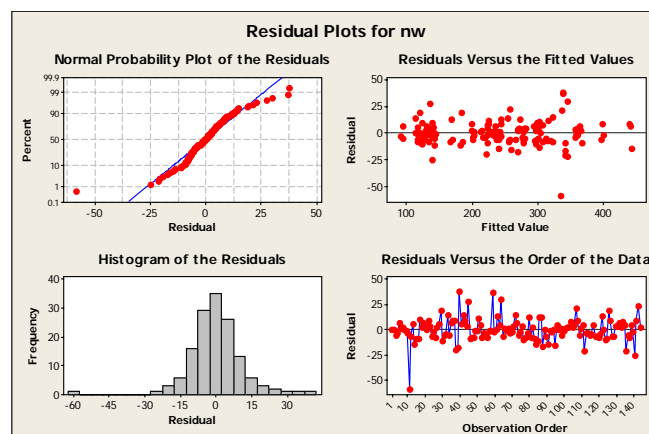


Figure 55 Residual plots of nose width in stage 2.

In Figure 55, the normal probability plot of residual resembles as a straight line. It shows that the underlying error distribution is normal. The model of plot of residuals and the fitted values is corrected because it does not correlate well as expected, the residuals are structureless and the assumptions are satisfied. Residual versus spindle speed is shown in Figure 56. The plot reveals that there are much less scatter in the residual at spindle speed of 15,000 and 18,000 rpm than at the spindle speed of 12,000 ipm Figure 57 plots the residual versus feed speed. The graph shows that there are much less scatter in the residual at feed speed of 180 ipm than at the feed speed of 360 ipm and Figure 58 displays the residual versus depth of cut. The plot depicts that there are much less scatter in the residual at a depth of cut of 0.1250 in. than at a depth of cut of 0.0625 in. In addition, the residual versus cutting distance displays in Figure 59.

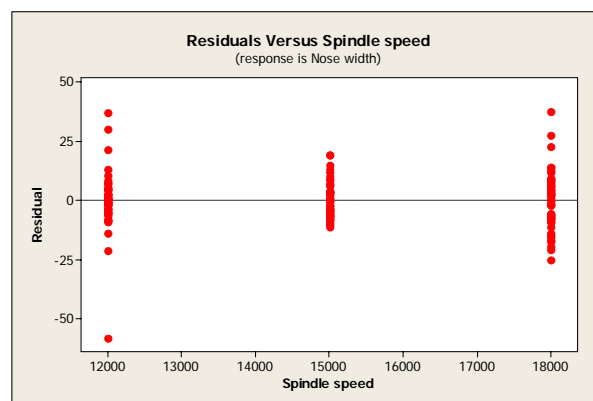


Figure 56 Residuals versus spindle speed at stage 2.

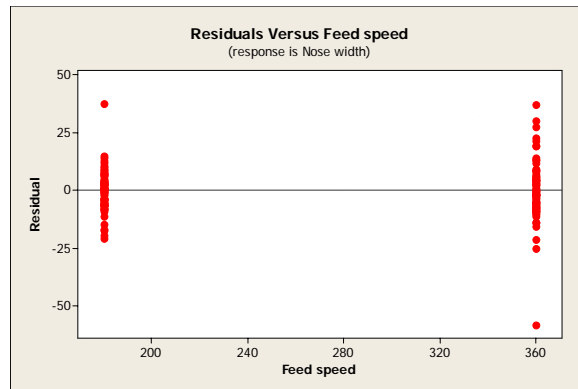


Figure 57 Residuals versus feed speed at stage 2.

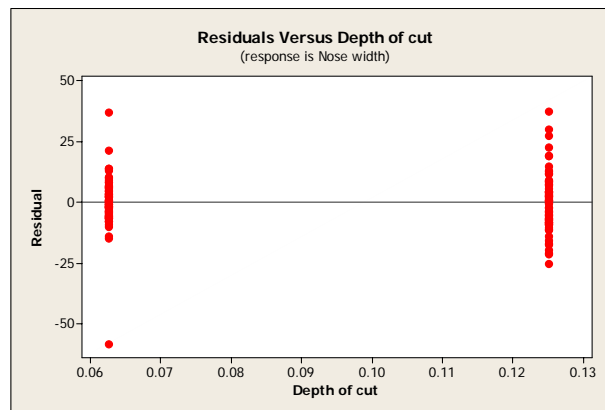


Figure 58 Residuals versus depth of cut at stage 2.

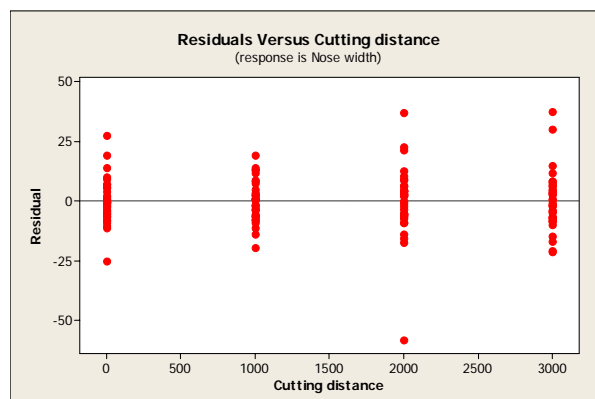


Figure 59 Residuals versus cutting distance at stage 2.

The main effect of spindle speed, feed speed, depth of cut and cutting distance are plotted in Figure 60. Spindle speed effect is 15,000 rpm, feed speed effect indicates mind inequality of nose width, with the treatment combination of 180 ipm possibly having larger nose width than 360 ipm., depth of cut effect reveals fairly of nose width, with the treatment combination of 0.0625 in possibly having larger nose width than 0.1250 in. and if the main effect is considered, three factors at a spindle speed of 15,000 rpm, a feed speed of 360 ipm and a depth of cut of 0.1250 in are needed to include to minimize the nose width form the blade test. However, any important interactions are necessary to be examined because the main effects do not have much meaning when the interaction significant affects.

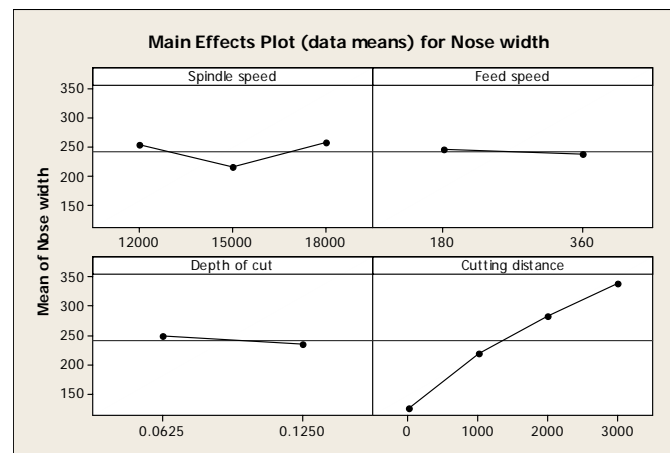


Figure 60 Plot of main effect of nose width in stage 2.

The spindle speed - feed speed interaction, the spindle speed - depth of cut interaction, the spindle speed – cutting distance interaction, the depth of cut – cutting distance interaction, the spindle speed - feed speed – depth of cut interaction, the spindle speed - feed speed – cutting distance interaction, the spindle speed - depth of cut – cutting distance interaction and the spindle speed – feed speed – depth of cut – cutting distance interaction are plotted in Figures 61 - 68. The spindle speed - feed speed interaction is shown that the feed speed effect is very small when the spindle speed is 15,000 rpm, as a result, it is possible to has smaller nose width at the spindle speed of 15,000 rpm and the feed speed of 360 ipm. The spindle speed - depth of cut

interaction indicates that depth of cut has smaller effect at 0.0625 in. The spindle speed – cutting distance interaction performs that spindle speed has smaller effect at 15,000 rpm. The depth of cut – cutting distance interaction performs that depth of cut has smaller effect at 15,000 rpm. As a result, the smaller nose width is obtained when a spindle speed is 15,000 rpm, a feed speed is 360 ipm and a depth of cut is 0.0625 in.



Figure 61 The interaction plot between spindle speed and feed speed.

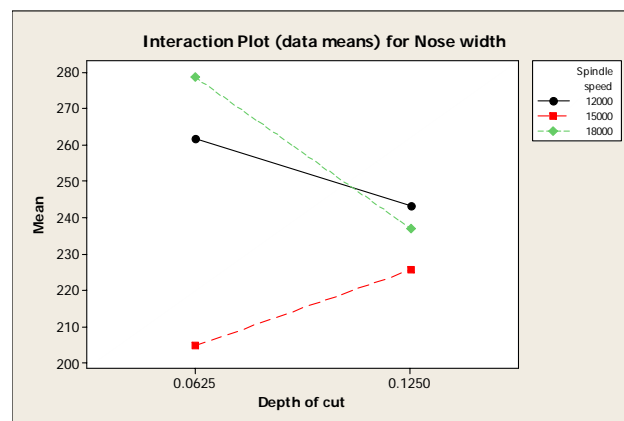


Figure 62 The interaction plot between spindle speed and depth of cut.

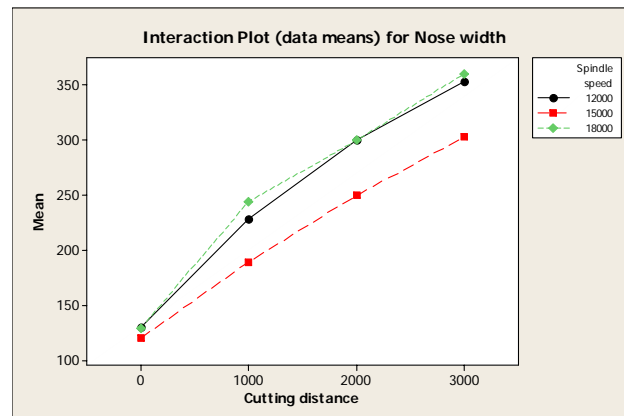


Figure 63 The interaction plot between spindle speed and cutting distance.

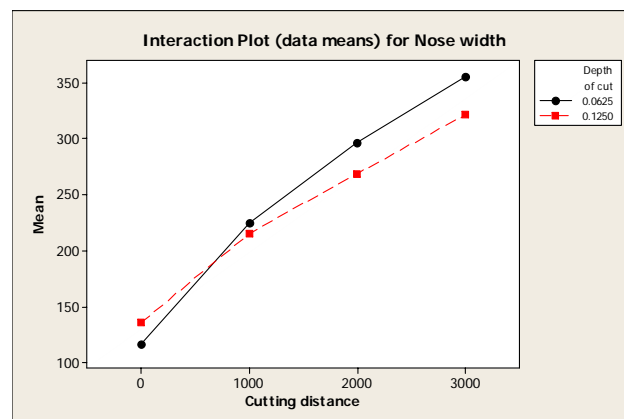


Figure 64 The interaction plot between depth of cut and cutting distance.



Figure 65 The interaction plot between spindle speed, feed speed and depth of cut.

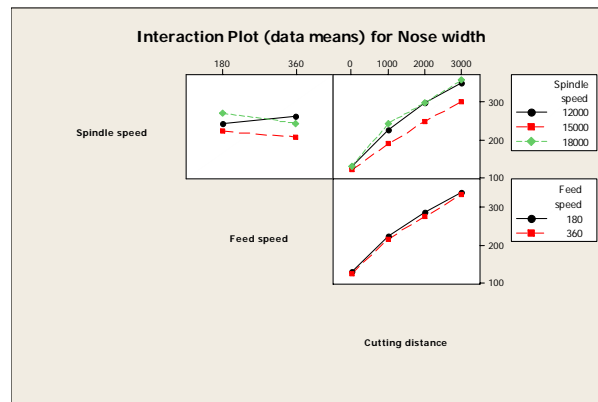


Figure 66 The interaction plot between spindle speed, feed speed and cutting distance.

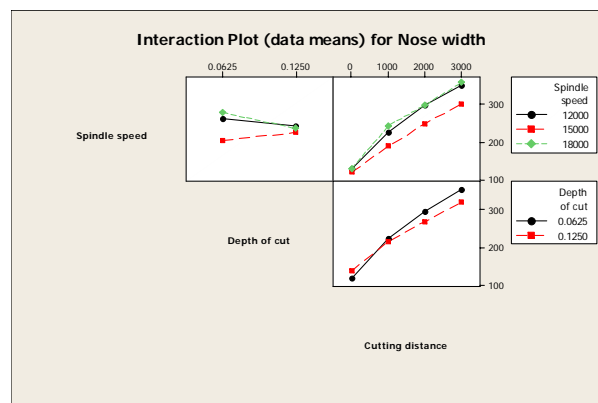


Figure 67 The interaction plot between spindle speed, depth of cut and cutting distance.

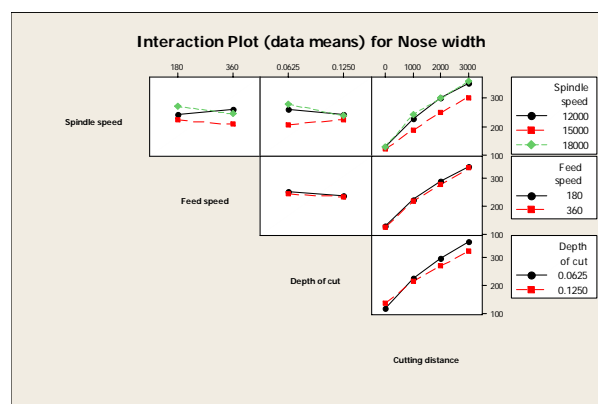


Figure 68 The interaction plot between spindle speed, feed speed, depth of cut and cutting distance.

In order to obtain a prediction model of optimization, a regression analysis on nose width versus spindle speed, feed speed, depth of cut and cutting distance is shown in Equation 31;

$$\begin{aligned} \text{Nose width } (\mu\text{in}) = & -95 + (0.0156 \text{ rpm}) + (0.608 \text{ ipm}) + (615 \text{ DoC}) + (0.0615 \text{ LF}) - \\ & (0.000046 \text{ rpm} \times \text{ipm}) - (0.0393 \text{ rpm} \times \text{DoC}) + (0.000003 \text{ rpm} \times \\ & \text{LF}) + (0.068 \text{ DoC} \times \text{LF}) + (0.000048 \text{ rpm} \times \text{ipm} \times \text{DoC}) - \\ & (0.000022 \text{ rpm} \times \text{DoC} \times \text{LF}) \end{aligned} \quad (31)$$

where rpm = spindle speed (revolution per minute)
 ipm = feed speed (inch per minute)
 DoC = depth of cut (inch)
 LF = cutting distance (feet)

For the case of surface roughness of parawood at cutting distance of 3000 feet, an analysis of variance for surface roughness table is shown in Table 17.

Table 17 Analysis of variance for surface roughness of parawood material at 3,000 linear feet with 90% confident interval.

Source	DF	SS	MS	F	P
Blocks	2	1972	986	0.56	0.577
Spindle speed (rpm)	2	458	229	0.13	0.878
Feed speed (ipm)	1	336	336	0.19	0.665
Depth of cut (in)	1	4265	4265	2.44	0.133
Spindle speed*Feed speed	2	8802	4401	2.51	0.104
Spindle speed*Depth of cut	2	4294	2147	1.23	0.313
Feed speed*Depth of cut	1	262	262	0.15	0.702
Spindle speed*Feed speed*Depth of cut	2	9487	4743	2.71	0.089
Error	22	38505	1750		
Total	35	68381			

$$S = 41.8359 \quad R\text{-Sq} = 43.69\% \quad R\text{-Sq (adj)} = 10.42\%$$

The result of analysis of variance considering P-Value shows that the interaction between spindle speed, feed speed and depth of cut has P-Value less than

0.10. As a result, the spindle speed – feed speed – depth of cut interaction significantly affects the surface roughness of parawood material at a cutting distance of 3000 feet. Normal probability plot of residual is shown in Figure 69. This plot could not resemble a straight line. It shows that the underlying error distribution is abnormal. The model of plot of residuals and the fitted values is incorrect because it is correlated well, the residuals are structured and the assumptions are unsatisfied.

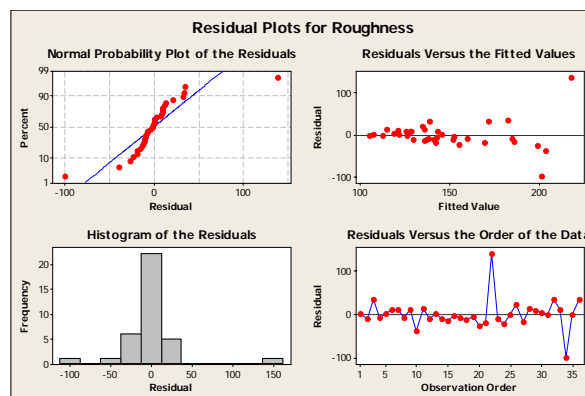


Figure 69 Residual plots for surface roughness at 3,000 linear feet.

To continue an analysis of surface roughness, Box-Cox technique used to transform the data. The Box-Cox plot of surface roughness, an analysis of variance table of transform data and the normal probability plot of the residual of transform data are presented in Figure 70, Table 18 and Figure 71, respectively.

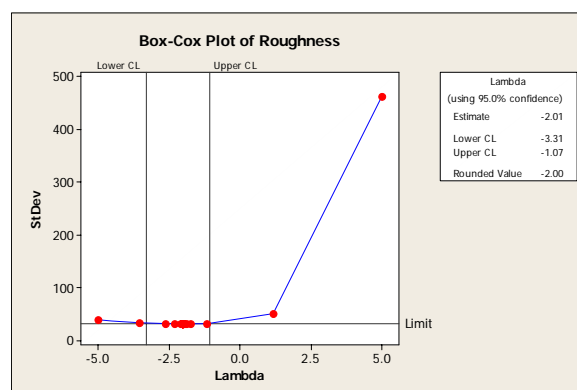


Figure 70 Box-Cox plot of surface roughness at stage 2.

Table 18 Analysis of Variance of transform data on step 2 with 90% confident interval.

Source	DF	SS	MS	F	P
Blocks	2	0.0000000	0.0000000	0.63	0.543
Spindle speed (rpm)	2	0.0000000	0.0000000	0.75	0.482
Feed speed (ipm)	1	0.0000000	0.0000000	3.04	0.095
Depth of cut (in)	1	0.0000000	0.0000000	3.07	0.093
Spindle speed*Feed speed	2	0.0000000	0.0000000	3.14	0.063
Spindle speed*Depth of cut	2	0.0000000	0.0000000	0.42	0.661
Feed speed*Depth of cut	1	0.0000000	0.0000000	0.13	0.722
Spindle speed*Feed speed*Depth of cut	2	0.0000000	0.0000000	6.66	0.005
Error	22	0.0000000	0.0000000		
Total	35				

$S = 0.0000159618$ $R\text{-Sq} = 57.24\%$ $R\text{-Sq (adj)} = 31.98\%$

The result of analysis of variance considering P-Value was found that feed speed, depth of cut, the spindle speed – feed speed interaction, and the spindle speed – feed speed - depth of cut interaction have P-Value less than 0.10. As a result, the main effect and the interaction above significantly affect the surface roughness of parawood workpiece at a cutting distance of 3,000 feet.

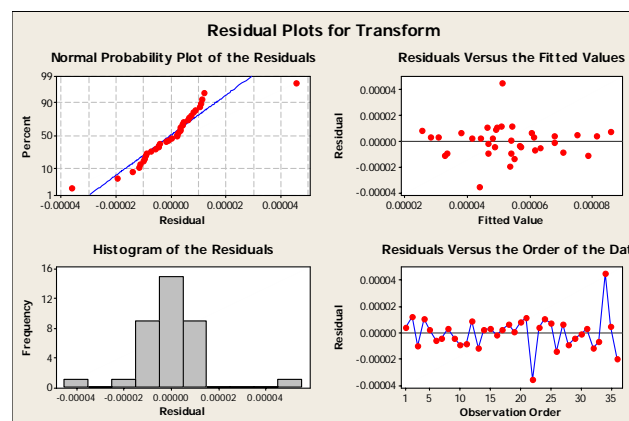


Figure 71 Normal probability plot of the residual of transform data.

In Figure 71, the normal probability plot of residual resembles as a straight line. It shows that the underlying error distribution is normal. The model of plot of

residuals and the fitted values is corrected because it does not correlated well as expected, the residuals are structureless and the assumptions are satisfied. Residual versus spindle speed is shown in Figure 72. The plot reveals that there are much less scatter in the residual at spindle speeds of 12,000 and 15,000 rpm than at the spindle speed of 18,000 ipm. Figure 73 displays the residual versus feed speed. The graph shows that there are much less scatter in the residual at a feed speed of 360 ipm than at a feed speed of 180 ipm and Figure 74 plots the residual versus depth of cut. The plot indicates that there are much less scatter in the residual at a depth of cut of 0.0625 in than at a depth of cut of 0.1250 in.

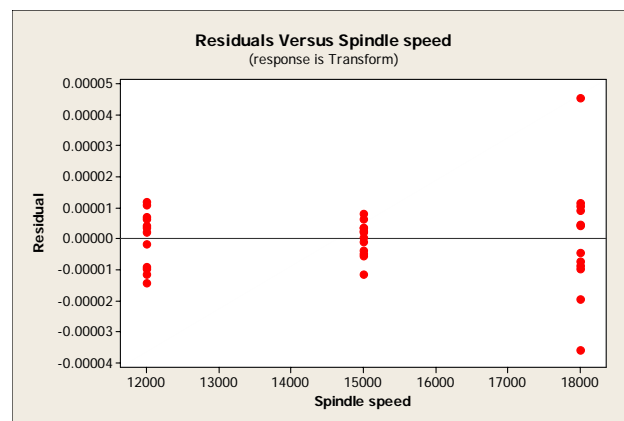


Figure 72 Residuals plot versus spindle speed.

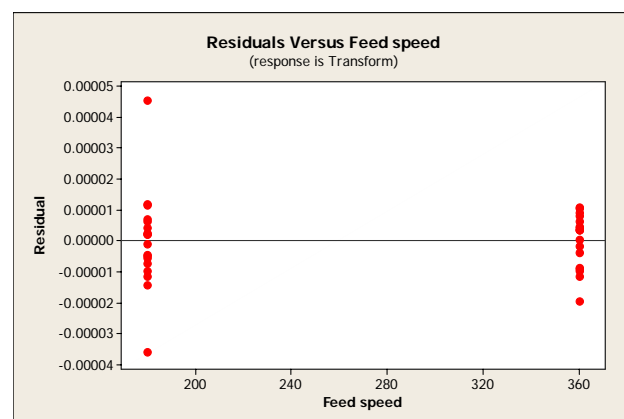


Figure 73 Residuals plot versus feed speed.

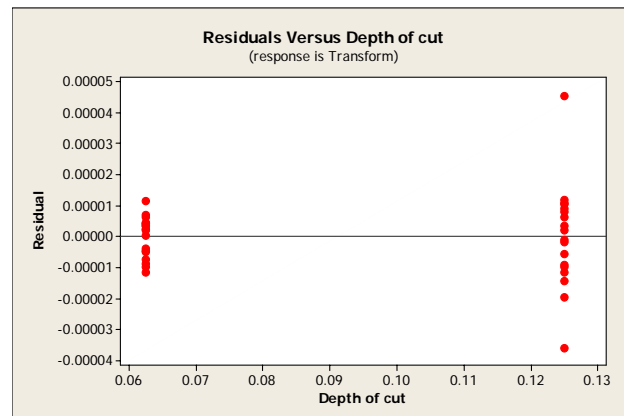


Figure 74 Residuals plot versus feed speed.

The main effect of spindle speed, feed speed and depth of cut are plot in Figure 75. The Spindle speed effect is 12,000 rpm, feed speed effect indicates smaller of surface roughness at 180 ipm more than 360 ipm and depth of cut effect also reveals smaller surface roughness of 0.0625 in than 0.1250 in. and if the main effect is considered, three factors at a spindle speed of 12,000 rpm, a feed speed of 180 ipm and a depth of cut of 0.0625 in are needed to include to minimize the surface roughness from workpiece. However, they are always necessary to examine any interactions that are important.

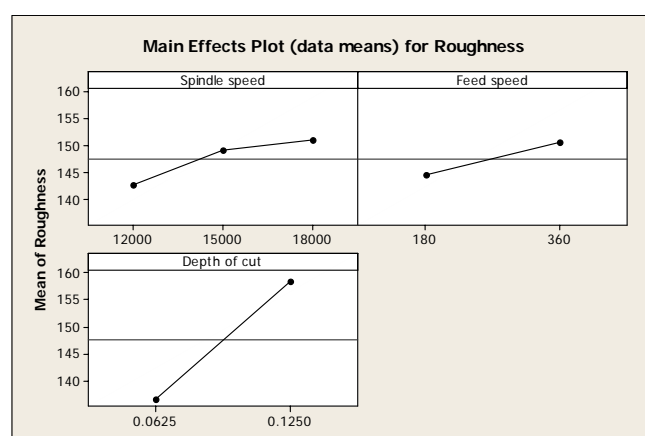


Figure 75 Main effect plot for roughness at stage 2.

The spindle speed - feed speed interaction and the spindle speed - feed speed - depth of cut interaction are plotted in Figures 76 and 77, respectively. The spindle speed - feed speed interaction reveals that the spindle speed and feed speed effect smaller surface roughness when a spindle speed is 12,000 rpm and a feed speed is 180 ipm. The spindle speed - feed speed - depth of cut interaction indicates that depth of cut has small effect at 0.0625 in. with feed speed at 180 ipm. As a result, the smaller surface roughness is obtained when a spindle speed is 12,000 rpm, a feed speed is 180 ipm and a depth of cut is 0.0625 in



Figure 76 Interaction plot between spindle speed and feed speed.

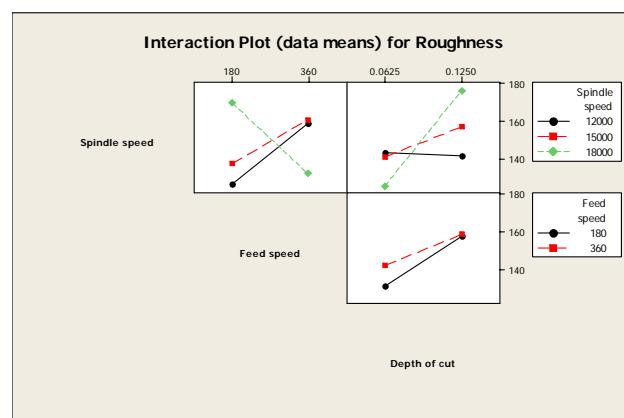


Figure 77 Interaction plot between spindle speed, feed speed and depth of cut.

From this research, it is found that the optimal cutting conditions for the range of machining parameters studied considering the conditions with the least cutting tool wear and the least splinter were at a spindle speed of 15,000 rpm, a feed speed of 360 ipm and a depth of cut of 0.0625 in. Additionally, it was discovered that the cutting conditions to minimize the surface roughness of machined parawood include a spindle speed of 12,000 rpm, a feed speed of 180 ipm and a depth of cut of 0.0625 in.

Due to restriction of experiment setup, the statistical analysis of regression model shows that the coefficient of determination of regression is very low, which means that the data of surface roughness is not enough to analyze regression model. Considering the surface quality of workpiece in machining process, it is necessary to use cutting condition include a spindle speed of 12,000 rpm, a feed speed of 180 ipm and a depth of cut of 0.0625 in. In addition, the condition with the least cutting tool wear is at a spindle speed of 15,000 rpm, a feed speed of 360 ipm and a depth of cut 0.0625 in.

To test of the regression model with a spindle speed of 12,000 rpm, a feed speed of 360 ipm, and a depth of cut of 0.1250 in on a cutting distance at 3,000 feet, it is shown that the nose width of the blade is 373.895 μin . Compared with the empirical data in Table 9, it can be seen that the nose width of an insert with the same condition is 344.97 μin . Using this data, it can prove that the regression model can be used to predict the nose width with 91.62% accuracy. Consequently, the regression model obtained in this work can be possibly used to predict the nose width of inserts in parawood machining process.

In addition, there are still have large amount of work needed to be done in the future for the understanding of parawood machining process. It mainly includes:

1. Analysis of the statistics for the surface finish in term of the normal probability plot of residual, and the regression model.
2. The relation between chip size and surface finish.

3. Data acquisition and statistical analysis for more effective approximation of tool wear and surface finish.

4. Application of the sensor systems for tool condition monitoring and the online control system on routing of workpiece subjected to its product quality and sensitivity of tool wear.

CONCLUSIONS

In this study, the effect of various machining parameters such as spindle speed, feed speed and depth of cut in the parawood machining process were investigated on the quality of parawood machined surface and the wear of the Tungsten Carbide (TC) cutting tool insert. The ranges of machining parameters studied in this research are spindle speeds of 12,000, 15,000 and 18,000 rpm, feed speeds of 180 and 360 ipm and depths of cut of 0.0625 and 0.1250 in. Using the statistical tool, the results show that the optimal cutting conditions for the range of machining parameters studied considering the conditions with the least cutting tool wear and the least splinter were found at a spindle speed of 15,000 rpm, a feed speed of 360 ipm and a depth of cut 0.0625 in. In addition, it was discovered that the cutting conditions to minimize the surface roughness of machined parawood, and as a result, the best surface quality, include a spindle speed of 12,000 rpm, a feed speed of 180 ipm and a depth of cut of 0.0625 in. The regression model was also obtained to predict the nose width in each cutting condition. This study provides more understanding on parawood machining process in order to identify the optimal cutting condition where high quality machined surfaces with less surface roughness, less tooling cost, less waste materials, and lower production time are obtained. The selection of optimal machining parameters can be greatly contributed to engineers and operators in the parawood furniture manufacturing industry in Thailand and other countries in terms of productivity improvement and cutting parameter selection during the wood machining process.

LITERATURE CITED

Anonymous. 1962 and 1995. USA Standard USAS B46.1-1962 and ASME standard B46.1-1995.

Anonymous. 1999. Mechatronic and Machine Tools. McGraw-Hill Companies, United states of America.

Arlai, T., P. Kaewtatip and K. Prommul. 2003. Influences of Various Working Parameter in Routing Process of Rubber Wood Using Tungsten-Carbide Routers, ME-NETT#17. National Conference, Prajinburi.

AsiaPulse News. 2003. Diary-Thailand Fair to Promote Parawood Furniture, Available Source: <http://www.asiapulse.com/>

Bailey, J. A., A. M. Bayoumi and J. S. Stewart. 1983. Wear of some Cemented Tungsten Carbide tools In Machining Oak. Wear. 85: 69-79.

Bayoumi, A. B. and J. A. Bailey. 1985. A Comparison of the Wear Resistance of Selected Steels and Cemented Carbide Cutting Tool Materials in Machining Wood. Wear. 105: 131-144.

Bayoumi, A. B., J. A Bailey, and J. S. Stewart. 1983. Comparison of the Wear Resistance of Various Grades of Cemented Carbides That May Find Application in Wood Machining. Wear. 89:185-200.

Chan, J. C., and W. L. Chen. 1999. A Tool Breakage Detection System Using an Accelerometer Sensor. Journal of Intelligent Manufacturing. 10 (2):187-197.

Design in wood. 2003., Available Source: <http://www.designsinwoodnc.com>

- Elanayar, S. V., T. Shin, and Y. C. S. Kumara. 1990. Machining Condition Monitoring for Automation Using Neural Networks. The winter Annual Meeting of The American Society of Mechanical Engineers. Monitoring and Control for Manufacturing Processes. PED. 44:85-100.
- Endler, I., K. Bartsch, A. Leonhardt, H. J. Scheibe, H. Ziegele, I. Fuchs and Ch. Raatz. 1999. Preparation and Wear Behavior of Woodworking Tools Coats with Superhard Layers. Diamond and Related Materials. 8:834-839.
- Forest Products Laboratory General Technical. 1999. Wood handbook, wood as an engineering material. The Forest Products Society, United States of America,
- Ko. P. L., Z. S. Liu, R. Cvitkovic, M. Donovan, R. Loewen and G. Krishnapper. 1999. Tool Wear Monitoring for Routing MDF. pp 609-619. Proceedings of 14th the International Wood Machining Seminar, Paris, France.
- Kohn, P. n. d. Utilization of Hardwoods Growing on Southern Pine Sites: Agriculture Handbook No 605. US Department of Agriculture forest service, United State of America.
- Kohn, P. 1964. Wood Machining Process. The Ronald Press Company, United State of America.
- Lim, G. H. 1995. Tool - Wear Monitoring in Machine Turning. Journal of Material Processing Technology. 51:25-36.
- Lin, S. B. and O. Masory. 1987. Gains Selection for a Variable Gain Adaptive Control System for Turning. Journal of Engineering for Industry. 109 (November):399-403.

Lundholm, T., E. Bergstrom, D. Enarson, L. Harder, B. Lindstrom, M. Nicolescu and B. Nilsson. 1992. New techniques Applied to adaptive controlled Machining. *Robotic and Computer-Integrated Manufacturing*. 9 (4/5):383-389.

Micheletti, G. F., W. Koenig, H. R. Vicor. 1976. In Process Tool Wear Sensors for Cutting Operations. *Annals of the CIRP*. 25 (2):483-496.

Groover, M. P. 1999. *Fundamentals of Modern Manufacturing Materials, Processes and System*. John Wiley & Sons, New York.

Mohan, G. D. and B. E. Klamecki. 1981-1982. The Susceptibility of Wood-Cutting Tools to Corrosive Wear. *Wear*. 74:85-92.

Montgomery, D. C. 2001. *Design and Analysis of Experiments*. John Wiley & Sons, United State of America.

Morita, T., S. Makisako and Y. Murase. 1999. Wear Characteristics of CNC-Router Bit in Up and Down Milling Processes. *Proceedings IWMS14*. 2 (September):663-669.

Prommul, K., P. Kaewtatip and T. Arlai. 2002. Study on Optimum Wood Cutting Conditions Using PCD. ME-NETT#16 National Conference, Phuket, Thailand.

Ratnasingam, J., H. F. Reid and M.C. Perkins. 2002. The Abrasive Sanding of Rubberwood (hevea Brasiliensis) an Industrial Perspective. *Holz als Roh-und Werkstoff*. 60 (1):191-196.

Ratnasingam, J., and M.C. Perkins. 1998. An Investigation into The Tool Wearing Characteristics of Rubberwood (Hevea Brasiliensis) Laminated Veneer Lumber. *Holz als Roh-und Werkstoff*. 56 (1):31-35.

- Rodkwan, S. and J. S. Strenkowski. 2003. A Numerical and Experimental Investigation of the Machinability of Elastomers, ME-NETT#17 National Conference, Prajinburi, Thailand.
- Rodkwan, S. 2002. A Numerical and Experimental Investigation of the Machinability of Elastomers. Ph.D. Dissertation. Department of Mechanical and Aerospace Engineering, North Carolina State University, United State of America.
- Rodkwan, S. 2000. In-Process Monitoring and Control on Routing of Melamine-Coated Medium Density Particleboard on a CNC Wood Router. Research Project Technical Summary Wood Machining and Tooling Research Program, North Carolina State University, United State of America.
- Scholl, M. and P. Clayton. 1987. Wear Behavior of Wood-Cutting Edges. *Wear*. 120: 221-232.
- Smith, T. 1996. An Experimental Investigation of the Power Requirements for High Speed CNC Router Spindles. Master thesis, Department of Wood and Paper Science, North Carolina State University, United State of America.
- Sheikh-Ahmad, J. Y. and J. A. Bailey. 1999. The Wear Characteristics of Some Cemented Tungsten Carbides in Machining Particleboard. *Wear*. 225-229:256-266.
- Strenkowski, J. S., A. J. Shih, S. Rodkwan, and M. A. Lewis. 2003. Machining of Elastomers – Experimental and Numerical Investigation. 2003 NSF Design Service and Manufacturing Grantees and Research Conference. Birmingham, Alabama, Jan 6-9.
- Strenkowski, J. S., A. J. Shih, M. A. Lewis, S. Rodkwan, and D. R. Poirier. 2002. Machining of Elastomers. 2002 NSF Design. Service and Manufacturing Grantees and Research Conference. San Juan, Puerto Rico, Jan. 4-7.

Tönshoff, H. K., J. P. Wulfberg, H. J. J. Kals, W. König and C. A. Van Luttervelt.
1988. Development and Trends in Monitoring and Control of Machining
Processes. *Annals of the CIRP*, 37 (2):611-622.

APPENDIX

APPENDIX A

Measurement of Moisture and Standard Measurement of Surface Roughness

A. Measurement of Moisture (Forest Products Laboratory General Technical, 1999)

The most accurate of measuring the moisture content is the oven method, in which this slices of the wood (without knot and other defects) to be tested are accurately weighted, heated in an oven or drying-chamber, repeatedly weighed until it has been established beyond question that all the moisture has been driven off. Then, the moisture loss can be calculated as:

$$\frac{(\text{Net weight} - \text{Dry weight})}{\text{Dry weight}} \times 100 \quad \dots\dots\dots a.1$$

While the result obtained by the oven is relatively reliable, it has to be performed in a laboratory or whenever the equipment is available. For fieldwork, the electrical moisture meter will give instantaneous readings accurate enough for most practical purposes. These meters work on the principle that the wood itself is a bad conductor of electricity and that any moisture present will facilitate the passage of an electrical current between two electrodes spaced apart. The measure of resistance to the passage of the current can be expressed in terms of moisture present as a percentage of the total bulk. One such a meter uses a transistorized sensing-plate to record the effect of the material being tested in a high-frequency electrostatic field; but most common forms of meter employ contact, clamp or drive in the pin electrodes attached to cable leads, with the meter actuated either direct from the mains, or with standard dry-cell high and low tension batteries. If only approximated moisture content is required, then the electrodes should be pushed into the surface at several points throughout the length of the board, not less than 4.5 mm. (3/16 in.) depth, and then the average of the reading is used. The range of measurements varies according to the type of meter, with a normal coverage of from 4 to 30 percent, and a margin of error of from 1 to 2 percent. It should be taken into account that the presence of mineral salts in the wood affects the readings. While some wood give large errors, especially in the upper moisture range, most manufacturers give a table of adjustment covering many of the commonly used woods.

B. Standard Measurement of Surface Roughness (ASME B46.1-1995)

In the means of engineering, surface is very complex and it consists of randomly distributed irregularities which are characterized by a wide range of height and spacing. Each surface characterization parameter relates to a selected topographical feature of the surface of interest. Surface texture is a result of the processing method. Surface obtained from casting, forging, or burnishing has undergone some plastic deformation. For surface that are machined, ground, lapped, or honed, the texture is a result of the action of cutting tools, abrasives, or other forces. It is important to understand that surfaces with similar roughness ratings may not have the same performance, due to tempering, subsurface effects, different profile characteristics, etc. The ability of a processing operation to produce a specific surface roughness depends on many factors. For example, in surface grinding, the final surface relies on the peripheral speed of the wheel, the speed of the traverse, the rate of feed, the grit size, the binding material and the state of dress of the wheel, the amount and the type of lubrication at the point of cutting, and the mechanical properties of the work pieces being ground. A small change in any of the above factors may have a marked effect on the surface produced.

Two of the most useful quantities in characterizing a surface are the roughness average (R_a) and Root Mean Square (RMS) roughness (R_q), as described in section 1 of ASME B46.1. A common method of measuring the roughness uses the motion of a sharp-pointed stylus over the surface and the conversion of the displacement normal to the surface into an output reading proportional to either the roughness average or the root mean square average. The stylus dimensions limit the minimum size of the irregularities which are included in the measurement. The specified value of stylus tip radius has been chosen to be small to include the effect of fine irregularities. Stylus radii ranging between 1 and 10 micrometer are fairly common. Since the stylus of such small radius is subject to wear and mechanical damage even when it made of wear-resistant materials, it is recommended that frequent check of the stylus to be made to ensure that the tip radius does not exceed the specified value.

Since most surfaces are not uniform, the fluctuations in readings can occur; therefore, the correct average reading will not be reached instantaneously. In using an instrument, a sufficient length of surface must be traversed to ensure that the full reading characteristic of the surface is obtained. This selection depends upon the cutoff selected. The roughness readings may also vary with location of the simple profile on the surface. In most machining processes, it is generally possible to obtain the adequate surface finish control with three measurements. If the process used produces parts that vary widely in roughness average or root mean square roughness over the surface, the use of statistical average of a number of measurements may be desirable. In general, surface contains irregularities characterized by a large range of widths. The instruments are designed to respond only to irregularity spacing less than a given value, called cutoff. In this section titled Definition of Surface Parameters for Profiling Methods several roughness height parameters are explained.

B.1, Profile height function $Z(x)$: the function used to represent the point-by-point deviations between the measured profile and the reference mean line.

B.2, Roughness average R_a : the arithmetic average of the absolute value of the profile height deviations recorded within the evaluation length and measured from the mean line. As shown in Figure A1., R_a equals to the sum of the shaded area of the profile divided by the evaluation length L , which generally includes several sampling lengths or cutoffs. For graphical determination of roughness, the height deviations are measured normal to the chart center line. Analytically, R_a is given by:

$$R_a = \frac{1}{L} \int_0^L |Z(x)| dx \quad \dots\dots\dots b.1$$

Root Mean Square (RMS) roughness R_q : the root mean square average of the profile height deviations taken with in the evaluation length and measured from the mean line is giving by

$$R_q = \sqrt{\frac{1}{L} \int_0^L Z^2(x) dx} \quad \dots\dots\dots b.2$$

The approximation can be written as:

$$R_q = [(Z_1^2 + Z_2^2 + Z_3^2 + \dots + Z_N^2) / N]^{1/2} \dots\dots\dots b.3$$

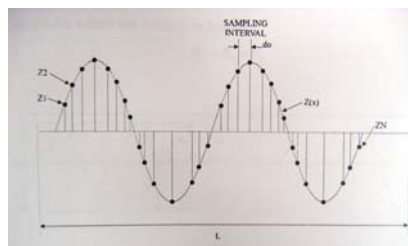
B.4 Maximum profile peak height R_p : is the distance between the highest point of the profile and the mean line within the evaluation length.

B.5 Maximum profile valley depth R_v : is the distance between the lowest point of the profile and the mean line within the evaluation length.

B.6 Maximum height of the profile R_t : is the vertical distance between the highest and lowest points of the profile within the evaluation length. The relationship of these variables can be shown as:

$$R_t = R_p + R_v \dots\dots\dots b.4$$

In section 4 of the standard, the measurement procedures for contact, skidded instruments are explained. The purpose of this section is to relate the uniformity of surface roughness evaluation among contact instruments, and to allow the specification of the desired surface texture values with assurance of securing repeatable results. Some of most important considerations in this section are the measurement direction (in general, perpendicular to the lay direction), the selection of the cutoff value, and the minimum traverse length for a specific cutoff value.



Appendix Figure A1 Calculation of roughness average R_a .

APPENDIX B

Data from Statistical Analysis

Data from Statistical Analysis

1. Determination of the Fundamental Machining Parameters.

1.1 General Linear Model: nose width versus spindle speed, feed speed, depth of cut and cutting distance

Factor	Type	Levels	Values
Blocks	fixed	3	1, 2, 3
Spindle Speed	fixed	2	12000, 18000
Feed Speed	fixed	2	180, 360
Depth of Cut	fixed	2	0.0625, 0.1250
Cutting Distance	fixed	4	0, 1000, 2000, 3000

Appendix B Table 1 Analysis of variance for nose width in step 1.

Source	DF	SS	MS	F	P
Blocks	2	326	163	0.67	0.516
Spindle speed (rpm)	1	718	718	2.94	0.092
Feed speed (ipm)	1	297	297	1.22	0.274
Depth of cut (in)	1	21735	21735	88.94	0.000
Cutting distance (ft)	3	681688	227229	929.82	0.000
Spindle speed*Feed speed	1	13079	13079	53.52	0.000
Spindle speed*Depth of cut	1	3220	3220	13.18	0.001
Spindle speed*Cutting distance	3	1096	365	1.49	0.225
Feed speed*Depth of cut	1	833	833	3.41	0.070
Feed speed*Cutting distance	3	1478	493	2.02	0.121
Depth of cut* Cutting distance	3	27091	9030	36.95	0.000
Spindle speed* Feed speed*Depth of cut	1	943	943	3.86	0.054
Spindle speed*Feed speed*Cutting distance	3	8092	2697	11.04	0.000
Spindle speed*Depth of cut*Cutting distance	3	1815	605	2.48	0.070
Feed speed*Depth of cut* Cutting distance	3	687	229	0.94	0.428
Spindle speed*Feed speed*Depth of cut * Cutting distance	3	2484	828	3.39	0.023
Error	62	15152	244		
Total	95	780735			

S = 15.6327 R-Sq = 98.06% R-Sq (adj) = 97.03%

Appendix Table B2 Work sheet for nose width at the first step.

No.	Block	RPM.	IPM.	DoC.	LF.	NW	FITS1	RESI1	RESI2
1	1	12000	180	0.0625	0	113.02	112.161	0.8589	-6.3294
2	1	12000	180	0.0625	1000	229.17	227.898	1.2722	15.8491
3	1	12000	180	0.0625	2000	293.67	298.534	-4.8645	-13.6224
4	1	12000	180	0.0625	3000	354.21	357.271	-3.0611	-47.0539
5	1	12000	180	0.1250	0	137.74	129.944	7.7955	2.8747
6	1	12000	180	0.1250	1000	214.7	212.984	1.7155	17.0455
7	1	12000	180	0.1250	2000	279.19	276.158	3.0322	18.7462
8	1	12000	180	0.1250	3000	305.51	304.238	1.2722	-17.7231
9	1	12000	360	0.0625	0	125.91	125.991	-0.0811	-6.5008
10	1	12000	360	0.0625	1000	217.33	220.001	-2.6711	-2.148
11	1	12000	360	0.0625	2000	276.56	334.048	-57.4878	-29.9853
12	1	12000	360	0.0625	3000	390.99	396.631	-5.6411	-2.6225
13	1	12000	360	0.1250	0	146.95	140.648	6.3022	-25.8868
14	1	12000	360	0.1250	1000	226.54	239.744	-13.2045	-2.5711
15	1	12000	360	0.1250	2000	269.98	278.354	-8.3745	-15.4055
16	1	12000	360	0.1250	3000	334.39	342.381	-7.9911	-7.2699
17	1	18000	180	0.0625	0	128.57	113.751	14.8189	-24.1206
18	1	18000	180	0.0625	1000	261.2	266.468	-5.2678	15.3768
19	1	18000	180	0.0625	2000	370.15	363.191	6.9589	31.1943
20	1	18000	180	0.0625	3000	448.26	439.108	9.1522	16.1718
21	1	18000	180	0.1250	0	148.27	138.238	10.0322	-1.893
22	1	18000	180	0.1250	1000	202.34	220.998	-18.6578	-12.5812
23	1	18000	180	0.1250	2000	252.9	269.381	-16.4811	-26.7794
24	1	18000	180	0.1250	3000	377.01	338.551	38.4589	32.5725
25	1	18000	360	0.0625	0	123.33	116.811	6.5189	-17.5364
26	1	18000	360	0.0625	1000	269.14	254.234	14.9055	45.4975
27	1	18000	360	0.0625	2000	308.38	298.361	10.0189	1.9614
28	1	18000	360	0.0625	3000	360.89	357.018	3.8722	-28.3047
29	1	18000	360	0.1250	0	164.01	135.958	28.0522	19.7224
30	1	18000	360	0.1250	1000	214.04	222.208	-8.1678	14.7665
31	1	18000	360	0.1250	2000	249.14	255.808	-6.6678	-5.1193
32	1	18000	360	0.1250	3000	287.97	294.388	-6.4178	-21.2752
33	2	12000	180	0.0625	0	115.62	116.296	-0.6761	-3.7294
34	2	12000	180	0.0625	1000	230.49	232.033	-1.5428	17.1691
35	2	12000	180	0.0625	2000	313.41	302.669	10.7405	6.1176
36	2	12000	180	0.0625	3000	366.06	361.406	4.6539	-35.2039
37	2	12000	180	0.1250	0	126.03	134.079	-8.0495	-8.8353
38	2	12000	180	0.1250	1000	213.38	217.119	-3.7395	15.7255
39	2	12000	180	0.1250	2000	275.24	280.293	-5.0528	14.7962
40	2	12000	180	0.1250	3000	300.25	308.373	-8.1228	-22.9831
41	2	12000	360	0.0625	0	128.61	130.126	-1.5161	-3.8008
42	2	12000	360	0.0625	1000	222.59	224.136	-1.5461	3.112
43	2	12000	360	0.0625	2000	375.2	338.183	37.0172	68.6547
44	2	12000	360	0.0625	3000	398.81	400.766	-1.9561	5.1975
45	2	12000	360	0.1250	0	144.31	144.783	-0.4728	-28.5268
46	2	12000	360	0.1250	1000	256.82	243.879	12.9405	27.7089
47	2	12000	360	0.1250	2000	287.09	282.489	4.6005	1.7045
48	2	12000	360	0.1250	3000	376.59	346.516	30.0739	34.9301

Appendix Table B2 Continued.

No.	Block	RPM.	IPM.	DoC.	LF.	NW	FITS1	RESI1	RESI2
49	2	18000	180	0.0625	0	110.23	117.886	-7.6561	-42.4606
50	2	18000	180	0.0625	1000	273	270.603	2.3972	27.1768
51	2	18000	180	0.0625	2000	358.26	367.326	-9.0661	19.3043
52	2	18000	180	0.0625	3000	428.42	443.243	-14.8228	-3.6682
53	2	18000	180	0.1250	0	131.21	142.373	-11.1628	-18.953
54	2	18000	180	0.1250	1000	237	225.133	11.8672	22.0788
55	2	18000	180	0.1250	2000	286.1	273.516	12.5839	6.4206
56	2	18000	180	0.1250	3000	325.97	342.686	-16.7161	-18.4675
57	2	18000	360	0.0625	0	120.72	120.946	-0.2261	-20.1464
58	2	18000	360	0.0625	1000	251.99	258.369	-6.3795	28.3475
59	2	18000	360	0.0625	2000	288.71	302.496	-13.7861	-17.7086
60	2	18000	360	0.0625	3000	359.64	361.153	-1.5128	-29.5547
61	2	18000	360	0.1250	0	137.78	140.093	-2.3128	-6.5076
62	2	18000	360	0.1250	1000	226.88	226.343	0.5372	27.6065
63	2	18000	360	0.1250	2000	244.49	259.943	-15.4528	-9.7693
64	2	18000	360	0.1250	3000	302.88	298.523	4.3572	-6.3652
65	3	12000	180	0.0625	0	115.62	115.803	-0.1827	-3.7294
66	3	12000	180	0.0625	1000	231.81	231.539	0.2706	18.4891
67	3	12000	180	0.0625	2000	296.3	302.176	-5.876	-10.9924
68	3	12000	180	0.0625	3000	359.32	360.913	-1.5927	-41.9439
69	3	12000	180	0.1250	0	133.84	133.586	0.254	-1.0253
70	3	12000	180	0.1250	1000	218.65	216.626	2.024	20.9955
71	3	12000	180	0.1250	2000	281.82	279.799	2.0206	21.3762
72	3	12000	180	0.1250	3000	314.73	307.879	6.8506	-8.5031
73	3	12000	360	0.0625	0	131.23	129.633	1.5973	-1.1808
74	3	12000	360	0.0625	1000	227.86	223.643	4.2173	8.382
75	3	12000	360	0.0625	2000	358.16	337.689	20.4706	51.6147
76	3	12000	360	0.0625	3000	407.87	400.273	7.5973	14.2575
77	3	12000	360	0.1250	0	138.46	144.289	-5.8294	-34.3768
78	3	12000	360	0.1250	1000	243.65	243.386	0.264	14.5389
79	3	12000	360	0.1250	2000	285.77	281.996	3.774	0.3845
80	3	12000	360	0.1250	3000	323.94	346.023	-22.0827	-17.7199
81	3	18000	180	0.0625	0	110.23	117.393	-7.1627	-42.4606
82	3	18000	180	0.0625	1000	272.98	270.109	2.8706	27.1568
83	3	18000	180	0.0625	2000	368.94	366.833	2.1073	29.9843
84	3	18000	180	0.0625	3000	448.42	442.749	5.6706	16.3318
85	3	18000	180	0.1250	0	143.01	141.879	1.1306	-7.153
86	3	18000	180	0.1250	1000	236.89	224.639	6.7906	16.5088
87	3	18000	180	0.1250	2000	276.92	273.023	3.8973	-2.7594
88	3	18000	180	0.1250	3000	320.45	342.193	-21.7427	-23.9875
89	3	18000	360	0.0625	0	114.16	120.453	-6.2927	-26.7064
90	3	18000	360	0.0625	1000	249.35	257.876	-8.526	25.7075
91	3	18000	360	0.0625	2000	305.77	302.003	3.7673	-0.6486
92	3	18000	360	0.0625	3000	358.3	360.659	-2.3594	-30.8947
93	3	18000	360	0.1250	0	113.86	139.599	-25.7394	-30.4276
94	3	18000	360	0.1250	1000	233.48	225.849	7.6306	34.2065

Appendix Table B2 Continued.

No.	Block	RPM.	IPM.	DoC.	LF.	NW	FITS1	RESI1	RESI2
95	3	18000	360	0.1250	2000	281.57	259.449	22.1206	27.3107
96	3	18000	360	0.1250	3000	300.09	298.029	2.0606	-9.1552

1.2 Regression Analysis: nose width versus spindle speed, feed speed, depth of cut and cutting distance.

The regression equation is

$$\begin{aligned} \text{Nose Width } (\mu\text{inch}) = & -283 + 0.0278 \text{ RPM} + 1.05 \text{ IPM} + 2550 \text{ DOC} \\ & + 0.132 \text{ LF} - 0.000073 \text{ RPM} \times \text{IPM} - 0.173 \text{ RPM} \\ & \times \text{DOC} - 4.52 \text{ IPM} \times \text{DOC} - 0.589 \text{ DOC} \times \text{LF} + \\ & 0.000367 \text{ RPM} \times \text{IPM} \times \text{DOC} + 0.000007 \text{ RPM} \\ & \times \text{DOC} \times \text{LF} \end{aligned}$$

Appendix Table B3 Regression analysis.

Predictor	Coef	SE Coef	T	P
Constant	-283.3	125.6	-2.26	0.027
Spindle speed	0.027777	0.008006	3.47	0.001
Feed speed	1.0530	0.4303	2.45	0.017
Depth of cut	2550	1278	1.99	0.049
Cutting distance	0.13245	0.01851	7.15	0.000
RPM x IPM	-0.00007299	0.00002884	-2.53	0.013
RPM x DOC	-0.17252	0.08199	-2.10	0.038
IPM x DOC	-4.524	4.354	-1.04	0.302
DOC x LF	-0.5888	0.2095	-2.81	0.006
RPM x IPM x LF	-0.00000000	0.00000000	-0.79	0.429
RPM x IPM x DOC x LF	0.00000000	0.00000004	0.07	0.948
RPM x IPM x DOC	0.0003671	0.0002921	1.26	0.212
RPM x DOC x LF	0.00000697	0.00000841	0.83	0.410

S = 23.5319 R-Sq = 94.1% R-Sq(adj) = 93.3%

Appendix Table B4 Analysis of variance.

Source	DF	SS	MS	F	P
Regression	12	734774	61231	110.58	0.000
Residual Error	83	45961	554		
Lack of Fit	19	30483	1604	6.63	0.000
Pure Error	64	15478	242		
Total	95	780735			

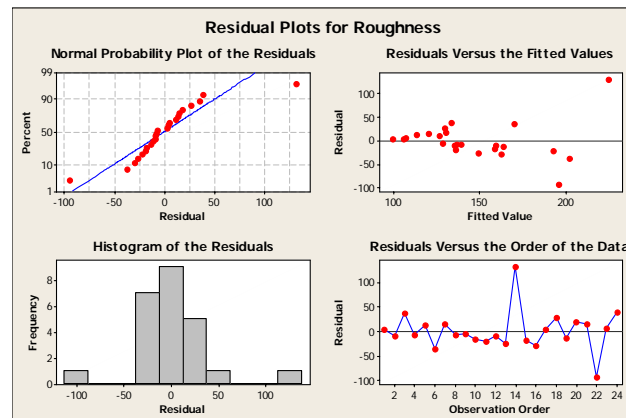
1.3 General Linear Model: surface roughness versus spindle speed, feed speed and depth of cut

Factor	Type	Levels	Values
Blocks	fixed	3	1, 2, 3
Spindle Speed	fixed	2	12000, 18000
Feed Speed	fixed	2	180, 360
Depth of Cut	fixed	2	0.0625, 0.1250

Appendix Table B5 Analysis of variance for roughness.

Source	DF	SS	MS	F	P
Blocks	2	3781	1891	0.75	0.491
Spindle speed (rpm)	1	416	416	0.16	0.691
Feed speed (ipm)	1	38	38	0.01	0.904
Depth of cut (in)	1	3626	3626	1.44	0.250
Spindle speed*Feed speed	1	7464	7464	2.96	0.107
Spindle speed*Depth of cut	1	4151	4151	1.65	0.220
Feed speed*Depth of cut	1	4794	4794	1.90	0.190
Spindle speed*Feed speed*Depth of cut	1	73	73	0.03	0.867
Error	14	35309	2522		
Total	23	59652			

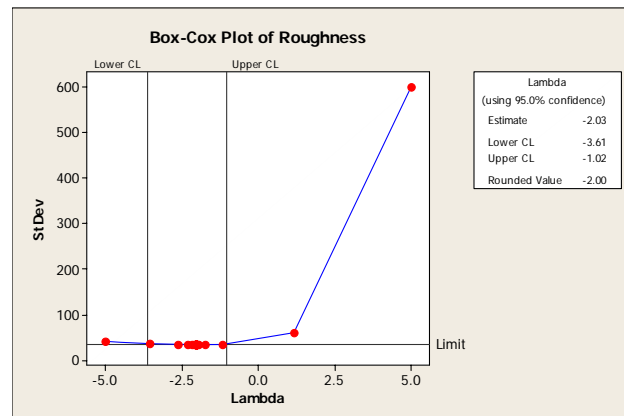
S = 50.2200 R-Sq = 40.81% R-Sq (adj) = 2.76%



Appendix Figure B1 Normal probability plot of residuals for surface roughness.

Appendix Table B6 Work sheet for surface roughness.

No.	Blocks	RPM	IPM	DoC	Rq	FITS1	RESI1	Transform	RESI1
1	1	12000	180	0.0625	108.11	105.599	2.511	8.56E-05	3.7E-06
2	1	12000	180	0.125	126.33	135.639	-9.309	6.27E-05	1.15E-05
3	1	12000	360	0.0625	205.89	170.122	35.768	2.36E-05	-1E-05
4	1	12000	360	0.125	128.56	136.642	-8.082	6.05E-05	1.05E-05
5	1	18000	180	0.0625	137.56	126.385	11.175	5.28E-05	-4.8E-06
6	1	18000	180	0.125	164.57	202.045	-37.475	3.69E-05	-1E-05
7	1	18000	360	0.0625	127.22	113.382	13.838	6.18E-05	-9.2E-06
8	1	18000	360	0.125	131.07	139.495	-8.425	5.82E-05	8.7E-06
9	2	12000	180	0.0625	121.98	128.653	-6.673	6.72E-05	-9.3E-06
10	2	12000	180	0.125	141.33	158.693	-17.362	5.01E-05	4.3E-06
11	2	12000	360	0.0625	171	193.176	-22.176	3.42E-05	5.7E-06
12	2	12000	360	0.125	149.11	159.696	-10.586	0.000045	3E-07
13	2	18000	180	0.0625	123.15	149.439	-26.289	6.59E-05	1.36E-05
14	2	18000	180	0.125	356.77	225.099	131.671	7.9E-06	-3.4E-05
15	2	18000	360	0.0625	117.78	136.436	-18.656	7.21E-05	6.4E-06
16	2	18000	360	0.125	132.62	162.549	-29.929	5.69E-05	1.27E-05
17	3	12000	180	0.0625	103.67	99.509	4.161	0.000093	5.5E-06
18	3	12000	180	0.125	156.22	129.549	26.671	0.000041	-1.6E-05
19	3	12000	360	0.0625	150.44	164.032	-13.592	4.42E-05	4.6E-06
20	3	12000	360	0.125	149.22	130.552	18.668	4.49E-05	-1.1E-05
21	3	18000	180	0.0625	135.41	120.295	15.115	5.45E-05	-8.8E-06
22	3	18000	180	0.125	101.76	195.955	-94.195	9.66E-05	4.39E-05
23	3	18000	360	0.0625	112.11	107.292	4.818	7.96E-05	2.8E-06
24	3	18000	360	0.125	171.76	133.405	38.355	3.39E-05	-2.1E-05

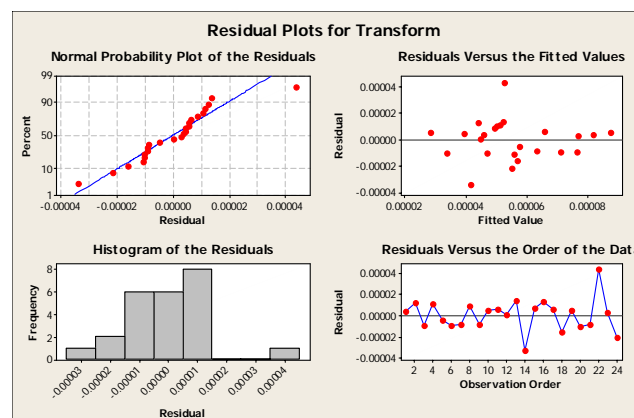


Appendix Figure B2 Box-Cox plot for surface roughness.

Appendix Table B7 Analysis of variance for transform.

Source	DF	SS	MS	F	P
Blocks	2	0.0000000	0.0000000	0.66	0.533
Spindle speed (rpm)	1	0.0000000	0.0000000	0.07	0.793
Feed speed (ipm)	1	0.0000000	0.0000000	1.11	0.310
Depth of cut (in)	1	0.0000000	0.0000000	2.20	0.160
Spindle speed*Feed speed	1	0.0000000	0.0000000	4.26	0.058
Spindle speed*Depth of cut	1	0.0000000	0.0000000	0.31	0.585
Feed speed*Depth of cut	1	0.0000000	0.0000000	1.31	0.272
Spindle speed*Feed speed*Depth of cut	1	0.0000000	0.0000000	3.36	0.088
Error	14	0.0000000	0.0000000		
Total	23	0.0000000			

$S = 0.0000192717$ $R\text{-Sq} = 49.90\%$ $R\text{-Sq (adj)} = 17.69\%$



Appendix Figure B3 Normal probability plot of residuals for transform data.

2. Determine the Optimal Solution in Parawood Machining Process.

2.1 General Linear Model: nose width versus spindle speed, feed speed, depth of cut and cutting distance.

Factor	Type	Levels	Values
Blocks	fixed	3	1, 2, 3
Spindle Speed	fixed	3	12000, 15000, 18000
Feed Speed	fixed	2	180, 360
Depth of Cut	fixed	2	0.0625, 0.1250
Cutting Distance	fixed	4	0, 1000, 2000, 3000

Appendix Table B8 Analysis of variance for nose width.

Source	DF	SS	MS	F	P
Blocks	2	286	143	0.75	0.476
Spindle speed (rpm)	2	52060	26030	136.19	0.000
Feed speed (ipm)	1	1942	1942	10.16	0.002
Depth of cut (in)	1	6175	6175	32.31	0.000
Cutting distance (ft)	3	895716	298572	1562.1	0.000
Spindle speed*Feed speed	2	14133	7067	36.97	0.000
Spindle speed*Depth of cut	2	24019	12009	62.83	0.000
Spindle speed*Cutting distance	6	11066	1844	9.65	0.000
Feed speed*Depth of cut	1	233	233	1.22	0.272
Feed speed*Cutting distance	3	379	126	0.66	0.578
Depth of cut* Cutting distance	3	15539	5180	27.10	0.000
Spindle speed* Feed speed*Depth of cut	2	1750	875	4.58	0.013
Spindle speed*Feed speed*Cutting distance	6	11143	1857	9.72	0.000
Spindle speed*Depth of cut*Cutting distance	6	14337	2390	12.50	0.000
Feed speed*Depth of cut* Cutting distance	3	854	285	1.49	0.223
Spindle speed*Feed speed*Depth of cut * Cutting distance	6	4003	667	3.49	0.004
Error	94	17967	191		
Total	143	1071601			

S = 13.8253 R-Sq = 98.32% R-Sq (adj) = 97.45%

Appendix Table B9 Work sheet of nose width at the second step.

No.	Blocks	RPM	IPM	DoC	LF	NW	FITS1	RESI1	RESI2
1	1	12000	180	0.0625	0	113.02	112.894	0.1257	-4.05
2	1	12000	180	0.0625	1000	229.17	228.631	0.539	34.729
3	1	12000	180	0.0625	2000	293.67	299.268	-5.5976	21.858
4	1	12000	180	0.0625	3000	354.21	358.004	-3.7943	5.027
5	1	12000	180	0.125	0	137.74	130.678	7.0624	5.229
6	1	12000	180	0.125	1000	214.7	213.718	0.9824	17.878
7	1	12000	180	0.125	2000	279.19	276.891	2.299	18.057
8	1	12000	180	0.125	3000	305.51	304.971	0.539	-19.934
9	1	12000	360	0.0625	0	125.91	126.724	-0.8143	-7.789
10	1	12000	360	0.0625	1000	217.33	220.734	-3.4043	8.436
11	1	12000	360	0.0625	2000	276.56	334.781	-58.221	-7.529
12	1	12000	360	0.0625	3000	390.99	397.364	-6.3743	31.705
13	1	12000	360	0.125	0	146.95	141.381	5.569	-8.654
14	1	12000	360	0.125	1000	226.54	240.478	-13.9376	9.597
15	1	12000	360	0.125	2000	269.98	279.088	-9.1076	-8.301
16	1	12000	360	0.125	3000	334.39	343.114	-8.7243	-5.23
17	1	15000	180	0.0625	0	133.8	123.668	10.1324	0.572
18	1	15000	180	0.0625	1000	201.96	199.491	2.469	-11.552
19	1	15000	180	0.0625	2000	241.63	235.198	6.4324	-52.165
20	1	15000	180	0.0625	3000	277.84	274.441	3.399	-96.239
21	1	15000	180	0.125	0	135.14	135.464	-0.3243	-7.786
22	1	15000	180	0.125	1000	208.4	199.821	8.579	2.583
23	1	15000	180	0.125	2000	280.54	276.918	3.6224	11.831
24	1	15000	180	0.125	3000	313.97	320.774	-6.8043	-17.63
25	1	15000	360	0.0625	0	89.38	91.758	-2.3776	-37.291
26	1	15000	360	0.0625	1000	159.27	167.028	-7.7576	-44.964
27	1	15000	360	0.0625	2000	238.01	235.831	2.179	-43.787
28	1	15000	360	0.0625	3000	300.89	294.791	6.099	-58.471
29	1	15000	360	0.125	0	139.06	119.728	19.3324	-5.387
30	1	15000	360	0.125	1000	170.56	181.618	-11.0576	-33.063
31	1	15000	360	0.125	2000	236.1	241.704	-5.6043	-26.7
32	1	15000	360	0.125	3000	308.48	313.338	-4.8576	-13.496
33	1	18000	180	0.0625	0	128.57	114.484	14.0857	-20.817
34	1	18000	180	0.0625	1000	261.2	267.201	-6.001	28.617
35	1	18000	180	0.0625	2000	370.15	363.924	6.2257	54.372
36	1	18000	180	0.0625	3000	448.26	439.841	8.419	49.286
37	1	18000	180	0.125	0	148.27	138.971	9.299	-5.071
38	1	18000	180	0.125	1000	202.34	221.731	-19.391	-12.472
39	1	18000	180	0.125	2000	252.9	270.114	-17.2143	-23.384
40	1	18000	180	0.125	3000	377.01	339.284	37.7257	39.255
41	1	18000	360	0.0625	0	123.33	117.544	5.7857	3.688
42	1	18000	360	0.0625	1000	269.14	254.968	14.1724	69.566
43	1	18000	360	0.0625	2000	308.38	299.094	9.2857	28.875
44	1	18000	360	0.0625	3000	360.89	357.751	3.139	1.453
45	1	18000	360	0.125	0	164.01	136.691	27.319	30.719
46	1	18000	360	0.125	1000	214.04	222.941	-8.901	23.736

Appendix Table B9 Continued.

No.	Blocks	RPM	IPM	DoC	LF	NW	FITS1	RESI1	RESI2
47	1	18000	360	0.125	2000	249.14	256.541	-7.401	1.822
48	1	18000	360	0.125	3000	287.97	295.121	-7.151	-16.361
49	2	12000	180	0.0625	0	115.62	116.303	-0.6826	-1.45
50	2	12000	180	0.0625	1000	230.49	232.039	-1.5493	36.049
51	2	12000	180	0.0625	2000	313.41	302.676	10.734	41.598
52	2	12000	180	0.0625	3000	366.06	361.413	4.6474	16.877
53	2	12000	180	0.125	0	126.03	134.086	-8.056	-6.481
54	2	12000	180	0.125	1000	213.38	217.126	-3.746	16.558
55	2	12000	180	0.125	2000	275.24	280.299	-5.0593	14.107
56	2	12000	180	0.125	3000	300.25	308.379	-8.1293	-25.194
57	2	12000	360	0.0625	0	128.61	130.133	-1.5226	-5.089
58	2	12000	360	0.0625	1000	222.59	224.143	-1.5526	13.696
59	2	12000	360	0.0625	2000	375.2	338.189	37.0107	91.111
60	2	12000	360	0.0625	3000	398.81	400.773	-1.9626	39.525
61	2	12000	360	0.125	0	144.31	144.789	-0.4793	-11.294
62	2	12000	360	0.125	1000	256.82	243.886	12.934	39.877
63	2	12000	360	0.125	2000	287.09	282.496	4.594	8.809
64	2	12000	360	0.125	3000	376.59	346.523	30.0674	36.97
65	2	15000	180	0.0625	0	120.72	127.076	-6.356	-12.508
66	2	15000	180	0.0625	1000	203.83	202.899	0.9307	-9.682
67	2	15000	180	0.0625	2000	238.01	238.606	-0.596	-55.785
68	2	15000	180	0.0625	3000	278.75	277.849	0.9007	-95.329
69	2	15000	180	0.125	0	135.14	138.873	-3.7326	-7.786
70	2	15000	180	0.125	1000	201.08	203.229	-2.1493	-4.737
71	2	15000	180	0.125	2000	283.36	280.326	3.034	14.651
72	2	15000	180	0.125	3000	339.01	324.183	14.8274	7.41
73	2	15000	360	0.0625	0	102.09	95.166	6.924	-24.581
74	2	15000	360	0.0625	1000	164.91	170.436	-5.526	-39.324
75	2	15000	360	0.0625	2000	237.09	239.239	-2.1493	-44.707
76	2	15000	360	0.0625	3000	301.96	298.199	3.7607	-57.401
77	2	15000	360	0.125	0	112.86	123.136	-10.276	-31.587
78	2	15000	360	0.125	1000	177	185.026	-8.026	-26.623
79	2	15000	360	0.125	2000	241.79	245.113	-3.3226	-21.01
80	2	15000	360	0.125	3000	328.71	316.746	11.964	6.734
81	2	18000	180	0.0625	0	110.23	117.893	-7.6626	-39.157
82	2	18000	180	0.0625	1000	273	270.609	2.3907	40.417
83	2	18000	180	0.0625	2000	358.26	367.333	-9.0726	42.482
84	2	18000	180	0.0625	3000	428.42	443.249	-14.8293	29.446
85	2	18000	180	0.125	0	131.21	142.379	-11.1693	-22.131
86	2	18000	180	0.125	1000	237	225.139	11.8607	22.188
87	2	18000	180	0.125	2000	286.1	273.523	12.5774	9.816
88	2	18000	180	0.125	3000	325.97	342.693	-16.7226	-11.785
89	2	18000	360	0.0625	0	120.72	120.953	-0.2326	1.078
90	2	18000	360	0.0625	1000	251.99	258.376	-6.386	52.416
91	2	18000	360	0.0625	2000	288.71	302.503	-13.7926	9.205
92	2	18000	360	0.0625	3000	359.64	361.159	-1.5193	0.203

Appendix Table B9 Continued.

No.	Blocks	RPM	IPM	DoC	LF	NW	FITS1	RESI1	RESI2
93	2	18000	360	0.125	0	137.78	140.099	-2.3193	4.489
94	2	18000	360	0.125	1000	226.88	226.349	0.5307	36.576
95	2	18000	360	0.125	2000	244.49	259.949	-15.4593	-2.828
96	2	18000	360	0.125	3000	302.88	298.529	4.3507	-1.451
97	3	12000	180	0.0625	0	115.62	115.063	0.5569	-1.45
98	3	12000	180	0.0625	1000	231.81	230.8	1.0103	37.369
99	3	12000	180	0.0625	2000	296.3	301.436	-5.1364	24.488
100	3	12000	180	0.0625	3000	359.32	360.173	-0.8531	10.137
101	3	12000	180	0.125	0	133.84	132.846	0.9936	1.329
102	3	12000	180	0.125	1000	218.65	215.886	2.7636	21.828
103	3	12000	180	0.125	2000	281.82	279.06	2.7603	20.687
104	3	12000	180	0.125	3000	314.73	307.14	7.5903	-10.714
105	3	12000	360	0.0625	0	131.23	128.893	2.3369	-2.469
106	3	12000	360	0.0625	1000	227.86	222.903	4.9569	18.966
107	3	12000	360	0.0625	2000	358.16	336.95	21.2103	74.071
108	3	12000	360	0.0625	3000	407.87	399.533	8.3369	48.585
109	3	12000	360	0.125	0	138.46	143.55	-5.0897	-17.144
110	3	12000	360	0.125	1000	243.65	242.646	1.0036	26.707
111	3	12000	360	0.125	2000	285.77	281.256	4.5136	7.489
112	3	12000	360	0.125	3000	323.94	345.283	-21.3431	-15.68
113	3	15000	180	0.0625	0	122.06	125.836	-3.7764	-11.168
114	3	15000	180	0.0625	1000	198.26	201.66	-3.3997	-15.252
115	3	15000	180	0.0625	2000	231.53	237.366	-5.8364	-62.265
116	3	15000	180	0.0625	3000	272.31	276.61	-4.2997	-101.769
117	3	15000	180	0.125	0	141.69	137.633	4.0569	-1.236
118	3	15000	180	0.125	1000	195.56	201.99	-6.4297	-10.257
119	3	15000	180	0.125	2000	272.43	279.086	-6.6564	3.721
120	3	15000	180	0.125	3000	314.92	322.943	-8.0231	-16.68
121	3	15000	360	0.0625	0	89.38	93.926	-4.5464	-37.291
122	3	15000	360	0.0625	1000	182.48	169.196	13.2836	-21.754
123	3	15000	360	0.0625	2000	237.97	238	-0.0297	-43.827
124	3	15000	360	0.0625	3000	287.1	296.96	-9.8597	-72.261
125	3	15000	360	0.125	0	112.84	121.896	-9.0564	-31.607
126	3	15000	360	0.125	1000	202.87	183.786	19.0836	-0.753
127	3	15000	360	0.125	2000	252.8	243.873	8.9269	-10
128	3	15000	360	0.125	3000	308.4	315.506	-7.1064	-13.576
129	3	18000	180	0.0625	0	110.23	116.653	-6.4231	-39.157
130	3	18000	180	0.0625	1000	272.98	269.37	3.6103	40.397
131	3	18000	180	0.0625	2000	368.94	366.093	2.8469	53.162
132	3	18000	180	0.0625	3000	448.42	442.01	6.4103	49.446
133	3	18000	180	0.125	0	143.01	141.14	1.8703	-10.331
134	3	18000	180	0.125	1000	231.43	223.9	7.5303	16.618
135	3	18000	180	0.125	2000	276.92	272.283	4.6369	0.636
136	3	18000	180	0.125	3000	320.45	341.453	-21.0031	-17.305
137	3	18000	360	0.0625	0	114.16	119.713	-5.5531	-5.482
138	3	18000	360	0.0625	1000	249.35	257.136	-7.7864	49.776

Appendix Table B9 Continued.

No.	Blocks	RPM	IPM	DoC	LF	NW	FITS1	RESI1	RESI2
139	3	18000	360	0.0625	2000	305.77	301.263	4.5069	26.265
140	3	18000	360	0.0625	3000	358.3	359.92	-1.6197	-1.137
141	3	18000	360	0.125	0	113.86	138.86	-24.9997	-19.431
142	3	18000	360	0.125	1000	233.48	225.11	8.3703	43.176
143	3	18000	360	0.125	2000	281.57	258.71	22.8603	34.252
144	3	18000	360	0.125	3000	300.09	297.29	2.8003	-4.241

2.2 Regression Analysis: nose width versus spindle speed, feed speed, depth of cut and cutting distance

The regression equation is

$$\begin{aligned}
 \text{Nose width } (\mu\text{in}) = & -95 + 0.0156 \text{ RPM} + 0.608 \text{ IPM} + 615 \text{ DOC} + 0.0615 \text{ LF} \\
 & - 0.000046 \text{ RPM} \times \text{IPM} - 0.0393 \text{ RPM} \times \text{DOC} + 0.000003 \\
 & \text{RPM} \times \text{LF} + 0.068 \text{ DOC} \times \text{LF} + 0.000048 \text{ RPM} \times \text{IPM} \times \\
 & \text{DOC} - 0.000022 \text{ RPM} \times \text{DOC} \times \text{LF}
 \end{aligned}$$

Appendix Table B10 Regression analysis.

Predictor	Coef	SE Coef	T	P
Constant	-95.4	106.1	-0.90	0.370
Spindle speed	0.015568	0.007554	2.06	0.041
Feed speed	0.6077	0.1938	3.13	0.002
Depth of cut	614.7	934.1	0.66	0.512
Cutting distance	0.06146	0.04934	1.25	0.215
RPM x IPM	-0.00004593	0.00001663	-2.76	0.007
RPM x DOC	-0.03925	0.06827	-0.57	0.566
RPM x LF	0.00000253	0.00000361	0.70	0.484
DOC x LF	0.0683	0.4993	0.14	0.891
RPM x IPM x LF	-0.00000000	0.00000001	-0.11	0.913
RPM x IPM x DOC	0.0000479	0.0001101	0.43	0.664
RPM x DOC x LF	-0.00002204	0.00003649	-0.60	0.547
RPM x IPM x DOC x LF	-0.00000001	0.00000006	-0.10	0.920

$$S = 33.7373 \quad R\text{-Sq} = 86.1\% \quad R\text{-Sq}(\text{adj}) = 84.8\%$$

Appendix Table B11 Analysis of variance.

Source	DF	SS	MS	F	P
Regression	12	922496	76875	67.54	0.000
Residual Error	131	149105	1138		
Lack of Fit	35	130852	3739	19.66	0.000
Pure Error	96	18253	190		
Total	143	1071601			

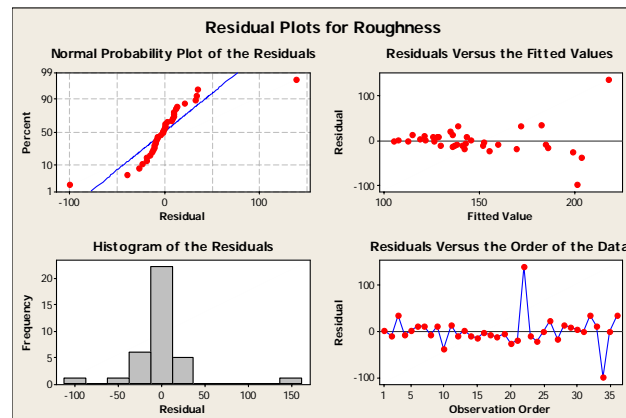
2.3 General Linear Model: surface roughness versus spindle speed, feed speed, depth of cut.

Factor	Type	Levels	Values
Blocks	fixed	3	1, 2, 3
Spindle Speed	fixed	3	12000, 15000, 18000
Feed Speed	fixed	2	180, 360
Depth of Cut	fixed	2	0.0625, 0.1250

Appendix Table B12 Analysis of variance for surface roughness in step 2.

Source	DF	SS	MS	F	P
Blocks	2	1972	986	0.56	0.577
Spindle speed (rpm)	2	458	229	0.13	0.878
Feed speed (ipm)	1	336	336	0.19	0.665
Depth of cut (in)	1	4265	4265	2.44	0.133
Spindle speed*Feed speed	2	8802	4401	2.51	0.104
Spindle speed*Depth of cut	2	4294	2147	1.23	0.313
Feed speed*Depth of cut	1	262	262	0.15	0.702
Spindle speed*Feed speed*Depth of cut	2	9487	4743	2.71	0.089
Error	22	38505	1750		
Total	35	68381			

S = 41.8359 R-Sq = 43.69% R-Sq (adj) = 10.42%



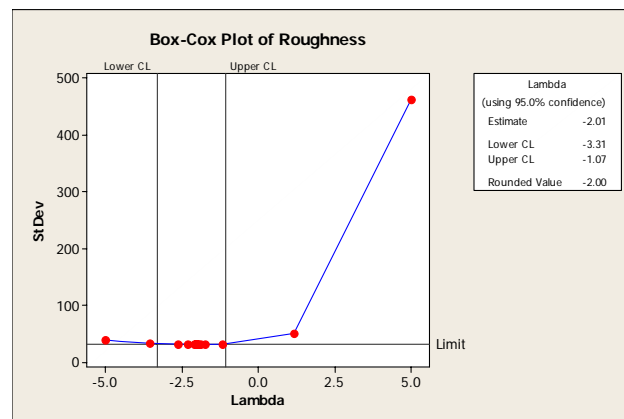
Appendix Figure B4 Normal probability plot of residuals for surface roughness.

Appendix Table B13 Work sheet of surface roughness in step 2.

No	Blocks	RPM	IPM	DoC	Rq	FITS1	RESI1	Transform	RESI1
1	1	12000	180	0.0625	108.11	107.181	0.929	8.56E-05	4.2E-06
2	1	12000	180	0.125	126.33	137.221	-10.891	6.27E-05	0.000012
3	1	12000	360	0.0625	205.89	171.704	34.186	2.36E-05	-9.9E-06
4	1	12000	360	0.125	128.56	138.224	-9.664	6.05E-05	1.09E-05
5	1	15000	180	0.0625	146.36	145.471	0.889	4.67E-05	2.5E-06
6	1	15000	180	0.125	131.62	121.271	10.349	5.77E-05	-5.6E-06
7	1	15000	360	0.0625	137.61	128.487	9.123	5.28E-05	-3.9E-06
8	1	15000	360	0.125	177.26	184.967	-7.707	3.18E-05	3.5E-06
9	1	18000	180	0.0625	137.56	127.967	9.593	5.28E-05	-4.4E-06
10	1	18000	180	0.125	164.57	203.627	-39.057	3.69E-05	-9.6E-06
11	1	18000	360	0.0625	127.22	114.964	12.256	6.18E-05	-8.8E-06
12	1	18000	360	0.125	131.07	141.077	-10.007	5.82E-05	9.1E-06
13	2	12000	180	0.0625	121.98	121.639	0.341	6.72E-05	-1.1E-05
14	2	12000	180	0.125	141.33	151.679	-10.349	5.01E-05	2.2E-06
15	2	12000	360	0.0625	171	186.162	-15.162	3.42E-05	3.5E-06
16	2	12000	360	0.125	149.11	152.682	-3.572	0.000045	-1.8E-06
17	2	15000	180	0.0625	151.49	159.929	-8.439	4.36E-05	2.2E-06
18	2	15000	180	0.125	122.22	135.729	-13.509	6.69E-05	6.4E-06
19	2	15000	360	0.0625	135.67	142.946	-7.276	5.43E-05	4E-07
20	2	15000	360	0.125	172.54	199.426	-26.886	3.36E-05	8.1E-06
21	2	18000	180	0.0625	123.15	142.426	-19.276	6.59E-05	1.15E-05
22	2	18000	180	0.125	356.77	218.086	138.684	7.9E-06	-3.6E-05
23	2	18000	360	0.0625	117.78	129.422	-11.642	7.21E-05	4.3E-06
24	2	18000	360	0.125	132.62	155.536	-22.916	5.69E-05	1.05E-05
25	3	12000	180	0.0625	103.67	104.941	-1.271	0.000093	7.2E-06
26	3	12000	180	0.125	156.22	134.981	21.239	0.000041	-1.4E-05

Appendix Table B13 Continued.

No.	Blocks	RPM	IPM	DoC	Rq	FITS1	RESI1	Transform	RESI1
27	3	12000	360	0.0625	150.44	169.464	-19.024	4.42E-05	6.3E-06
28	3	12000	360	0.125	149.22	135.984	13.236	4.49E-05	-9.1E-06
29	3	15000	180	0.0625	150.78	143.231	7.549	0.000044	-4.7E-06
30	3	15000	180	0.125	122.19	119.031	3.159	0.000067	-8E-07
31	3	15000	360	0.0625	124.4	126.247	-1.847	6.46E-05	3.5E-06
32	3	15000	360	0.125	217.32	182.727	34.593	2.12E-05	-1.2E-05
33	3	18000	180	0.0625	135.41	125.727	9.683	5.45E-05	-7.1E-06
34	3	18000	180	0.125	101.76	201.387	-99.627	9.66E-05	4.56E-05
35	3	18000	360	0.0625	112.11	112.724	-0.614	7.96E-05	4.5E-06
36	3	18000	360	0.125	171.76	138.837	32.923	3.39E-05	-2E-05

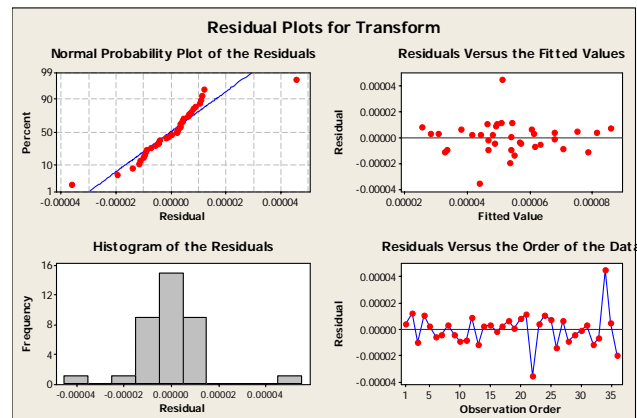


Appendix Figure B5 Box-Cox plot for surface roughness.

Appendix Table B14 Analysis of variance for transform.

Source	DF	SS	MS	F	P
Blocks	2	0.0000000	0.0000000	0.63	0.543
Spindle speed (rpm)	2	0.0000000	0.0000000	0.75	0.482
Feed speed (ipm)	1	0.0000000	0.0000000	3.04	0.095
Depth of cut (in)	1	0.0000000	0.0000000	3.07	0.093
Spindle speed*Feed speed	2	0.0000000	0.0000000	3.14	0.063
Spindle speed*Depth of cut	2	0.0000000	0.0000000	0.42	0.661
Feed speed*Depth of cut	1	0.0000000	0.0000000	0.13	0.722
Spindle speed*Feed speed*Depth of cut	2	0.0000000	0.0000000	6.66	0.005
Error	22	0.0000000	0.0000000		
Total	35				

S = 0.0000159618 R-Sq = 57.24% R-Sq (adj) = 31.98%



Appendix Figure B6 Normal probability plot of residuals for transform data.

APPENDIX C

Calculation

The regression equation model of nose width

$$\begin{aligned} \text{Nose width } (\mu\text{in}) = & -95 + 0.0156 \text{ RPM} + 0.608 \text{ IPM} + 615 \text{ DOC} + 0.0615 \text{ LF} - \\ & 0.000046 \text{ RPM} \times \text{IPM} - 0.0393 \text{ RPM} \times \text{DOC} + 0.000003 \text{ RPM} \times \\ & \text{LF} + 0.068 \text{ DOC} \times \text{LF} + 0.000048 \text{ RPM} \times \text{IPM} \times \text{DOC} \\ & - 0.000022 \text{ RPM} \times \text{DOC} \times \text{LF} \end{aligned}$$

Example, to test of regression equation model of nose width, give spindle speed at 12,000 rpm feed speed 360 ipm, depth of cut at 0.1250 in at 3000 linear feet.

from regression model

$$\begin{aligned} \text{NW } (\mu\text{in}) = & -95 + 0.0156 (12,000) + 0.608 (360) + 615 (0.125) + 0.0615 \\ & (3,000) - 0.000046 (12,000 \times 360) - 0.0393 (12,000 \times 0.125) + \\ & 0.000003 (12,000 \times 3,000) + 0.068 (0.125 \times 3,000) + 0.000048 \\ & (12,000 \times 360 \times 0.125) - 0.000022 (12,000 \times 0.125 \times 3,000) \\ = & 375.205 \mu\text{in} \end{aligned}$$

from Table 9., nose width of an insert at spindle speed at 12,000 rpm feed speed 360 ipm, depth of cut at 0.1250 in at 3000 linear feet is 8.7543 then percent (%) of accuracy for nose width is

$$100 - ((375.205 - 344.97) \times 100 / 344.97) = 91.24\%$$

Appendix Table C1 was shown nose width from regression equation model at several linear feet.

Appendix Table C1 Result of nose width of insert using regression model.

PW*	Variables			Nose Width (μin)			
	Spindle Speed (rpm)	Feed Speed (ipm)	Depth of Cut (in)	Cutting Distance (feet)			
				0	1,000	2,000	3,000
1	12,000	180	0.0625	117.723	202.973	288.223	373.473
2	12,000	180	0.1250	133.165	206.165	279.165	352.165
3	12,000	360	0.0625	134.283	219.533	304.783	390.033
4	12,000	360	0.1250	156.205	229.205	302.205	375.205
5	18,000	180	0.0625	150.145	245.145	340.145	435.145
6	18,000	180	0.1250	154.090	228.590	303.090	377.590
7	18,000	360	0.0625	120.265	215.265	310.265	405.265
8	18,000	360	0.1250	133.930	208.430	282.930	357.430
9	15,000	180	0.0625	133.934	224.059	314.184	404.309
10	15,000	180	0.1250	143.628	217.378	291.128	364.878
11	15,000	360	0.0625	127.274	217.399	307.524	397.649
12	15,000	360	0.1250	145.068	218.818	292.568	366.318

* Parawood

CURRICULUM VITAE

NAME : Miss Siripen Supadarattanawong

BIRTHDATE : January 20, 1978

BIRTH PLACE : Ratchaburi, Thailand

EDUCATION	:YEAR	INSTITUTION	DEGREE/DIPLOMA
	2001	Kasetsart University	B.S., Agricultural Engineering

POSITION/TITLE : Graduate student

WORK PLACE : Faculty of Engineering, Kasetsart University

SCHOLARSHIP/AWARDS : Excellence Student Award (Master degree), Kasetsart University, 8/2003

Graduate Research Traveling Scholarship (Roundtrip Transportation between Bangkok, Thailand – Raleigh, NC, USA), Faculty of Engineering, Kasetsart University, 4/2003

Best Project Award (Software for Measurement), Kasetsart University, 8/2002

Kasetsart University – TUA Exchange Student Scholarship, Department of Agricultural Engineering, Tokyo University of Agriculture (TUA), Japan, 10/2001-11/2001